curtin
University of Technology
Perth Western Australia

ROGER L. CLIFTON

PROCESSING METHODS FOR MULTICHANNEL RADIOMETRIC DATA WITH APPLICATION TO ATMOSPHERIC RADON

PROCESSING METHODS FOR MULTICHANNEL RADIOMETRIC DATA WITH APPLICATION TO ATMOSPHERIC RADON

By

Roger L. Clifton

A thesis presented as part of the requirements for the Degree of Master of Applied Science at Curtin University of Technology.

December 1989

ABSTRACT

Airborne multichannel radiometric data are collected for lithology mapping. Established processing methods efficiently extract the potassium and thorium distributions, but confuse the uranium in the ground with the radon gas it releases into the atmosphere.

This thesis uses the multichannel character to help separate the true uranium signal from the radon effects. The processing is reviewed and some methods for reducing the effects of radon are examined.

Radon effects are found to be related to height effects. A new height calibration procedure is proposed, and a topography sensitive procedure is established.

A Poisson noise data set is synthesized. Signal-to-noise studies are performed and smoothing requirements are investigated. Noise levels are successfully investigated in the Fourier domain. Reduction to Fourier components at acquisition is proposed.

Improved procedures for the extraction of principal components are developed. A promising new method using Fourier cosine coefficients is introduced. Changes in the processing sequence are proposed to reduce storage costs and improve precision.

The representation of factors in terms of principal components is shown to be practical and an example radon factor is constructed and tested.

ACKNOWLEDGMENTS

My supervisors were Associate Professor B H O'Connor (Principal Supervisor), Dr D Pridmore and Mr P Dunn. I particularly wish to thank Aerodata through Dr D Pridmore for supplying the survey data from the Aerodata multiclient surveys of Queensland and Dr M Lynch for initiating the project and for the use of his personal Amiga computer as a graphing terminal.

Curtin University supplied the computing and the NAG package used in the diagonalization procedure. Dr P J Rye optimized the fast Fourier transform. The meteorological data were provided by the Queensland Bureau of Meteorology.

TABLE OF CONTENTS

LIST OF TABLES

LIST OF FIGURES

CHAPTER I

INTRODUCTION

1.1 Background

The natural gamma radiation from the Earth's surface correlates with the mineral distribution. The proportions of the three radioactive elements, potassium, uranium and thorium are often found to be approximately constant across a rock type and so provide a means of mapping lithology from the air (Schwartzer et al., 1972).

Contractors' aircraft fly at roughly constant ground clearance above the uneven surface, collecting a grid of radiometric data. This is currently processed to produce a radiometric map which falls short of directly showing the rock units, due to various effects which are not directly related to the lithology. One of these problems is the presence in the air between ground and detector of the radioactive gas, radon, which gives a spurious uranium signal.

The spectrum is distorted by Compton scattering in the material between the emitter and detector and in the detector. The distortion or its absence thus includes information on the whereabouts of the emitter, but it is currently suppressed when averaging into windows and stripping out the overlap. Extraction of the effective altitude (Dickson et al. 1981), and estimation of

atmospheric radon (Bailey, 1986) have been studied.

The flying height and low measured count rates result in noisy spectra when accumulated over short time intervals such as one second. The sample spectra are very noisy and extracting useful information requires the application of delicate statistical procedures. The main limitation to such extraction has been seen as a lack of computing power (Grasty et al., 1985). To offset this, multichannel data are currently condensed in three wide windows each of which collects more of the radiation from one element than the other two, as well as a total-count window. This condensation alleviates the problems of noise and computing time but damages much of the information content (Dickson et al., 1981).

It is reasonable to anticipate the availability of sufficient computing power to apply the much more demanding software. Presently the airborne geophysical contractors in W.A. are installing multichannel acquisition units. The time is appropriate to review the multichannel techniques, in particular, with reference to suppressing the effects of radon.

1.2 Objectives

The information latent in the multichannel data was to be examined. Processing methods were to be developed to extract more information from the data than is presently achieved.

Existing procedures to suppress the radon effects in the images were to be examined and possible new procedures studied.

1.3 Methodology

One significant element in the method was the use of raw commercial data. From the outset, pragmatic decisions in the balance of quality and quantity had to be made. This approach made possible the extraction of a subset apparently showing a strong airborne radon signal.

After the literature was studied, the published multichannel methods were to be tested. Preliminary reading found that very little has been published which is specifically multichannel. However, the thesis by B H Dickson (1980) developed the important factor analysis. The nearest equivalent in the journals is the subsequent paper by B H Dickson et al., (1981) and later papers refer to both.

Factor analysis is not often used in radiometrics, so it was expected that much development work would be necessary. The necessary principal components analysis, or PCA, is vulnerable to the high noise levels so this problem had to be overcome before factor analysis could be seriously undertaken.

It was expected that radon studies would come to include attenuation and height effects. This proved to be so. Some elucidation was necessary and the implied changes to the calibration for height were investigated.

Any multichannel method which could address the radon problem was to be used. Fourier analysis was expected to be productive and a fast

Fourier transform program was obtained for the purpose. Other topics attempted were the use of ordinate scale transforms, deconvolutions by gaussians and dephased spectra, and also the second derivatives.

1.4 Structure of thesis

The following chapter (II) is a literature review and aims to present the state of the subject without particular reference to radon. A certain amount of commentary is included. The debt to the Canadian workers is apparent.

Chapter III, "Preliminary considerations" expands on the theoretical background relevant to radon studies including its spatial distribution. A data set containing an appearance of radon is identified and the probable cause discussed. The relationship with altitude is discussed in some detail. A proposal for the altitude calibration of multichannel systems is made.

Chapter IV, "Possible approaches to radon correction" scans briefly through each of a range of possibilities. A method for locating the vertical whereabouts of the radon is demonstrated. Various spatial techniques are then addressed. These include methods which might be applied to existing commercial window data sets. Following are the sections which deal specifically with multichannel data, using the spectral behaviour of the radon for identification and removal.

In Chapter V, the principal component extraction and optimization receives detailed attention, particularly the suppression of noise

interference. A new contribution to the field is made in the Fourier domain extraction of principal components. Principal components are extracted and compared.

In Chapter VI, factor analysis is applied to derive an example radon factor. This example is a preliminary trial left unextended by the lack of time available, and does not exhaust the subject. The altitude relationship is developed further with factors.

There is a brief discussion in the concluding Chapter VII.

A short Appendix shows the connection between least squares fitting of spectra and projections in linear vector space.

A Glossary follows the Appendix. A certain amount of definition and elucidation of the terms is made. The literature is detailed in the list of References. A subject Index is found at the rear.

The literature review follows immediately.

CHAPTER II

CURRENT RADIOMETRIC PRACTICE

2.1 Introduction

The theory, acquisition, processing and interpretation of airborne gamma ray spectrometry data are outlined here as a literature review.

2.2 Applications of gamma ray data

Airborne radiometric data were first collected for uranium exploration and are still collected for that purpose, with fixed wing aircraft taking the first survey and helicopter surveys following up areas of interest on a finer grid.

The principal use is in mapping the lithology associated with exploration targets in hard rock. However some exploration targets have distinct signatures of their own. Calcrete frequently gives a strong uranium signal (Butt, Horwitz and Mann, 1977) and may reach recoverable grade (Western Mining Corporation, 1975). Bauxite often contains enhanced levels of thorium (Butt, Horwitz and Mann, 1977) and heavy mineral sands have been sought successfully in Western Australia (Starkey, 1970). The Ranger uranium deposits of the

Northern Territory were discovered in a detailed airborne radiometric survey (Smith, 1985).

Radiometric surveying is not confined to hard rock studies. Sedimentary processes can in principle be assessed from radiometric data. Whereas thorium is deposited by the pH change met on entering seawater (Mason 1966), uranium is deposited in reducing conditions, so the ratio U/Th can indicate the environment of deposition (Adams and Weaver, 1958).

Monitoring of snow thicknesses has been developed for routine use in the Soviet Union (Dmitriev et al., 1973) and elsewhere. A related technique is the monitoring of soil saturation for flood control (Grasty, 1976d).

Environmental monitoring authorities are increasingly attending to fall-out from industrial activities. Cesium-137, a fission product, has a photopeak at 662 keV which can be routinely monitored with airborne equipment. Following the Chernobyl accident of 1986, the authorities of several countries spontaneously reported their monitoring data to the International Atomic Energy Authority which became a clearing-house for radiation information (International Atomic Energy Authority, 1987).

Military activities can also involve airborne radiometrics. The current distribution of plutonium and fission products from the British weapons testing in Australia was reviewed using airborne radiometrics.

Environmental monitoring need not be confined to induced

radioactivity; the uranium series content of many industrial wastes may be high enough to allow monitoring with standard equipment. Fly ash, for instance has 37 Bq kg^{-1} compared to sand at 7 Bq kg^{-1} (Mathew and Beretka, 1983). Thorium-containing wastes from mineral sands processing may also be monitored from the air through the characteristic emissions of the daughter, Tl-208.

Radon diffusing out of the soil into buildings forms a health hazard, being believed to be the main cause of lung cancer after smoking (Pearce, 1987). With thoron, its contribution to the total annual human exposure of 2.5 mSv is estimated to be 51% in Britain (National Radiological Protection Board, 1989). In Australia at least one radon effusion from sediments has been located by airborne spectrometry, at Stratham, 10 km south of Bunbury, W.A. (Dunn, pers. comm., 1987). Airborne monitoring may be appropriate when such radon concentrations occur in populated areas.

As the applications of airborne surveying are expected to increase, the related applications of stationary equipment, such as raw material monitoring, are also likely to increase.

2.3 Radioactivity and the Earth

The terrestrial elements beyond iron were formed in a supernova which left a large range of radioactive isotopes, each of which contributed radioactivity over a period similar to its half-life. The geological timescale of billions of years may be inferred from the major activities remaining in the Earth's crust (Mason, 1966). These are the three currently significant radionuclides, K-40 with a

half-life of 1.28 Ga, Th-232 at 14.0 Ga and U-238 at 4.47 Ga. Having a half-life of 0.7 Ga, U-235 is largely expended, but still contributes 5% of the activity of uranium.

The three elements are represented at various concentrations throughout the Earth's crust, in proportions reflecting the early magmatic events, subsequent metasomatism and later weathering.

When the product of a nuclear decay is itself radioactive with a half life shorter than that of its parent, the daughter will accumulate until its activity equals that of the parent. This state is referred to as radioactive equilibrium. Both U-238 and Th-232 give rise to naturally occurring series of daughters in equilibrium whereas the series associated with U-235 and Th-233 only become significant after man-caused events.

Disequilibrium in the uranium series can occur naturally when one of the daughters is depleted or enriched in a material by a geochemical or physical process. For instance, uranium can be easily mobilized in acid and oxidizing conditions and can be moved from its daughters (Ward, 1981). Similarly, radium can be leached out and radon gas can diffuse away. Detection of disequilibria could be used as an indicator for the causing process (Saunders et al., 1987).

The radioactive isotope of potassium is K-40 of which 11% decays to Ar-40 by electron capture with a gamma emission and 89% to Ca-40 in a beta decay (Adams and Dams, 1970). Potassium-argon dating is an established procedure in geochronological studies and the ratio of Ca-40 to total calcium is being investigated for similar purposes (Nelson and McCulloch, in press).

2.4 Nuclear emissions

Any nuclear decay involves the transition of a nucleus to a lower energy state. The energy difference is often partly carried away by an emitted particle such as an electron in beta decay, or a helium nucleus in alpha decay. In the case of beta decay, such as K-40 to Ca-40, the electron competes with the simultaneously emitted photon and neutrino for the energy, so the gamma spectrum resulting is spread exponentially across the low energies (Adams and Dams, 1970). The minority process (11%) for K-40 involves an electron capture to Ar-40 and a subsequent gamma emission, or de-excitation, with all the yield being delivered by the photon. Consequently its photon spectrum has a sharp photopeak. (See Figure 2.1, page 11.) This peak, at 1.46 MeV, is commonly used to detect potassium.

A Rn-222 nucleus decays with two alpha emissions to the short-lived Po-218 then to Pb-214. The Pb-214 beta decays to Bi-214 with a prompt de-excitation giving rise to a set of gamma-ray decays, the most useful of which is the 352 keV emission. The Bi-214 subsequently beta decays to Po-214 and de-excites giving a complex spectrum which includes all the significant emissions above 352 keV (Beck,1972). (See Figure 2.2, page 12.)

Other and subsequent decays are not significant here: the two radon daughters Pb-214 and Bi-214 are considered to be the immediate source of the "uranium spectrum" observed with airborne sodium iodide detectors. (See for instance, Grasty, 1973.)

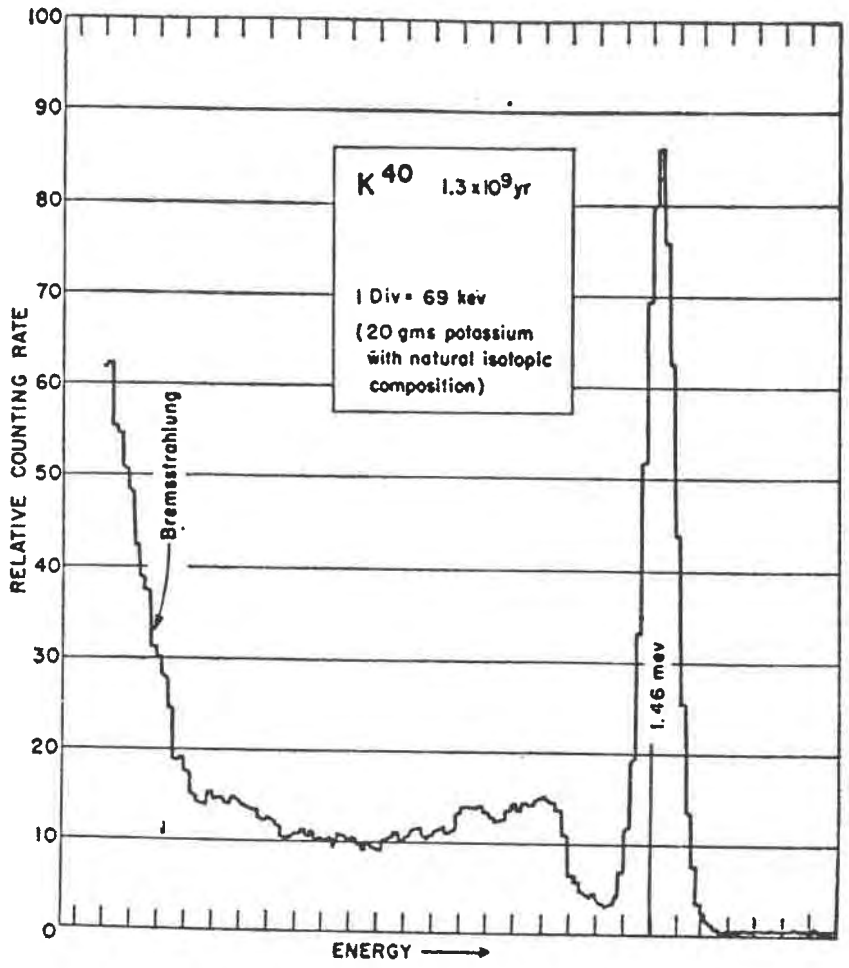

FIGURE 2.1

Potassium Spectrum

Spectrum of potassium decay taken with an NaI detector. The peak at 1.46 Mev is due to the excited Ar-40 daughter, the exponential curve at the left is due to the competing beta decay to Ca-40. The Compton spectrum runs from the low energies up to the shoulder near 1.2 MeV. (After Adams and Dams, 1970)

Uranium series ($4n + 2$)

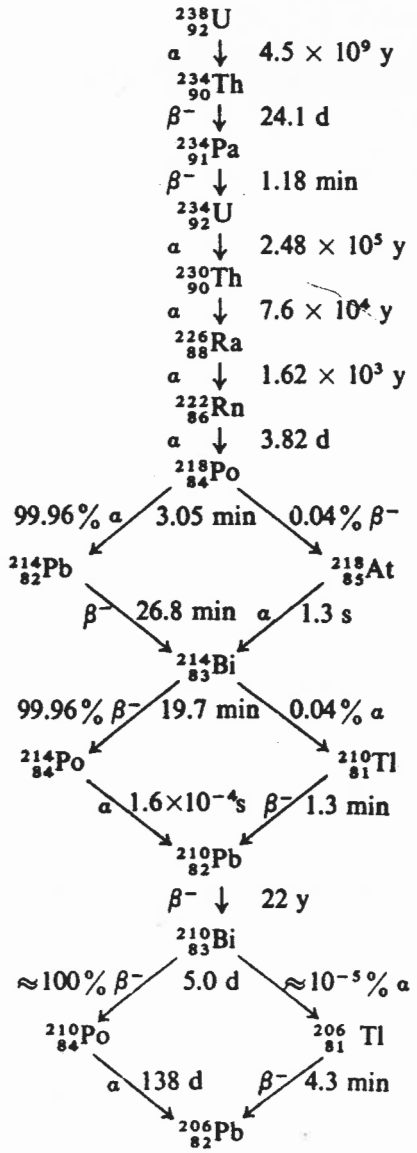

FIGURE 2.2

Uranium Decay Series

The radon daughters are the isotopes below Rn-222, the bismuth daughters are those isotopes below Bi-214. (From Hansson, 1972)

In the thorium series, similar decay chains occur, see Figure 2.3, page 14. The peaks between 0.3 and 3 MeV in the thorium series mainly arise from Tl-208 and Ac-228 (Adams and Dams, 1970). Although the series includes a radon member, Rn-220 (thoron), the half-life of this gas is short at 55 seconds. Airborne thoron is usually neglected in lithological mapping studies, however it is nevertheless considered to contribute 4% of the average radiation exposure to humans in Britain (National Radiological Protection Board, 1989).

In both the uranium and thorium series, alpha, beta and gamma decays all occur. As the gamma rays pass through the intervening matter Compton scattering redistributes some of the energies, giving rise to continuous spectra with superimposed peaks. (See Figures 2.4 and 2.5, on pages 15 and 16.) The characteristic gaussian shapes of the photopeaks alone are used in the window method of acquiring counts. The poor spectral resolution of the NaI detector limits the choice for the uranium window to the relatively isolated emission at 1.764 MeV, and even this vicinity is overlapped by two thorium peaks at 1.592 and 1.594 MeV. The thorium window is placed around the 2.62 MeV emission from Tl-208.

2.5 Interaction of gamma radiation with matter

Alpha radiation attenuates in a few tens of millimetres of air, beta radiation a few centimetres and gamma rays penetrate a few hundred metres, so only the latter can reach the detector in the aircraft.

Thorium series ($4n$)[1]

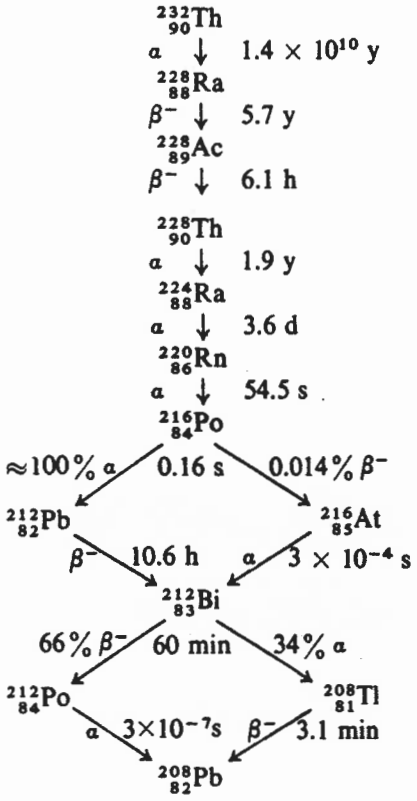

FIGURE 2.3

Thorium Decay Series

The most significant emitter in radiometric surveying is Tl-208. The Rn-220 is chemically identical to Rn-222, but the short half-life stops it drifting far. Its contribution is usually neglected in airborne radiometric mapping.

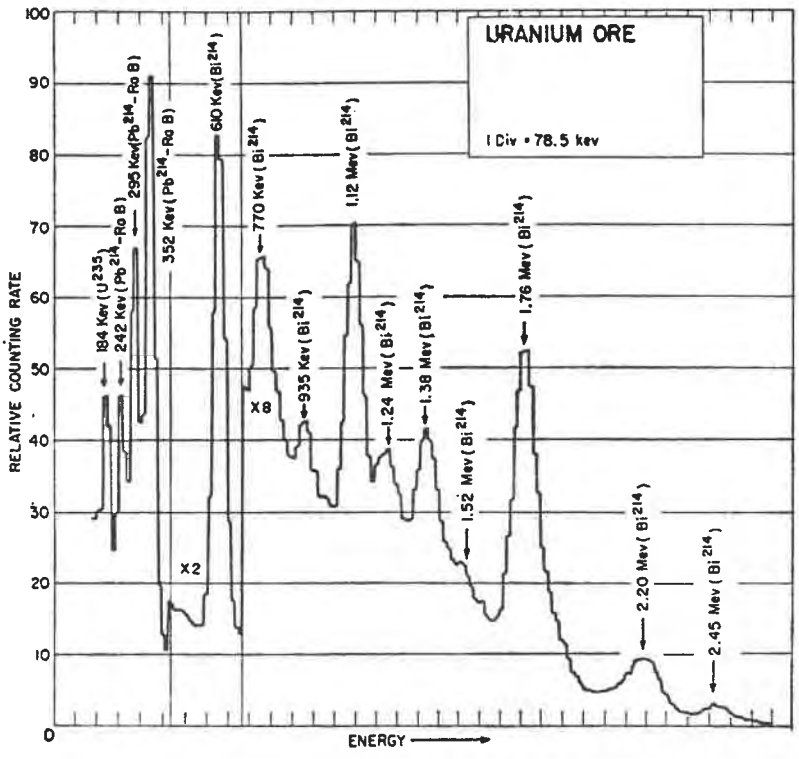

FIGURE 2.4

Uranium Spectrum

Spectrum of uranium series in equilibrium, taken with a sodium iodide detector. (From Adams and Dams, 1970).

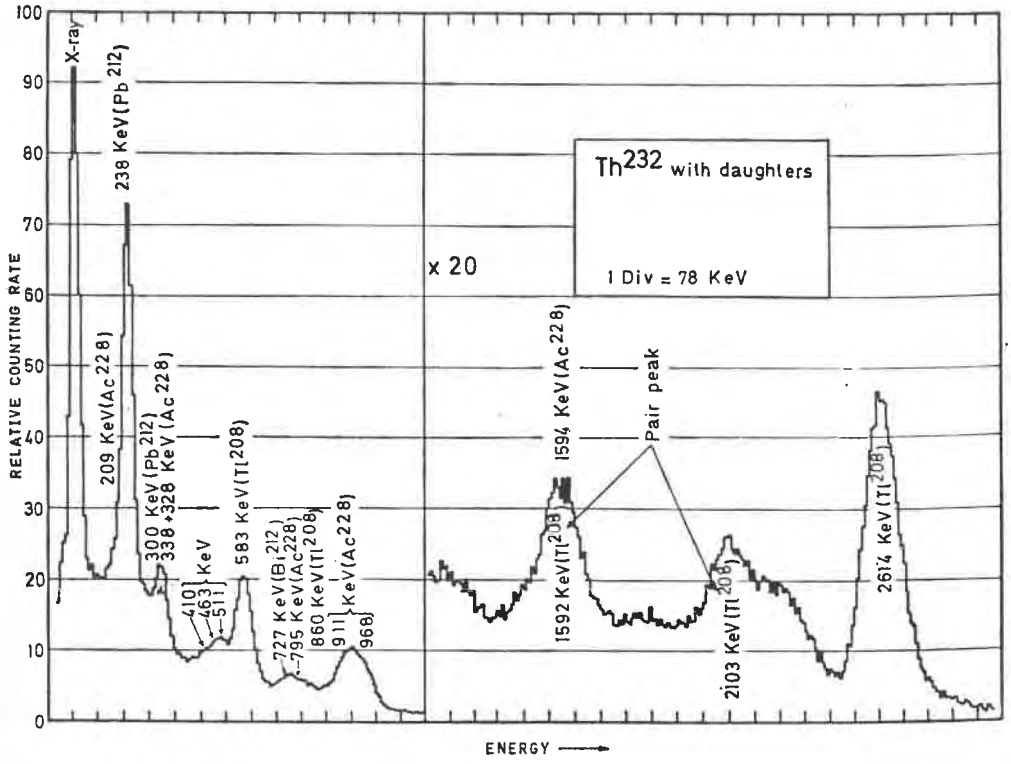

FIGURE 2.5

Thorium Spectrum

Spectrum of thorium series in equilibrium, taken with a sodium iodide detector. (From Adams and Dams, 1970).

There are many mechanisms by which a gamma ray loses its energy interacting with matter, of which three are of significance at the energies of interest here. These are photo-electric absorption, Compton scattering and pair production.

At 100 keV, which is past the low energy end of most airborne gamma detection systems, the photoelectric effect makes a significant contribution to attenuation. Here the photon liberates a bound electron, with the excess energy appearing as the kinetic energy of the electron. For higher energy gamma photons, photoelectric absorption is less likely.

Compton scattering is somewhat less significant at higher energies than lower, but is the dominant process across the spectra of interest. The photon interacts with an electron but some of the momentum and energy is carried off by a secondary, or scattered photon. The energy of the scattered photon is variously less than that of the incoming photon, creating a characteristic spectrum with a continuum of photons whose deflections rise to a maximum value about 0.25 MeV less than the original. The maximum can be often recognized on spectra as "the Compton edge" appearing 0.20-0.25 MeV below a significant peak. See Figure 2.6, page 18, where a sharply defined incoming beam has been scattered to create a Compton spectrum alongside the unscattered peak.

Although annihilation radiation, bremsstrahlung and coherent radiation all deviate the beam, only Compton radiation is considered

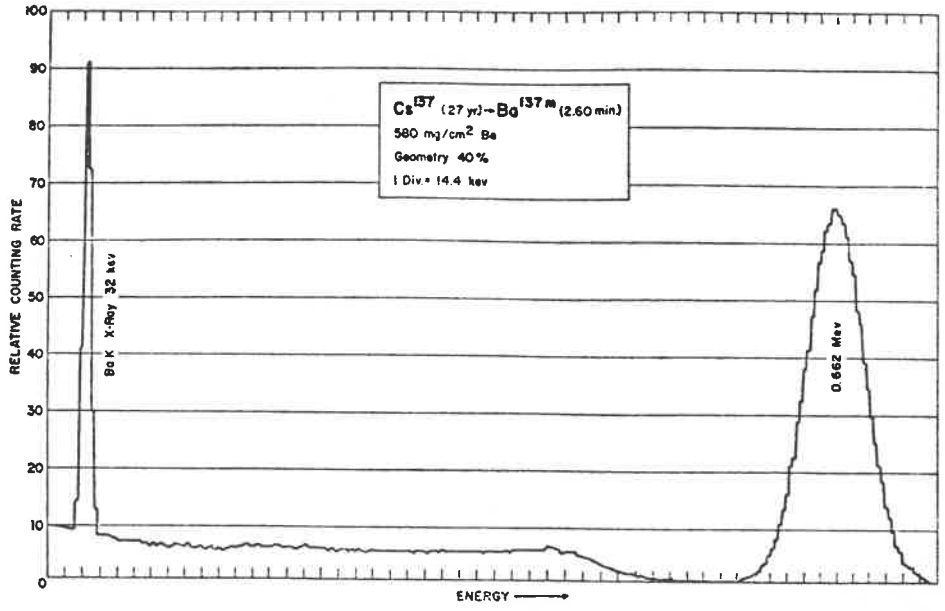

FIGURE 2.6

Cesium Spectrum

Cesium-137 spectrum taken with an NaI detector. The spectrum is characteristic of Compton scattering, the main peak at 662 keV being echoed by a shoulder near 400 keV and a continuum below that. (After Adams and Dams, 1970)

by Beck and de Planque (1968) to significantly affect the angular distribution.

The angle between the incident and scattered photons is implicit in the following equation:

$$1/E' - 1/E = 1/mc^2 \ (1- \cos(\theta))$$

where E and E' are the energies of the primary and secondary photons and mc^2 is the rest mass energy of the electron. Given that a detailed spectrum could be obtained, the angular distribution dependence of the scattering contains information on the intervening material between emitter and detector (Beck and de Planque, 1968) and may even be made to yield information on its chemistry (Cooper, 1985). However, although there is some angular variation in the sensitivity of commercial detectors (Grasty, 1976a) and much in the so-called upward-looking crystals there is no specifically angular-sensitive equipment in the present generation of spectrometer systems.

Above 1.022 MeV, a photon has enough energy to create an electron-positron pair. The electron is quickly stopped in the crystal, but the positron is converted into two photons of 512 keV. "Escape peaks" result from the escape of one or both of the annihilation photons from the crystal.

For incident photons above 1.022 MeV, the likelihood of pair-production increases. The most energetic of the useful radioelement emissions is the thorium series line of Tl-208 at 2.6 MeV, which has two minor escape peaks at 2.1 MeV and 1.6 MeV. Otherwise, the pair-production is always a minor process and is usually neglected

(Bailey, 1986).

2.6 Attenuation of gamma rays

A Compton process is as likely to scatter a tightly bound electron as a free electron (Lapp and Andrews, 1972), so that the amount of Compton scattering is proportional to the electron density. Except for particularly hydrogenous materials, this scattering is approximately proportional to the mass density along the path (Adams and Dams, 1970). Consequently, mass attenuation coefficients are quoted in units of square metres per kilogram (m^2 kg^{-1}) or in units of metres of air at standard pressure and temperature.

Laboratory derived measurements refer to a collimated beam, approximately parallel. Effective attenuations refer to a plane source whereby a more realistic detector collects scattered photons that would have been lost from a parallel beam. The distribution of attenuating material in each system of air, aircraft and equipment is peculiar to that installation and operating altitude and so must be calibrated separately.

The attenuation is greater at the low energies, as seen on Figure 2.7, page 21. The mid-range value of 0.0062 m^2 kg^{-1} at 1.0 MeV on the Figure implies a half-value thickness of approximately 100 m of air, and since the attenuation is inversely proportional to the density, 110 mm of water or perhaps 50 mm of soil. Similarly, a density of 3.7 Mg m^{-3} for sodium iodide (Weast, 1984) implies a half value thickness of 30 mm which is indicative of the size of crystal

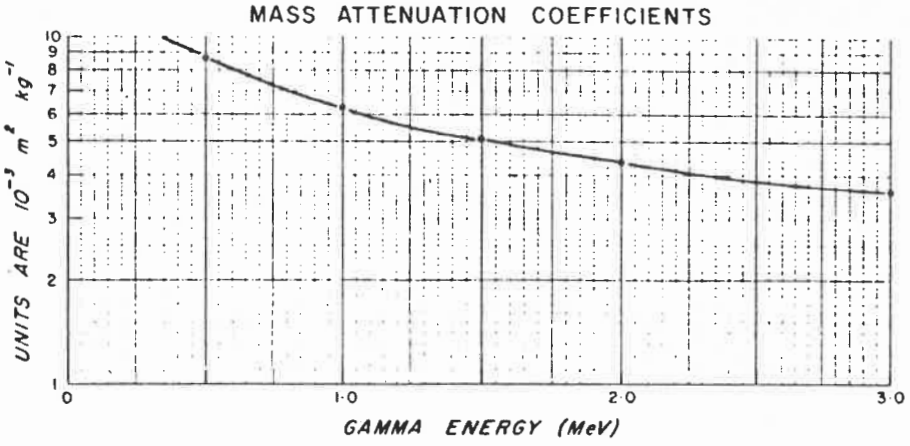

FIGURE 2.7

Mass Attenuation Coefficients

Mass attenuation coefficients as a function of the energy. These are measures of the loss of photons from a collimated beam. (From Seigbahn, 1965).

needed for collecting most of the energy of the common gamma rays.

The figure of 100 m of air indicates the need for low flight and gives rise to the concept of a footprint, a circle of investigation on the ground which is the source for 90% of the useful photons when the ground is uniformly active (Duval, 1971). The footprint is relatively insensitive to decreasing flight altitude, having a radius of 210 m at 70 m but 100 m at 20 m altitude (Duval, 1977). Aircraft surveys commonly take readings every second, or 50-60 m along the flight path, so footprints from adjacent readings at 60 m altitude normally overlap.

The figure of 110 mm for water indicates a sensitivity to soil moisture content (Kogan et al., 1969, quoted by Grasty et al., 1973). This amount of attenuation is equivalent to about a metre of snow, or dense forest. Median forest in the U.S. has a density on the ground of 35 kg m^{-2} (Grasty, 1982a) equivalent to 35 mm of water.

Because there is negligible content of the three radioelements in lake waters and little in seawater (Mason, 1966), bodies of water transmit little radiometric signal.

The short length for soil implies that evidence of the rock beneath the weathered zone can only be indirect. Conversely it implies that the information content of radiometric data can be confidently related to the topmost material.

There is more attenuation at the lower energies than the higher, being 0.010 m^2 kg^{-1} at 0.35 MeV and 0.0035 m^2 kg^{-1} at 3.0 MeV. The threefold difference in half-value thickness implies a threefold

increase in the height sensitivity at the low energies.

2.7 Gamma ray detectors

Detection of gamma rays usually uses the property of certain materials to scintillate. A gamma ray excites a path in the material and the subsequent de-excitation yields a shower of photons in the visible range. A useful scintillator must be dense to maximize collection of the secondary photons. It must also be transparent so that the photons may be collected. For this purpose a photomultiplier is mated to the scintillator and the resulting current pulse is then processed to allocate an energy to the incoming gamma ray (Harshaw, 1988).

Crystalline sodium iodide with thallium doping, NaI(Tl), is the most common scintillator. An installation usually has several crystals, each of perhaps four litres with its own photomultiplier and pre-amplifier. Commercial units often have a total of 16 or 33 litres of crystal, and research units such as that of the Canadian Geological Survey have 50 litres. The manufacturing method of growing single crystals from the melt limits the shape of sodium iodide to block forms, a limitation not shared by the plastic scintillators.

Scintillating polymers such as polystyrene or polymethylstyrene with a few percent of dopants may be extruded, moulded or shaped to a large range of shapes and volumes (Hurlbut, 1985). This ease of forming allows the design of detectors with geometries more complex

than that of the single crystal detectors. The plastic scintillators are cheaper and more robust but lack density, needing three times the volume of the sodium iodide for a similar energy resolution. Non-spectrometric applications may bring the plastic scintillators into more common use, such as the sideways looking detectors proposed by Parker Gay and Lyons (1978) for locating localized sources in low flight, or the anticoincidence counters proposed by Cowan and Crabb (1981).

2.8 Airborne detection of gamma rays

The successes of the airborne geiger counters in the 1940's in finding associations with the known uranium deposits led to the establishment of airborne radiometrics as a contract industry. However the rate of discovery remained low (Darnley, 1971).

The geiger counter is a total-count instrument; it does not distinguish between photons of different energies. Nevertheless interpreters have become familiar with total-count maps so they are still usually required from spectrometer surveys.

The signal-to-noise ratio for each element is highest in the vicinity of a photopeak, where the counts due to that element rise above those due to the other causes. The "three-window" equipment accumulates the count rate in windows around each of these peaks as well as a large total count window, which emulates the signal received by the earlier Geiger-Muller tubes. A fifth, cosmic window is often collected from 3 to 6 MeV, to allow removal of coincident cosmic background from the lower windows.

Once the multichannel acquisition equipment had been thoroughly developed for spectral studies in the laboratory it was inevitable that it began to appear in airborne surveying. Darnley et al. (1968) advocated its implementation and subsequently the Canadian Geological Survey Skyvan aircraft was fitted with a multichannel channel unit. Although the practice has spread, it has not displaced the three-window equipment, in part because computing power remained inadequate to handle the large volumes of low value data that resulted.

A reading then consists of a set of at least three values from the window equipment, and hundreds, commonly 256, values from the multichannel equipment. Compare Figure 2.8, page 26, with Figure 2.9, page 27, the mean of about a thousand seconds of flight. The major peaks are identified on Figure 2.9, page 27.

2.9 Correlation with the ground

An element's concentration tends to vary less across a rock type than when the lithology changes (Ahrens, 1965, p79-82). Schwartzer and Adams (1973) found that radiometric boundaries in the soil coincided with changes in the parent rock type.

The gamma spectrometric data are normally handled as though the window counts are linear combinations of the concentrations of potassium, uranium and thorium in the vicinity of the detector. As

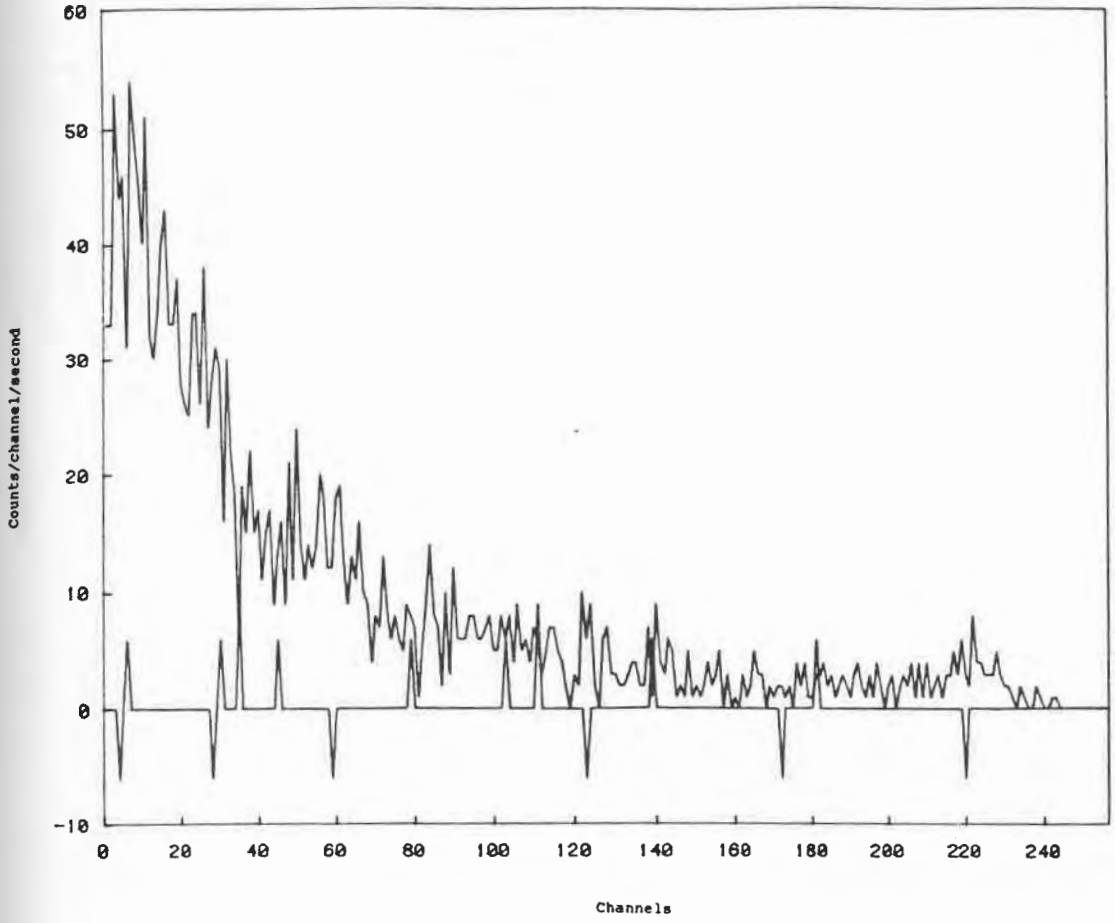

FIGURE 2.8

Typical One-second Multichannel Reading

From Aerodata's (1987) flight line 4013. The spiky character is due to Poisson noise. The spikes on the axis identify the main photopeaks. Compare with Figure 2.9, page 27.

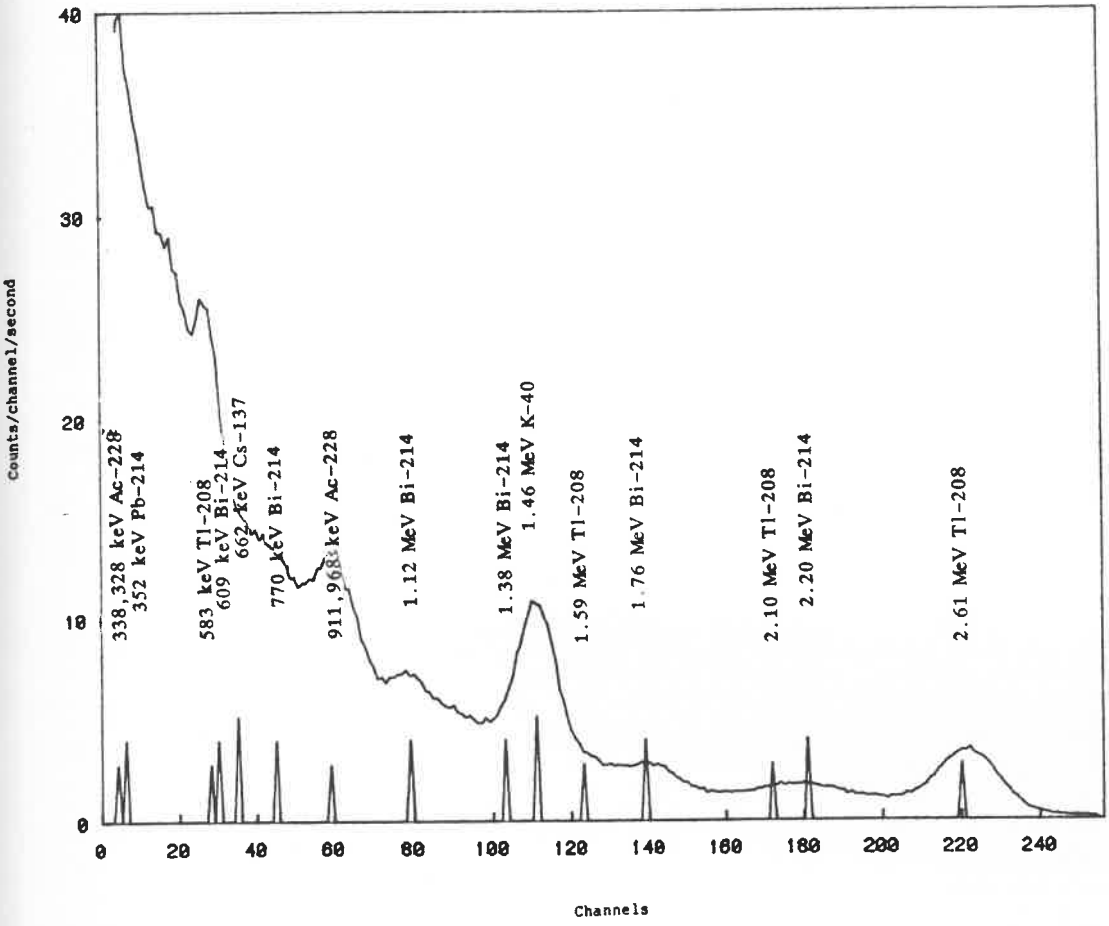

FIGURE 2.9

Mean Spectrum of Line 4013

Average spectrum of a representative line, 4013, of 1044 readings. The spikes on the axis identify the main photopeaks. The lowest spikes indicate the thorium series, mainly of emissions of Tl-208. The higher spikes indicate theuranium series, mainly of Bi-214. The K-40 and Cs-137 lines are also shown. (See also Figure 2.8, page 26.)

far as this assumption is true, the method can be regarded as a geochemical mapping technique.

The assumption is modestly successful in down-hole work. The few hundred millimetres of rock just beyond the wall of the hole are representative of the stratum being sampled. In particular, the Th/K ratios are used by well-logging contractors to make estimates of the lithology down-hole (Serra, 1984).

The contrast in signal between shales and sandstones is used extensively to correlate those rock types when drilling for hydrocarbons (Schlumberger, 1972). This contrast is improved when the uranium signal is removed, as it has less correlation with the clay mineral content than the thorium and potassium.

The correlation between the signal and underlying rock is weaker with airborne data. The surface layer being sampled has undergone a series of geochemical processes since it was part of the bedrock and these may have distorted the previous proportions. Disequilibria may occur in the uranium series, with radium being leached or radon gas diffusing away (Saunders et al., 1987). The correlation is further weakened in the presence of transported overburden. Nevertheless, consistent expressions of the parent rock are seen in the daughter soils (Schwartzer and Adams, 1973).

Lithologic boundaries were often visible in the total count data (Demnati and Naudy, 1975). Potassium, uranium and thorium tend to reach the upper crust together as products of late stage magmatic differentiation so they tend to increase together as the rock types range from ultra-basic to acidic (Adams, 1954). Much of the

radiometric variation in a survey is due to changes associated with the acidity of the rock type.

The three-window data increase the capacity of the worker to infer geologic units. However it remains restricted by the lack of counts in the neighbourhood of the photopeaks. Detection is limited to the number of photons per second per square metre available for collection, so detection is limited by the volume of sodium iodide used to intercept them. The survey reported by Demnati and Naudy (1975) used only a 6.5 litre crystal. Even so, they were able to distinguish features delineated by the potassium, thorium and Th/K ratio, as well as the total count.

The potential profitability of airborne radiometrics for delineating lithological boundaries has continued to draw the attention of the industry. With the rising confidence has come a willingness to mount larger and heavier crystals, with contractors flying up to 16 or 33 litre crystals.

2.10 Cosmic rays and the solar wind

The cosmic ray flux is a stream of nuclear particles, electrons and photons of very high energies, typically GeV (Lapp and Andrews, 1972), and sometimes exceeding 10^{25} eV (1.6 MJ) (Fischer, 1988). It is approximately isotropic and has been ascribed to the acceleration of nuclei by the intense magnetic field around neutron stars (Fischer, 1988) and the intense fields in the galactic centres. These particles give rise to hard secondary gamma rays in the atmosphere which may reach the ground level but are more frequently

represented at the surface by showers of scattered gamma rays.

The interaction of the nuclear particles with the Earth's magnetic field causes high latitudes to receive a greater contribution from cosmic rays than low latitudes. However all latitudes receive some contribution to the continuous background of environmental gamma radiation.

The solar wind is a stream of much lower energy (keV and less) nuclei, mainly protons, which interacts with the Earth's magnetic field sufficiently to distort it. Significantly for radiometric surveying, the magnetic field varies as the solar wind changes, causing fluctuations in the cosmic ray secondary flux reaching ground level (Lapp and Andrews, 1972).

The bulk distortion of the magnetic field by the solar wind may cause a diurnal variation in the background radiation as the solid Earth rotates inside the distorted shield, but any effect appears to be less than temporal changes in atmospheric radon effects. On the other hand, the more transient solar flares sometimes cause the background to increase by as much as an order of magnitude for several days (Lapp and Andrews, 1972).

2.11 Cesium and radon interference

There is a small and declining contribution due to fallout from early weapons testing in the atmosphere. In particular, Cs-137 with a half-life of 30 years has a gamma transition at 0.662 MeV and a broad spectrum below that. (See Figure 2.6, page 18.) This part of

the spectrum is generally avoided largely because of the cesium contribution (Dickson et al., 1981).

However the main source of background radiation is the series of decays due to the uranium daughter, radon-222. As an inert gas this diffuses into and through the soil pores and appears intermittently at the surface. Once clear of the soil the radon is transported according to the prevailing micrometeorology, which may not mix it into the general air mass for some time. The half-life of 3.82 days allows it to spread through the troposphere.

The window method cannot distinguish between radon and uranium. Between 50-70% of the signal which is ascribed initially to uranium arises from the airborne radon (Dickson, 1980). Although much of the spurious signal appears to be blurred out by the atmospheric movement, much also remains as stripes on the map, caused by changes in the radon level between the flights, or local changes along the line caused by flying across distinct air masses.

Removal of the effects from the maps has remained a recurrent problem in radiometrics. It is addressed in more detail in the following Chapters.

2.12 Background removal

Background consists of those counts which do not correlate with the ground distribution of radioelements. These are: the cosmic radiation; the aircraft radioactivity; and the decay of airborne radon. The background varies over time, and so must be measured in

the field for subsequent removal during processing. Fluctuations arise particularly in cosmic radiation and in the proportion of atmospheric radon.

It has been common practice to fly a test line at relatively high altitude, about 1000 m, for background estimation. (Wilkes, 1976). This procedure removes the detector to a level of maximum shielding from ground sources without greatly increasing the exposure to cosmic radiation. There is an assumption that the radon concentration is the same in the main air mass as near the production flying height. Removal of the system from the air layer in which it collects the data may mean that it samples a misleading airborne radioactivity. The practice is declining.

The shielding from ground sources is improved if a large body of water is available for flying over. Ideally it should be several times wider than the flying height and long enough for a long reading. Although commonly available in some parts of Canada, large bodies of water in convenient flying range of a survey are rare in Australia. The occurrence of potassium evaporites in salt lakes makes that alternative questionable in this country.

The "upward looking crystal" method averages the readings of a separate detector flown onboard with its crystal shielded from the ground. Photons arriving from the side and overhead are intercepted. Once the geometry of the cargo space required this to be arranged with underlying lead (Foote, 1968, quoted in Dickson et al., 1981). It is now possible to use the mass of the main crystal as the shield.

The use of such an upward-looking crystal tends to remove backscattered photons or "skyshine" as well as cosmic and local radioactivity. Skyshine is predominantly low energy, with smooth sections in the spectrum that co-vary with the higher energy photopeaks from which the primary photons came. It contributes perhaps 5 to 10% of the signal above 0.3 MeV (Lovborg et al., 1976). Since its removal will tend to sharpen the spectrum, the loss of counts is not undesirable as it is likely to improve resolution. The sharpening would need to be considered in any procedure that made use of the Compton scattered counts.

Dickson et al. (1981) proposed estimation of airborne radon from a comparison involving the apparent attenuation in the uranium channel with the known ground clearance. Bailey (1986) showed that certain information could be better extracted if upward looking data were available.

Another method obtains a variation of background, due to airborne radon, as a residual along the flight line (Green, 1987). This method assumes that the three elements correlate strongly in the survey, and that the atmospheric radon is constant along the line. The method is discussed further in Chapter IV.

It may be possible to use the higher attenuation at the lower energies (see Section 2.6, page 20) to estimate atmospheric radon. The low energy, 352 keV, line for Pb-214 is particularly shielded from true ground emitters, so any contravariance with the higher energy radon line at 1.76 MeV is a measure of the airborne radon (Grasty, 1982b).

The background spectra are stripped from the data, subtracted window by window. As it is a subtraction of an estimate of a noisy background from a total signal the procedure requires alertness of the interpreter to the possibility that a fluctuation in the background may have been left imprinted on the otherwise corrected data.

The resulting data are considered to originate from the presence of the three radioactive elements in the ground below the aircraft. The readings are considered to be linear combinations of three model spectra, each of which is the response to unit concentration of one of the radioelements.

2.13 Calibration

Concrete pads containing known proportions of the radioactive elements have been laid down at several airports around the world. As the sources are embedded and distributed over a fairly wide angle compared to the detector in an aircraft parked above, the pads allow the collection of relatively realistic model spectra. Calibration procedures are established for ground spectrometers (Killeen and Cameron, 1977) as well as aircraft systems (Grasty, 1976b). There are currently no pads for aircraft in Australia.

Airborne data can be reduced with these model spectra without correcting for non-uniform, non-planar distribution of the real sources in the field. As such the results are frequently represented in effective concentrations. The latter are the

radiometrically equivalent concentrations of emitters which are uniformly distributed in a flat half-space at the indicated distance in air.

Field calibrations are occasionally used for obtaining model spectra but the practice is considered inferior. These calibrations are performed in the field to monitor the performance of the instruments, by placing relatively active sources on the ground below or strapped to the outside skin of the aircraft. Routinely obtained with uranium and thorium, they are not obtained for potassium as the required sample mass is too great to transport.

Calibration in flight is possible if the ground concentrations are known and the background can be adequately estimated. Permanent standard flight calibration ranges with the ground concentrations assayed have been set up in other parts of the world, but only recently has one been set up in Australia, at Dalgety in New South Wales. The assaying allows the model spectra for each radioelement to be determined for the response of the system in operating conditions. If the field of ground sampling is wide enough, it also allows various altitudes to be flown during calibration so that the height dependence, or effective attenuation coefficients, may be obtained. The main requirements for a calibration flight range are laid out by Charbonneau and Darnley (1970).

2.14 Reduction of the data: stripping ratios

The three model spectra are then fitted to the data to obtain the amplitude of the three radioelements' signals. Early multichannel laboratory data were once fitted and stripped out by hand, but computers now allow the least squares fitting technique to be used efficiently (Salmon, 1960).

Fitting of the three model spectra to each reading is equivalent to solving a system of three simultaneous equations. With the coefficients, here called stripping ratios, determined during calibration, the solutions are applied automatically. (See for instance, Killeen and Carmichael, 1970, or Dickson, 1980.) The multichannel equivalent is readily obtained as a generalization, using the style of Grasty et al. (1985) :

Let $\{c_i\}$ represent the three concentrations at some calibration station, and let $\{x_j\}$ represent the corresponding count rates after background correction. There will be a sensitivity matrix $\underline{A}$ such that

$$x_j = \Sigma_i \, a_{ij} \, c_i \ .$$

Once estimates of the count rates $\{x_j\}$ have been accumulated at sufficiently many stations, the inverse may be calculated for use on routine readings $\{x_j'\}$ from stations of unknown concentrations $\{c_i'\}$ thus–

$$c_i' = \Sigma_j \, a_{ij}^{-1} \, x_j \ .$$

The index i runs over the three concentrations, whereas the index j runs over the number of channels, usually 3 or 256, depending on whether window or multichannel data are being used. In window

processing the stripping ratios form the 3x3 matrix $\underline{A}^{-1}$, some of whose elements are zero. (See Table 1, page 38).

The transformation redistributes the counts so that the new set of counts resembles the readings from an instrument which had separately recorded the respective emissions of each radioelement.

The method will fail if the equations are badly conditioned (McSharry, 1973) which can occur if the energy limits on the window settings drift significantly from the optimum or if so few counts have been used that a statistical fluctuation distorts the proportions. Conditioning must also be examined when designing calibration pads- there must be sufficient independent variation of the radioelements for their model spectra to be extracted cleanly (Killeen and Carmichael, 1970). In a general sense, any matrix manipulation of numbers of low signal-to-noise ratio involves risks of burgeoning errors.

Multichannel readings have typically 256 channels, implying a need for perhaps thousands of calculations for each reading. Such computation is becoming increasingly practical with the current improvements in computing power, but so far (1988) it is considered unreasonably demanding. Instead the separate channel counts are normally summed together when they fall in the limits of the three windows, thereby simulating the older equipment and enabling standard processing.

Methods which use the multivariate character of multichannel data are described by Dickson (1980) and applied by Dickson et al.

TABLE 1

Stripping ratios for a window acquisition system

Each of the three windows' count rates includes a contribution from each of the three elements in proportion to its concentration. In practice, some of the proportions are so low as to be neglected and so are zero in the table. The Greek letters are the common identifications. The figures quoted here are those used in one series of flights from the Aerodata (1987) survey.

	Potassium in:	Uranium in:	Thorium in:
Potassium window	1.000	τ= 0.744	β= 0.430
Uranium window	0	1.000	α= 0.335
Thorium window	0	ϵ= 0.062	1.000

(1981), Grasty et al. (1985) and Bailey (1986). There is a recognition that much of the information content remains unused in the data (Grasty et al., 1985) with the heavy computing load considered the main limitation.

The window settings recommended by the International Atomic Energy Authority (1976) have been found to be an optimum for the estimation of the three elements (Grasty et al., 1985) when the data taken from the reading are restricted to the three windows. However, an increase in the number of windows can allow an improvement in the estimations. Grasty et al. (1985) recommended ten windows and quoted the best settings. B H Dickson (1980) obtained improvements in the error estimates with decreasing window sizes down to 50 keV, which is only four channels wide in current multichannel equipment.

The stripping ratios vary with height and overburden and geometry of the source (Wormald and Clayton, 1975) due to the varying proportion of Compton-scattered photons. Lovborg et al. (1976) estimate increases in the three-window stripping ratios of about 0.03 in 50 m increase of ground clearance. This result implies that the application of the stripping procedure without accounting for the effective altitude involves a loss of precision.

2.15 Correction to constant ground clearance

Standard operational flying procedure requires pilots to maintain constant ground clearance, a requirement that is only readily met in topography of low relief. The deviations from the nominal flying height cause variations in the attenuation in the air between the

detector and the sources. Correction is routinely applied.

The processing assumes that the aircraft is flying at constant altitude above a uniformly active plane surface (Godby et al., 1952 quoted in Wilkes, 1976). Any variation in relative height as given by the radar altimeter is then treated as an independent circumstance of the aircraft above a uniform plane.

Even this straightforward model gives rise to a difficult integral which is approximated by an exponential of the form (Godby et al., 1952):

$$N(0) = N(h).\exp(-\mu\ h^2)$$

where N is the count rate, h is the height above a uniform plane source and μ is the linear attenuation coefficient for the energy range used. The more mathematically exact expression of this relationship is given by Godby et al. (1952) as a Bessel function. The value of the refinement is not great: Darnley (1971) considered that any height correction at all is pointless if the data have a standard deviation of 20% and the height varies by less than a hundred feet. In practice the correction to standard flying height H from indicated height h is usually taken as (Wilkes, 1988):

$$N(H) = N(h).\exp(-\mu(h-H))$$

where N and μ are the count rate and attenuation coefficient respectively, for each window. The correction is applied afresh to each reading along the path of the aircraft.

The method assumes that contributions from sources which are not vertically below the aircraft are all at the altitude given by the

radar altimeter during the reading being corrected. Topographic effects (see Figure 2.10, page 42) are not accounted for, although geometric models of the flight line could be constructed from the ground clearances of successive readings. Neither does the method allow for any effect of a variation in the ground activity in the area contributing to the reading. In the case of a localized source, the attenuation coefficient used in the standard correction is that for the infinite plane source, but the effective attenuation is about three times greater than that for a point source. (See Figure 2.11, page 43.) A consequence is an increase in the detection range for localized deposits at lower flight clearances, which is seen by Parker Gay and Lyons (1978) as justification for lower flying.

Although there is much consideration given in the literature to noise in the radiometric channels, there is less attention given to noise in the radar altimeter readings used to correct them. Yet the instruments can be noisy. Smoothing of the altimeter data was considered by Duval (1977), whose intention was to suppress the imprint of topography. Light smoothing has become a common practice. If the altimeter data are used to characterize the terrains or to suppress their effects, more frequent altimeter readings would be needed than the usual rate of once every second of flight.

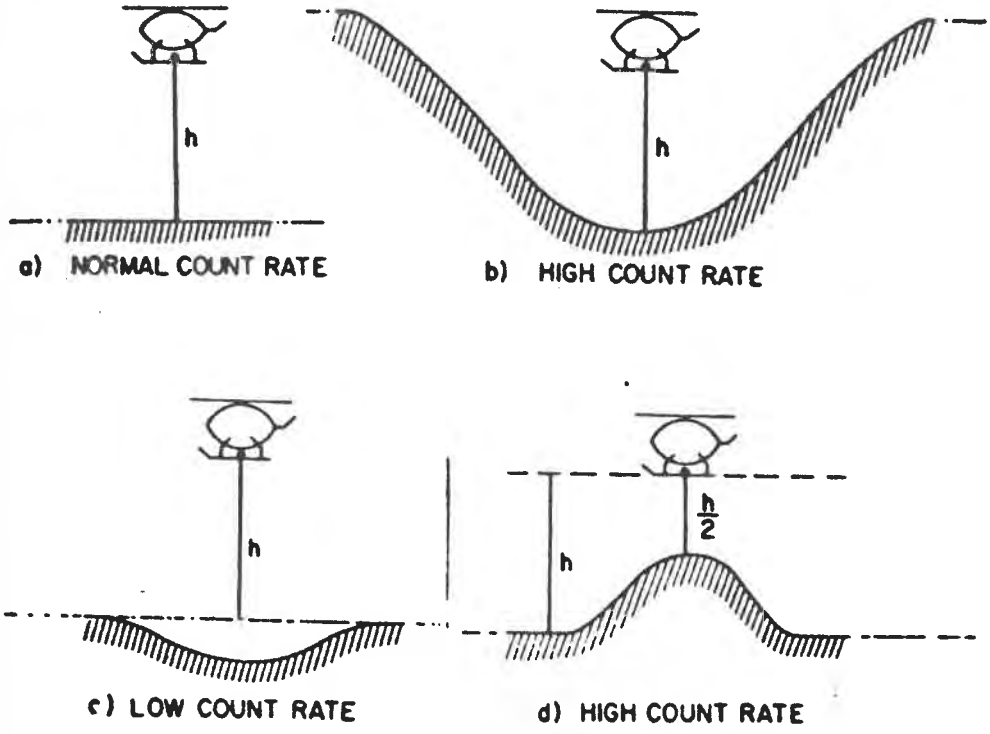

FIGURE 2.10

Effect of Topography

(From Grasty, 1976a)

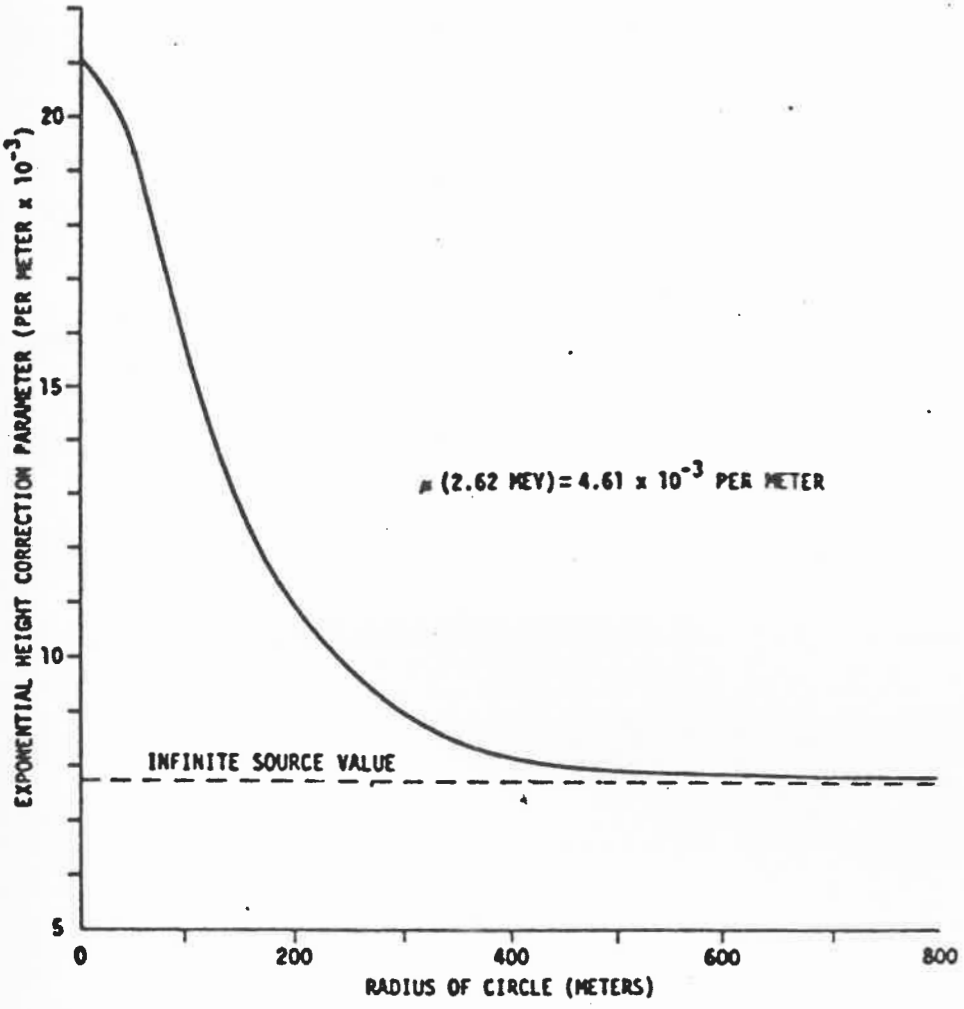

FIGURE 2.11

Attenuation and Width of Source

Effect of narrow sources on attenuation coefficients for a flying height of 122 m. (From Grasty 1976d)

2.16 Smoothing and deconvolution

The effective concentrations or the corrected counts of the three elements are then calculated at each point on the flight lines, which are then regridded and interpolated into a two dimensional map or image. During these steps a certain amount of enhancement is performed. Most significant of these is the suppression of noise, both spectral and spatial.

Spectral noise arises in multichannel data partly because the equipment provides for the acquisition of more independent variables, typically 256, than the low count rates allow of discrimination, yet each independent channel contributes noise from the inevitable statistical fluctuation. If a variable cannot be discriminated, the freedom to describe it is useless. Most of the 256 "degrees of freedom" are redundant and can be sacrificed to reduce the associated noise.

Much of the spatial noise on raw radiometric maps is expressed as a short scale visual noise, which tends to whiten a luminous three-colour image and darken a printed equivalent. The longer scales of noise have a lower amplitude but can cause dislocations, or stripes, along the flight lines.

The spatial noise can be tolerated or reduced by applying smoothing filters in the image processing later in the sequence. It is also possible to transform the data into frequency form by using Fourier transforms and then to filter out the spatial and spectral noise such as is done in the processing of seismic data (see for instance,

Robinson and Trietel, 1980). In a similar way, Grasty (1976c) proposed removal of the higher spatial frequencies to enhance the remaining signal band when deconvolving.

Deconvolution is a numerical procedure to remove a repeated function from across a data set. In radiometrics, the process of detection and recording leaves such a repeated imprint, called the spreading function, the transfer function or impulse response.

Deconvolution of broad spatial features is a potentially valuable technique where the feature can be specified. It has been applied to down-hole gamma logs for the discrimination of thin beds and edges to beds (Scott, 1963). The borehole geological impulse response was defined by Conaway and Killeen (1978) for a simple inverse filter. However, it should be noted that there is very low background in borehole data, removing one of the uncertainties that make deconvolution of airborne data risky. Cooper (1977) has sketched out some of the considerations required when attempting deconvolution.

Specification of the spreading function to be deconvolved from airborne data has been attempted by Grasty (1976c) who obtained the Fourier transforms of the anomaly at flight altitude due to a point source and also for a prism lying across the flight path.

A Fourier deconvolution of a spatial quantity requires the assumption of constant height along enough length or area of data for the transform to be taken. Deconvolving filters, on the other hand, are localized procedures and so may be adapted as the height changes along a data set.

Spectral smoothing, that is, smoothing out the ragged character of a spectrum, is in a sense, being performed when condensing the multichannel data into windows. The International Atomic Energy Authority (1976) boundaries for the three window condensation do provide an optimum signal-to-noise ratio for the three concentrations (Grasty et al., 1985) but that "smoothing" removes all other degrees of freedom beyond those three major quantities.

The resulting data set forms a two dimensional image in each of the quantities of interest. Where the data are available in the spectral form it is still possible to extract useful quantities other than the three concentrations, such as the ratios or more subtle spectral patterns. These and the concentrations are called factors.

2.17 Factors

In this thesis, the term "factor" will be used to refer to any contribution to the variance whose cause can be physically defined and has a spectral expression as a function of energy, such as the effective ground concentration of potassium. This is distinct from term "component".

The term "components" refers to certain orthogonal functions of energy which can be used in linear combination to reconstruct or decompose the spectra. In this way there will be as many possible components as there are independent degrees of freedom in the data, which the number of independent factors cannot exceed. This maximum

number is referred to as the dimensionality of the data.

Essentially, window data are 3-dimensional: there are three element windows collected in such a way that the three elements' spectra dominate the variance. The model spectra of the three elements are the factors and the concentrations are their amplitudes, apart from a constant factor. As discussed earlier, in Section 2.9, page 25, the concentrations correlate, so their spectra also will correlate. Since the space is three-dimensional, there are only three components, and only three independent factors can be obtained as linear combinations of the components at once.

Typically, multichannel data sets are 256 dimensioned. Since most of the 256 degrees of freedom are redundant, only a few components are needed to span a subspace of extractable information. In any case, there can only be as many factors as can be physically defined and can be expressed by the available components.

Grasty et al. (1985) recommend ten windows which do allow up to ten independent factors to be extracted. But the spectral boundaries are unlikely to be optimal for many factors of interest to the interpreter as they are primarily designed for estimation of the concentrations of the three radioelements.

2.18 Presentation

The data are regridded and usually presented in contour or pseudocolour maps for each reduced variable and as combined three-

coloured maps. Figure 2.12, page 49, shows a section of a commercial contour map of the effective thorium concentration. Although other presentations are available, contour and coloured maps of the effective concentrations most powerfully suggest the distribution of the three elements. However they also present distractions, particularly those due to variations in the attenuating ground cover.

Since the three windows have similar attenuation in the overburden, and assuming that the three elements have similar proportions across a rock type, it follows that the ratios of the channels would represent the rock unit regardless of the variation in overburden. These ratios are vulnerable to low values in the denominator, so their maps also are noisy, with the noise worsening in areas of heavy cover, such as swamp. Although variations in air-path due to topography (Wormald and Clayton, 1975) or variations in water-path due to soil moisture for instance may be considered as inert attenuators, the same cannot be said for sand-drifts or sheetwash clays, which add their own signature at the same time as they suppress the signal of the local material.

Each source contributes to several adjacent readings, so the more closely spaced sources overlap. Consequently there is very little useful information at wavelengths similar to the station spacing. The signal-to-noise ratio is high, so these wavelengths are often filtered out before presentation as a map. The surviving wavelengths near those cut off may still be visible in the map, as may be seen in Figure 2.12, page 49.

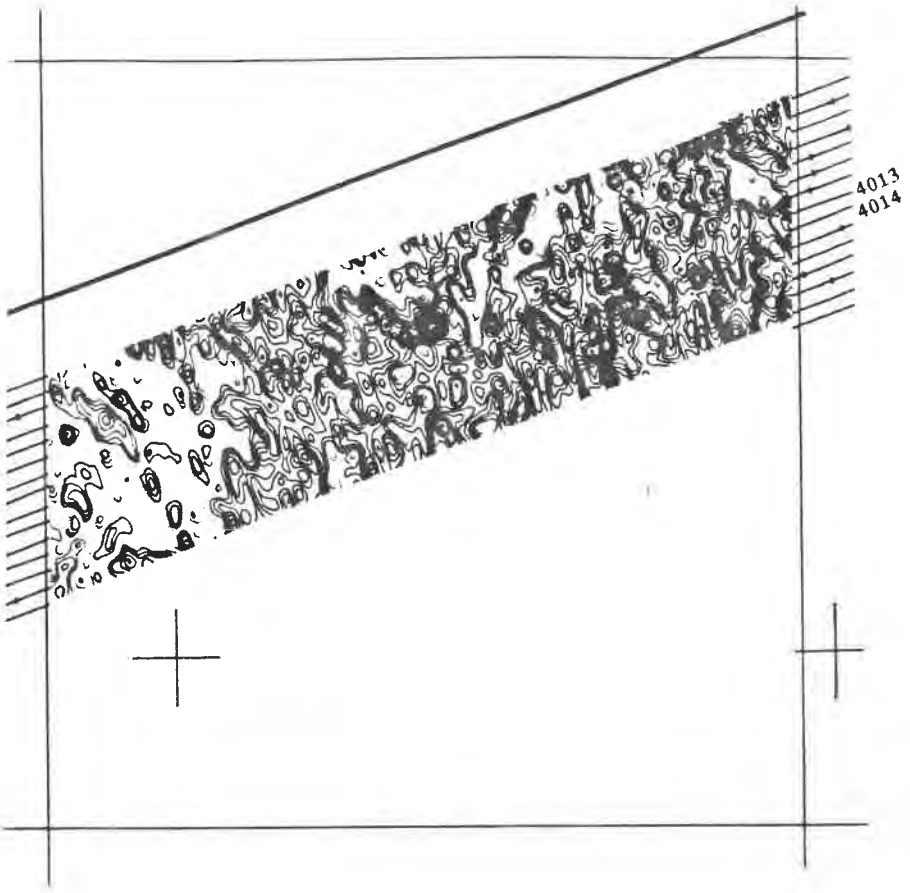

FIGURE 2.12

Part of a Commercial Raw Image for Thorium

The subset is shown superimposed on the flight lines, whose spacing at 200 m lends scale to the Figure. Software has lightly smoothed and interpolated the data along and across the lines to give a field of coloured contours. After further corrections and image processing, the full map is available for sale. From Aerodata (1987).

Another method presents the values at each grid point or reading in a triangle diagram, placed at the position of each station (Wilkes, 1976). This method allows all three concentrations to be represented on the same map, but is slow to read. An older technique is to present the profiles arrayed across the map. A related format presents the surface implied by the contours in isometric, or perspective view.

Increasingly, images are stored and handled in magnetic media and displayed in luminous form on visual display units.

2.19 Image processing

Cordell and Knepper (1987) argue that shading maps, or images, using a scale with high data density most powerfully represents geophysical data. They also argue for monochrome, as it is easier to reproduce with the current generation of equipment. Myers (1988) argues for coloured images as being a natural information medium to the human interpreter, and for an image size of 512 by 512 pixels so that the limit of resolution is within sight of the user.

The data are often sold to the client in magnetic form. This medium facilitates the application of various direct image processing techniques such as enhancement of areas of faint signal when they are of interest. Being readily reprocessed, this form also allows more indirect methods such as taking the ratios if they are not already taken, the passing of edge enhancement functions, and levelling of baseline shifts, such as those caused by atmospheric radon.

2.20 Effective altitude

The effective altitude is the amount of attenuator required to give a spectrum the appearance characteristic of a detector system at that altitude in air above a uniform ground source. It is measured in metres of air equivalent. This definition conforms to that of Dickson (1980) as quoted by Bailey (1986).

If there is an increase in the amount of attenuator between emitter and detector, the proportion of scattered radiation increases. Since these photons have lost energy during scattering, the spectrum softens; it loses prominence near the photopeaks and gains intensity between them. As a consequence, the residue left behind after removal of background and the fitting of the model spectra contains direct information of the intervening attenuating material.

B L Dickson et al. (1979) used the ground level residue at the uranium 609 keV peak to measure the overburden on a near-surface uranium deposit. Grasty (1982a) used the spill of counts from the potassium photopeak into an adjacent window to make estimates of snow depths between the aircraft and ground in a single flight.

B H Dickson (1980) used factor analysis to formalize a method of this estimation from multichannel data. He obtained what amounted to height factors for each element by multivariate analysis of the data obtained when covering the pads at Breckenridge, Ottawa with various thicknesses of plywood. His overburdens arrived at using the scattering in the thorium data were almost as good as those obtained using the potassium spectrum, but the method requires quite

long counting times. He concluded that reasonable estimations would require a kilometre of flight-line data using the 50 L fixed-wing system of the Geological Survey of Canada.

Dickson et al. (1981) studied the effect of thicknesses of attenuator for each of the elements and was able to produce a model spectrum for the altitude effect on each element. Bailey (1986) developed a physical model to describe the effect. Since the amplitude of that characterizing height spectrum depends on the concentration of the element, the presence of each element should be seen as a height dependent factor with two spectral components.

With increasing thickness of attenuator, the amount of deflection due to scattering increases. As effective altitude increases, the lower energies become more isotropic whereas the photopeaks become collimated toward the vertical. If the angular distributions of the gamma ray flux could be measured as well as the counts, their stronger dependence on attenuator thickness might allow a better determination of the effective altitude. In connection with the age of fission product fallout, Beck and de Planque (1968) consider that it might be possible to estimate the depth distribution of the emitter in the soil from the radiometric angular distribution.

It is with similar logic that Bailey (1986) advocated the use of upward looking crystals for the estimation of atmospheric radon as a negative effective altitude extracted from the uranium signal.

2.21 Terrain and topographic effects

Any repeating pattern in the ground surface forms a terrain. Workers such as Schwartzer et al. (1972) foresee considerable value in the use of airborne radiometrics in terrain analysis.

A repeating pattern in the topography is an example. Even uniformly radioactive ground will leave the imprint of its topography in the data (see Figure 2.10, page 42). Unless the ground clearance varies only slowly, the usual height correction (see Section 2.15) will incompletely suppress the variation since it assumes a plane source. Clark (1971, quoted in Duval, 1977) modelled several idealized topographic features, and found the height correction to be imprecise.

Laterites and calcretes can set up characteristic terrains (Butt, 1981), with the recurrence of flat topped hills with sharp gradients at the edges. Since both materials have radiometric signature, so do their associated terrains. An interpreter may compare the topographic profile with the radiometrics to infer the presence of a high thorium laterite, or a uranium-bearing calcrete, for example.

Another example is dune country, where the sand of the dunes has been sorted clean of the more radioactive clay. An interpreter may observe a correlation between low radiometric signal and rolling terrain; and then infer sand dunes. Similarly the high clay contents of playas may be expected to create an identifying signature of radiometric highs over flat stretches of ground.

Topography should be available from the barometric and radar

altitudes if they are recorded sufficiently often. Parker Gay and Lyons (1978) consider the topographic profile to be a valuable data set in its own right, allowing the interpreters to supply their own knowledge of rock types relative to the terrain.

2.22 Summary

The literature of airborne radiometrics has been reviewed with some commentary. No particular emphasis has been placed on radon suppression, a subject which will be addressed in the following Chapter. There is a certain amount of multichannel information in the technical literature, with relatively little appearing in exploration text books. It is apparent that research is being done, without radical changes having appeared in practice. The main workers in the multichannel studies are in Canada, particularly Dr R C Bailey at the University of Toronto and Dr R L Grasty at the Geological Survey of Canada. In Australia, the work of Dr B L Dickson is pre-eminent.

The window method of radiometric data analysis is a matured technique, with radon suppression an outstanding problem. This problem may be better addressed with appropriate multichannel techniques, as they become practical.

CHAPTER III

RADON- PRELIMINARY CONSIDERATIONS

3.1 Introduction

The achievement of solutions to the problem of the effects of airborne radon required an examination of the various physical phenomena as well as the data processing considerations. The mechanism of the appearance of excess airborne radon is of interest as it has implications for the whereabouts of the radon and its spectral effects. The chapter begins with a discussion of the causes and the meteorological and spectral behaviours.

A specimen data set containing a significant change in signal due to airborne radon was needed. A selection was made from a search of some data made available by Aerodata P.L. (1987). The likelihood of radon being present in the selected data set was examined.

The stochastic noise content was examined and means of noise suppression relative to the useful signal was discussed.

A practical distinction between the useful uranium signal and the spurious radon effects was sought in the spectral evidence. To this end the attenuation behaviour was studied in some detail. The relationship between the airborne radon and the patterns in the data was found to be interwoven with the effects of altitude.

The Behaviour of Radon

3.2 The spectral difference due to airborne radon

The search for measures of the airborne radon effects required the project to address the types of variation in the data. It was considered appropriate to seek a fourth degree of freedom -beyond the three ground concentrations- that in some way expressed the variation in airborne radon. Once this behaviour was identified, a radon estimate R was to be found which quantified the amount of the total "uranium" signal due to the effects of airborne radon. This radon estimate would be of use to the industry to isolate that part of the uranium signal due solely to the concentration of uranium in the ground:

$$U_{litho.} = U_{total} - R$$

Accordingly, a characteristic distinction was sought between the spectra due to the uranium series in the ground and that caused by radon in the air. The spectra are otherwise equivalent. Under similar physical conditions, the NaI-acquired spectrum of radon-222 must be taken as the spectrum of natural uranium, as the radon daughters Pb-214 and Bi-214 (see Figure 2.2 on page 11) are the only significant uranium daughters distinguishable in the NaI-acquired spectrum between 0.3 and 3 MeV (see Figure 3.1 on page 57). There is not enough detail in the readings or calibration spectra to resolve any of the emissions due to the other uranium daughters.

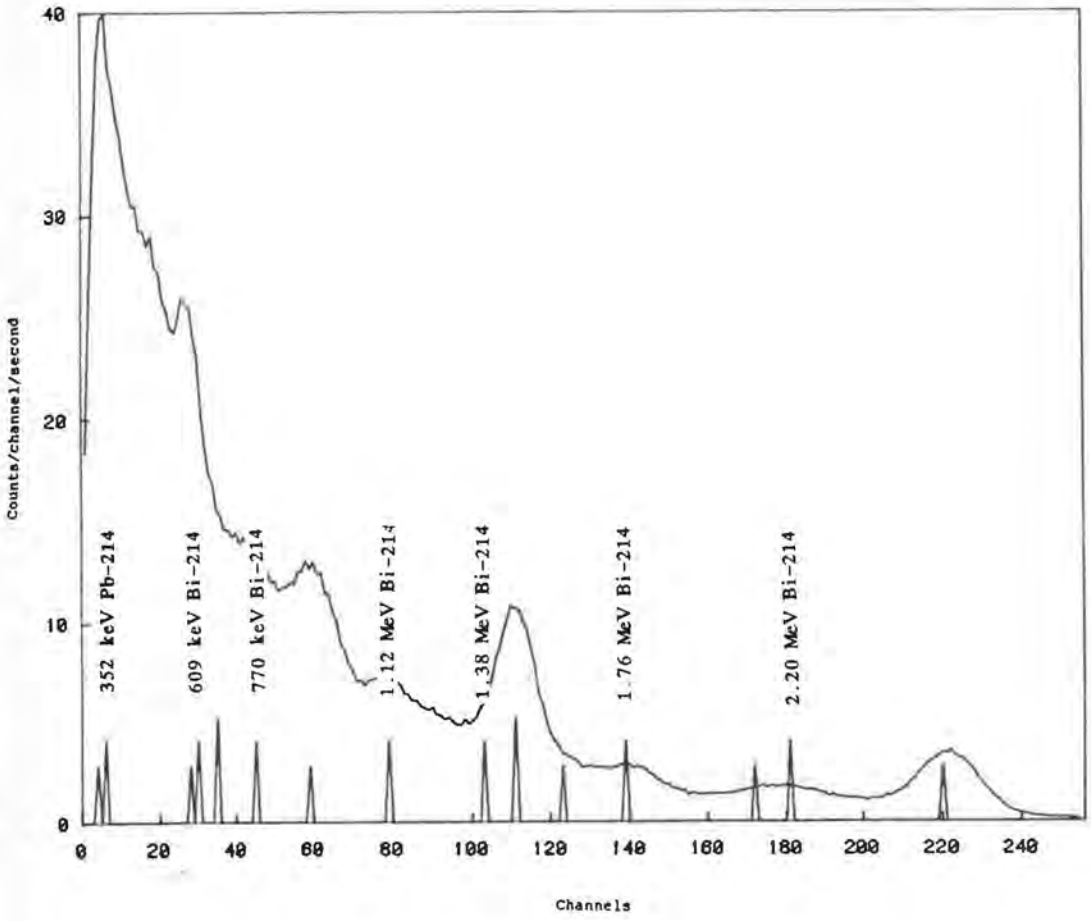

FIGURE 3.1

Emissions of Radon Daughters

The energies of the significant emissions of Rn-222 are shown as spikes against the channel numbers used in these data. Apart from a single line of Pb-214 at 352 keV, they all arise during the decay of Bi-214 into Po-214. The mean spectrum of line 4014 is shown superimposed. Compare with the spectrum of a uraninite sample, Figure 2.4 on page 15.

Except possibly in the event of fresh precipitation the Pb-214 and Bi-214 are in equilibrium with each other, so the spectrum of the uranium in the land surface below the aircraft was taken to be equivalent to that of radon, similarly attenuated by the intervening soil and air.

There is a difference in the spectra caused by a significant increase in the amount of attenuation between the source and detector. Due largely to the increased scattering at the lower energies (see Section 2.6 on page 20), this effect allows the estimation of the amount of overburden on a uranium deposit from the field spectra (B L Dickson et al., 1979). It is of interest to extend the estimation to soil, vegetation, water, snow or air separation in general airborne surveys. In the work that follows, the approximation is made, following B H Dickson (1980), that the difference can be measured as if it were due to an attenuating layer of air.

There is a strong peak of Pb-214 at the relatively low energy of 352 keV (see Figure 2.4 on page 15) which has been proposed by Grasty (1982b) for radon estimation instead of the Bi-214 lines. Any disequilibrium effects would need to be understood, but are unlikely to be great since the half-life of the transition between the two nuclides is only 20 minutes. Regardless, the contribution by Pb-214 to the spectrum is only at the lowest energies, which are rarely used. It is sufficiently accurate to speak of the spectrum of Bi-214 as the spectrum of both radon and uranium, when the attenuation is equal.

On the basis of these considerations, a difference of the appropriate form between the detected spectrum and that expected of a ground uranium distribution can be attributed to the free radon. The relation between R and the amount of the spectral difference will depend on the attenuation distribution of the radon. Two examples serve to illustrate the range of distributions.

3.3 Radon in the atmosphere

Radon is produced by alpha decay in the soil or rock. The recoiling radon nuclei have too much energy (typically 100 keV) to be stopped by the gas in the soil pores. In dry soil they come to rest in the solid grains (Kerrigan and O'Connor, 1989) and some then diffuse into the pore spaces. If the radon gas does not move further in the soil pores, its subsequent gamma ray signal is attenuated similarly to the radon remaining fixed in the solid rock; it is only when it moves into a position of different attenuation relative to the detector that it confuses the inference of the uranium concentration. Primarily, the radon confuses by a change in the amplitude of the spectrum and secondly by a change in its shape.

An example can be taken to show a change in amplitude of the signal with no change in spectral shape.- If the radon intermittently escapes into the air above the soil and is swept away, the drop in signal can cause stripes in the map of the inferred uranium. An adjacent line collected before the escape has a relative step in the amplitude of the spectrum, but there is no change in its shape because there is no change in the attenuator.

The opposite extreme is met when the aircraft flies into a pocket of radon-containing air, such as might be leaving the near-surface zone in a morning thermal. (See Figure 3.2 on page 61.) Here there is minimal attenuation and a disproportionate transmission of the low-energy end of the spectrum. The spectrum has changed shape as well as amplitude.

It is to be noted that these two extreme cases can be caused by the same quantity of displaced radon. A procedure that allows inference of the quantity of radon from a measure of the attenuation effect will estimate zero free radon in the first (buried radon) case and excessive free radon in the second (nearby airborne radon) case. Yet the two cases are equally undesirable when mapping the uranium concentration. Clearly the mapping methods are limited by the working assumptions of the free radon distribution.

If there is sufficient change of spectral shape to quantify, and the airborne distribution can be confidently estimated, then the attenuation effect can be used to measure the proportion of the signal due to the ground sources. The groundwork for such methods will be developed further in this thesis.

A complete description of the free radon activity from spectral evidence alone would require several independent values to be determined at each element of area where the radon is to be estimated. Some function of the sequence of values would then yield the radon quantity estimate. One value alone could not quantify the free radon activity; but it would allow a first approximation of the

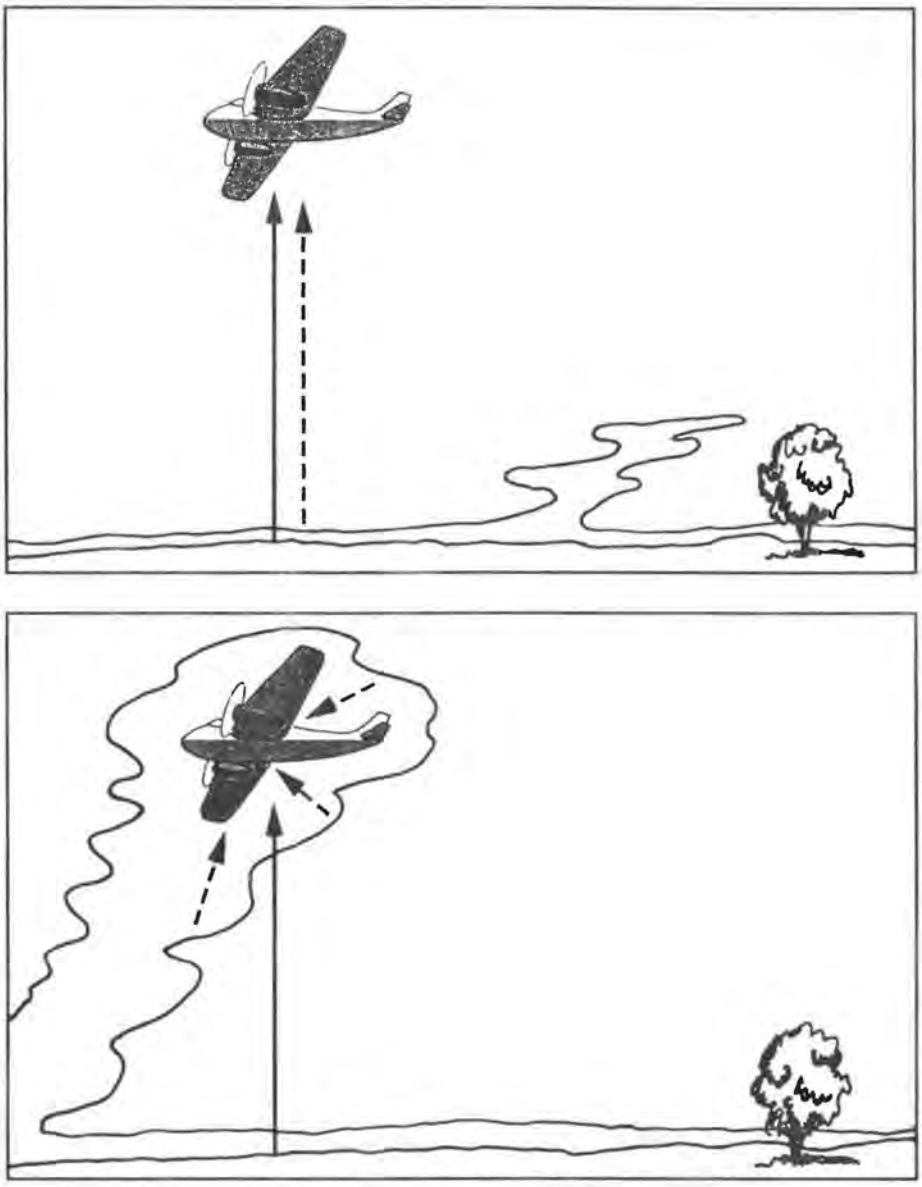

FIGURE 3.2

Ambiguity of Range when Detecting Airborne Radon

When exhaled radon lies close to the ground surface its signal suffers a similar amount of attenuation to that from the uranium series still embedded in the ground. When a pocket of radon-enriched air is encountered by the aircraft, the detector receives the radon signal with minimum attenuation.

free radon signal received, which is the quantity relevant to uranium mapping.

This value is the relationship between a quantified change in shape and the amount of spurious uranium signal, referred to earlier as the radon estimate, R. Clearly R depends functionally on the vertical distribution assumed by the worker during the processing.

Considerations of noise in the currently available one-second commercial data make the extraction of more than one value inadvisable. Even that value would have to be related to the adjacent readings to improve the reliability: B H Dickson (1980) had to use 10 second intervals to reliably calculate a similar estimate, the potassium overburden. Although his data were obtained at the less sensitive height of 97 m, his equipment was better calibrated and used more (50 L) crystal. The potassium overburden is likely to be more reliable than the radon estimate, so the prospects of achieving a high level of signal in any inference of the radon are not great.

This thesis attends mainly to the simplest models, whereby the radon estimate derived at any point is a single number.

3.4 Radon excursions due to moisture

How the radon excursions arise is not fully understood. It is appropriate to examine some possible mechanisms.

The capacity of solid surfaces to cool the adjacent air at night-time gives rise to dew and fog. The negative buoyancy of the cooler

air can cause an air mass to drift off the high ground and accumulate in low ground. This may cause an air mass already enhanced in radon activity to associate with a fog patch without necessarily any relationship between the radon gas and the droplets. Across a survey, there may then be a tendency for uranium-window activity to occur in low ground, as observed by Butt et al. (1977). Such activity would have the half-life of Rn-222 of 3.8 days rather than the half-life of Bi-214 at 20 minutes. Darnley et al. (1968) observed an association with fog but did not estimate the half-life.

On the other hand, when dew forms in the bottom several hundred metres of night-time still air, the circulating droplets are able to adsorb the charged decay products of radon. Grasty (1973) implied this mechanism when describing the activity of fresh snow. Once the droplets have deposited on the outermost surfaces of the vegetation and exposed materials, a layer of activity has formed with the maximum thickness of air and the minimum of other attenuation. This activity shows very little spectral distinction from uranium in the ground.

As radon daughters rather than radon gas have been adsorbed on the droplets then the characteristically shorter half-life (approx. 20 minutes for both Pb-214 and Bi-214) allows the activity to clear quickly (Grasty, 1973). Furthermore, the radon daughters can only be scavenged from the depth of air in the inversion, already similar in magnitude to the range of the airborne detector. This model does not appear to adequately explain the quantities of spurious signal from Bi-214 and Pb-214.

Moreover, the meteorological phenomenon most commonly associated with a radon excursion is rain rather than fog. Clifford et al. (1981) tabulated several sets of radon excursions against the rainfall as recorded in the nearest meteorological posts. Results of a correlation analysis of their data is shown in Table 2 on page 65. The correlations are rather weak, the stronger results giving a rate of increase of the radon signal near 5% per millimetre of rain.

A model for the effect of rainfall on dry soil may be inferred from the work of Kerrigan and O'Connor (1989) and others. Consider that most aerated soils will have a water film spread over the soil grains. A radon nucleus produced in an alpha decay,

$$Ra\text{-}226 \rightarrow Rn\text{-}222 + He\text{-}4$$

has a recoil energy of 100 keV which is often sufficient to allow the nucleus to escape from the soil particle grain and be stopped either in another soil particle or in the water film.

Consider also that a wet soil will always be evaporating a water vapour into any atmosphere which is short of 100% relative humidity. The thickness of the water film at any depth will vary according to the vapour pressure gradient and the permeability of the soil above it. The gradient will be particularly affected by a change of the top surface from a sun-dried state to a saturated micro-environment with free water droplets. Without itself contributing to the mass of the water films, a fall of rain or dew lying on the surface may still allow the temporary accumulation of a water film which would otherwise have evaporated from the subsoil.

TABLE 2

Correlation of Rainfall against Radon Excursions

Clifford et al. (1981) tabulated rainfall of the locality against the radiation levels compared to the average for the station. Their data have been reprocessed to seek the sensitivity to rain. Many of their rainfalls were shown only as "trace" and so have been omitted from the regressions. The resulting gradients suggest a general response of total signal, as detected by their upward looking NaI detector, of 5% per millimetre of rain.

Table	State	Correlation	Response
LXV	Oklahoma	0.795 *	4.55% mm^{-1} *
LXVI	N.Mexico	0.072	11.4% mm^{-1}
LXVII	Texas	0.155	1.25% mm^{-1}
LXVIII	N.Dakota	0.529 *	5.26% mm^{-1} *

An increase in the proportion of water to solid mineral implies that the freshly formed radon will increasingly come to rest in water rather than solid. From the water the radon readily diffuses into the gas in the soil pores and thence into the atmosphere. Its rate of diffusion is unaffected by changes in the humidity.

By this process the wetness of the surface may cause exhalation of radon from the interior of the soil. Supporting evidence for this model of the radon excursions is also found in the monazite studies. These studies have shown a 50% increase in exhalation of Rn-220 from monazite samples to occur when 5% water is added to dry samples (Kerrigan and O'Connor, 1989). The behaviour of Rn-222 is likely to be similar.

It is reasonable to ascribe radon excursions to the growth of water films in the soil pores during wet conditions. The experimental set-up used in the work on monazite may present appropriate means of testing such propositions.

3.5 Mechanisms and measurement of the vertical development

When a layer of air near the ground persists unstirred by upper winds it can be expected to accumulate radon diffusing from the soil. Conversely, an air mass which has travelled over ocean for some weeks will be almost clean. As air masses tend to stratify, it is appropriate to examine factors affecting the vertical distribution of radon.

The air in the first few centimetres and metres above the soil remains for a time which depends partly on its height above the ground. The residence time is a function of the amount of mixing reaching that height.

The whereabouts of radon in the atmosphere above tree height is controlled by layer formation and layer dissipation. The characteristic vertical mixing velocity is about 1 m s^{-1} whereas the horizontal velocities are larger, perhaps 10 m s^{-1}. Consequently horizontal uniformity is to be expected to be more common than vertical uniformity, and the vertical distribution to be more significant than the horizontal.

Thermals provide a mechanism for the mixing of near-surface air into the air above. The sun heats the soil and vegetation within a few centimetres above. The adjacent air warms, becomes buoyant and lifts off. It may remain trapped in the vicinity of higher, cooler obstructions, such as shrubs, trees, or crops. This constitutes a layer closer to the aircraft. Although only a few metres of

absolute distance may be involved, the change in attenuation can be significant: 10 kg m^{-2} of intervening vegetation has a mass attenuation equivalent to 10 m of air.

Daytime thermals liberate trapped air and deliver it as high as the lapse rate permits. An inversion layer near the operating height will stop the thermals and allow a local accumulation of radon, vertically localized but horizontally spread. Such interface accumulation has been observed by Darnley (1971). The effect in a radiometric image would be a general uranium bias. If the inversion clears before all the flight lines were completed, a long stripe with a strong, relatively uniform, spectral signature might be seen. On the other hand, active thermals at flying height must create a noisy imprint with a non-uniform distribution in the data.

Some of the Bi-214 residuals selected by Green (1987) are shown in Figure 3.3 on page 69. These are derived from the uranium means of flight lines at 150 m. They are suggestive of a surface or near-surface activity being mixed into the atmosphere as the day progresses.

It is clear that the vertical whereabouts depends on the prevailing meteorology and is quite variable. Yet in practice assumptions have to be made; for instance, flying over a test line or over water or the use of baseline averages are averaging procedures that seek to establish a reference estimate for the whole atmosphere for that period. (See for instance, Wilkes, 1988.)

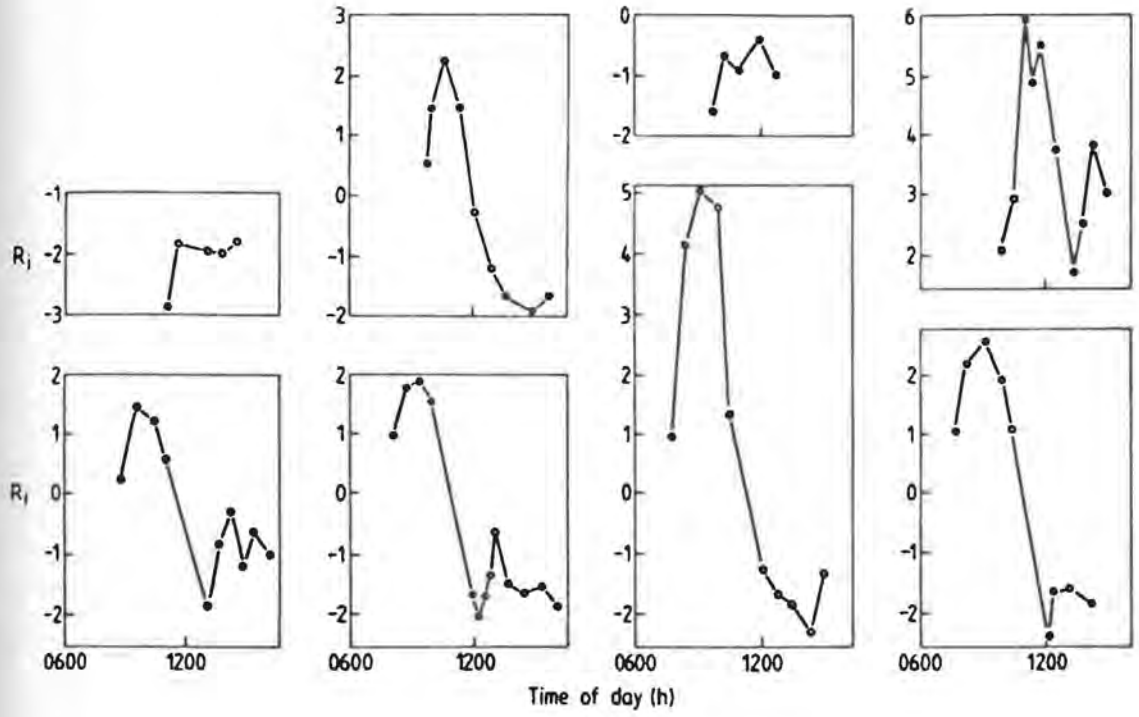

FIGURE 3.3

Uranium Residuals and Time of Day

A selection of radon quantifiers obtained by Green (1987), showing decay as the day advances. This quantity is the uranium residual, or discrepancy between the uranium mean of each line and the mean expected on the basis of its potassium and thorium means. The expectation is given by regressing uranium line means against the potassium and thorium line means. From Green (1987).

The flying of test lines at successively higher altitudes for the estimation of the cosmic contribution may allow the estimation of the gross vertical gradient in the radon at the same time if the equipment is multichannel. When window equipment is in use, the assumption is usually made that the radon is constant (Wilkes, 1988).

The use of an upward-looking crystal assumes a certain vertical uniformity to infer the total airborne radon contribution to the uranium channel. This allows the radon estimate to change horizontally as often as the upward crystal is sampled.

The vertical separation of airborne radon from the parent rock provides a behavioural distinction between it and the uranium series in the ground. The spectral expression of the behaviour will be used to characterize the effects of airborne radon.

The Data Set

3.6 Identification of a data set with a radon step

Some multiclient data, currently being collected by one of the supporters of the project, were scrutinized for the presence of a radon step. To maintain confidentiality, the location was given only as the locality of Charters Towers, Queensland.

A Geometrics 256-channel multichannel analyser had been used with eight four-litre NaI crystals. Data had been stored on magnetic tape without special attention being paid to the quality control.

Some 100 000 seconds of multichannel flight data representing about 6000 km of grid in lines of about a thousand seconds duration each were examined.

The average spectrum of each line was compared to that of the next. At the same time, the size of the 609 keV hump was monitored, that is, the average sum of counts in the 609 keV peak over and above the average of the spectrum on either side was recorded. The 609 keV emission is a high intensity, low energy emission of Bi-214 (Beck, 1972) and so is expected to be particularly sensitive to the decaying airborne radon near the aircraft.

Both the spectral plots and the peak counts showed a distinct drop between the lines named 4013 and 4014. Subsequent radiometric maps show the same jump, despite the smoothing. An example is seen in Figure 3.4 on page 72.

The average flying heights of both lines was 58 m, although the standard deviation of 10 metres on line 4013 was twice that of line 4014 at 5 metres. Also similar was the gain shift, measured by comparing the counts on either side of the nominal position of the main thorium series peak at 2.67 MeV. The statistics of the neighbouring lines are detailed in Table 3 on page 73.

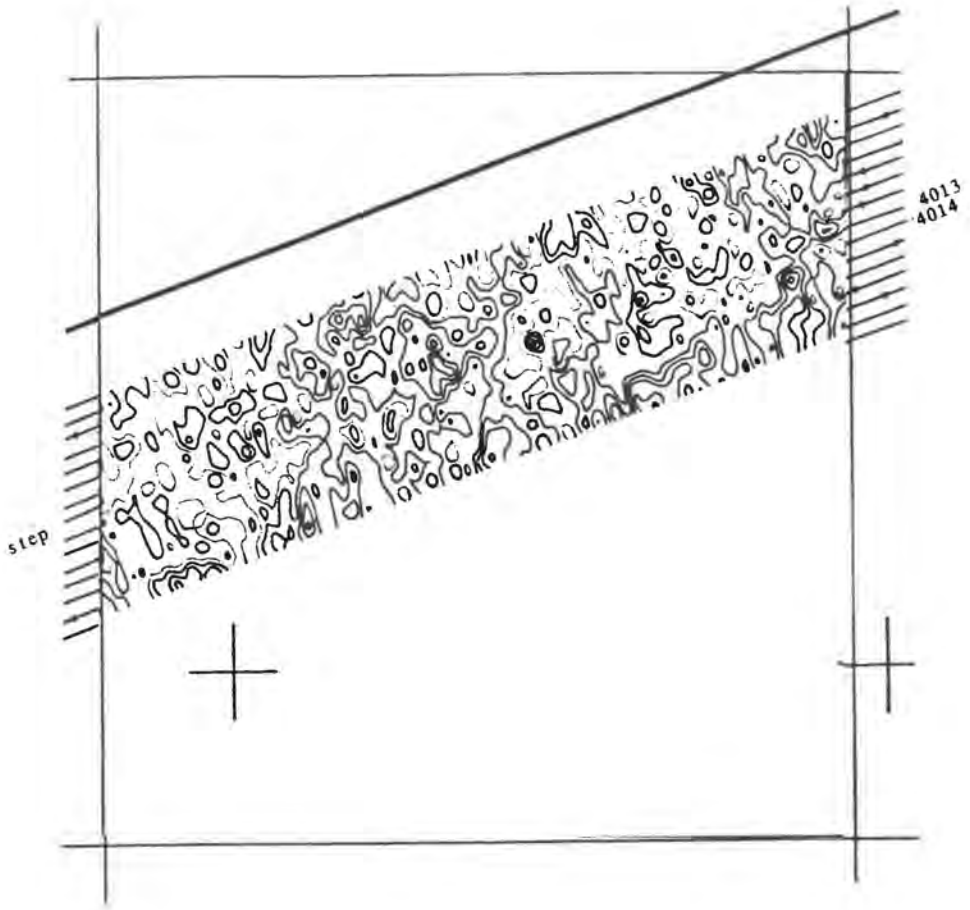

FIGURE 3.4

Part of the Raw Image for Uranium

Image of raw uranium counts after stripping but before image processing. Lines 4013, 4014 run along the middle. Interpolation has created a smoothing effect. Possibly the processing worker has invoked extra smoothing to suppress the step, but it is still evident. The flight line grid is superimposed, its 200 m spacing giving scale to the image. Same area as Figure 2.12 on page 49.

TABLE 3

Acquisition summary of some flight lines

The average sum of counts in the 609 keV peak above the average of the spectrum on either side is seen to show a distinct drop between lines 4013 and 4014. The gain shifts, here showing little change, are measured by comparing the counts on either side of the nominal position of the main thorium series peak at 2.67 MeV. The total count and the potassium, uranium and thorium counts are also shown averaged.

Log entry	Line No	Samples	Gain Shift	609 keV hump	N	K	U	Th
2nd June:								
4th file	4001.0W	1140	30.3	15.7	2387	205	61	90
5th file	4002.0E	1264	29.8	17.8	2411	200	64	91
6th file	4003.0W	1152	31.3	20.7	2408	199	65	92
7th file	4004.0E	1244	32.1	23.1	2489	203	68	95
8th file	4005.0W	1152	29.2	21.8	2300	186	64	88
9th file	4006.0E	1232	30.2	22.9	2334	188	65	89
10th file	4007.0W	1124	28.2	24.7	2282	184	64	86
11th file	4008.0E	1196	29.2	23.8	2281	181	65	87
12th file	4009.0W	1132	26.9	23.5	2220	171	64	85
13th file	4010.0E	1212	29.1	25.7	2240	174	64	86
14th file	4011.0W	1088	26.4	25.1	2146	164	63	83
15th file	4012.0E	1208	27.6	23.4	2174	169	63	84
16th file	4013.0W	1044	26.7	23.0	2180	171	62	84
5nd June:								
34th file	4014.0E	1176	23.6	15.2	1993	160	53	79
35th file	4015.0W	1080	25.9	15.0	2041	163	54	81
36th file	4016.0E	1180	28.3	15.9	2006	155	55	80
37th file	4017.0W	1064	25.0	15.1	2004	152	55	81

When the average spectra of the two lines are subtracted and smoothed, the result can be seen to be dominated by the uranium spectrum. Compare Figures 3.5 and 3.6 on pages 75 and 76, the spectrum of the difference, with Figure 3.7 on page 77, which is a smoothed uranium calibration spectrum. At the far left in Figure 3.4 on page 72 is a rising spectrum cut off near the 350 keV peak by the acquisition equipment. The major peak around channel 30 can be identified with the Bi-214 peak at 609 keV. Other details on the smoothed curve are readily matched with the positions of the main uranium series peaks, see Figure 2.4 on page 15. It is apparent that the spectrum of the difference between the two lines is dominated by the spectrum of the radon daughters.

It was concluded that the line 4013 has distinctly more "radon" signal than the adjacent line 4014. Accordingly, the pair of lines 4013 and 4014 was taken as the main reference data set.

3.7 The weather during acquisition

It is appropriate to seek a meteorological event which could have given rise to the apparent radon step. The flight logs for the two lines revealed that they were flown on two different dates several days apart, the higher signal appearing on the second and the lower signal appearing on the fifth of June, 1987. The times of the flights are unknown.

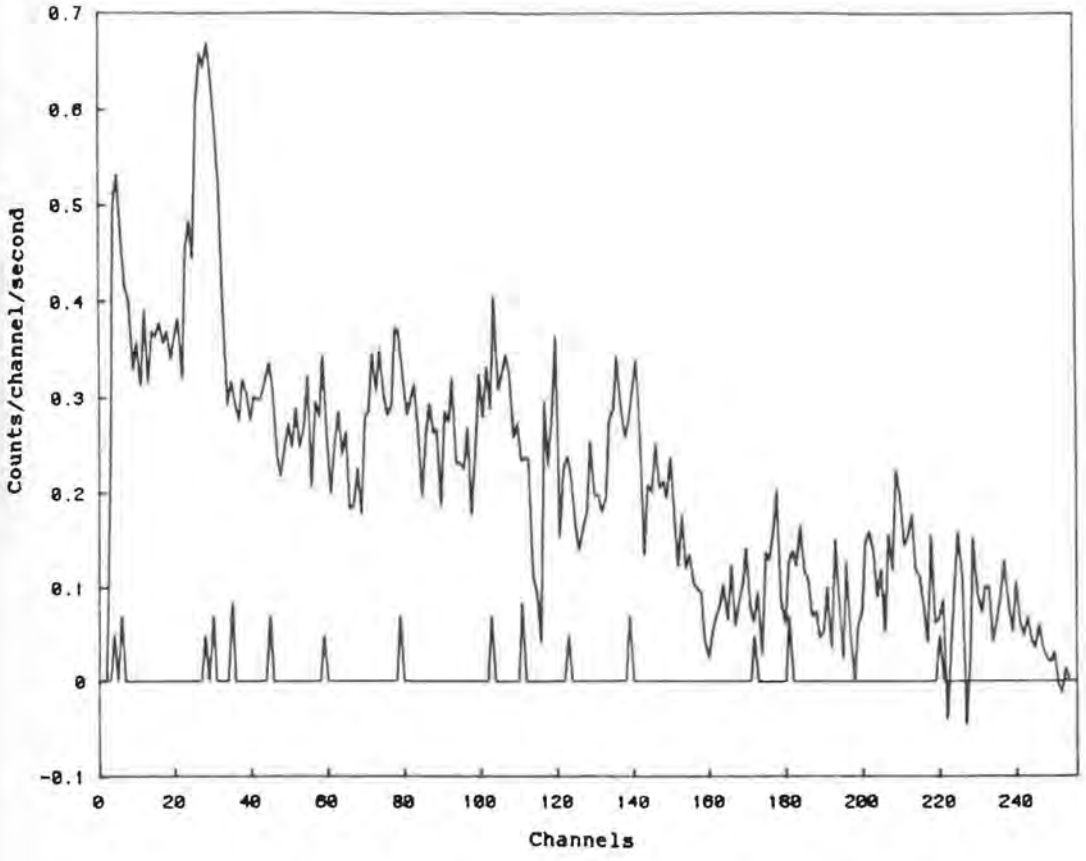

FIGURE 3.5

Difference between Mean Spectra of Lines 4013, 4014

These averages differ by only a few percent so the scaled up result includes much noise. The spikes on the horizontal axis identify the expected emission lines. Only the 609 keV emission from the uranium series is prominent before the smoothing, the result of which is shown in Figure 3.6 on page 76.

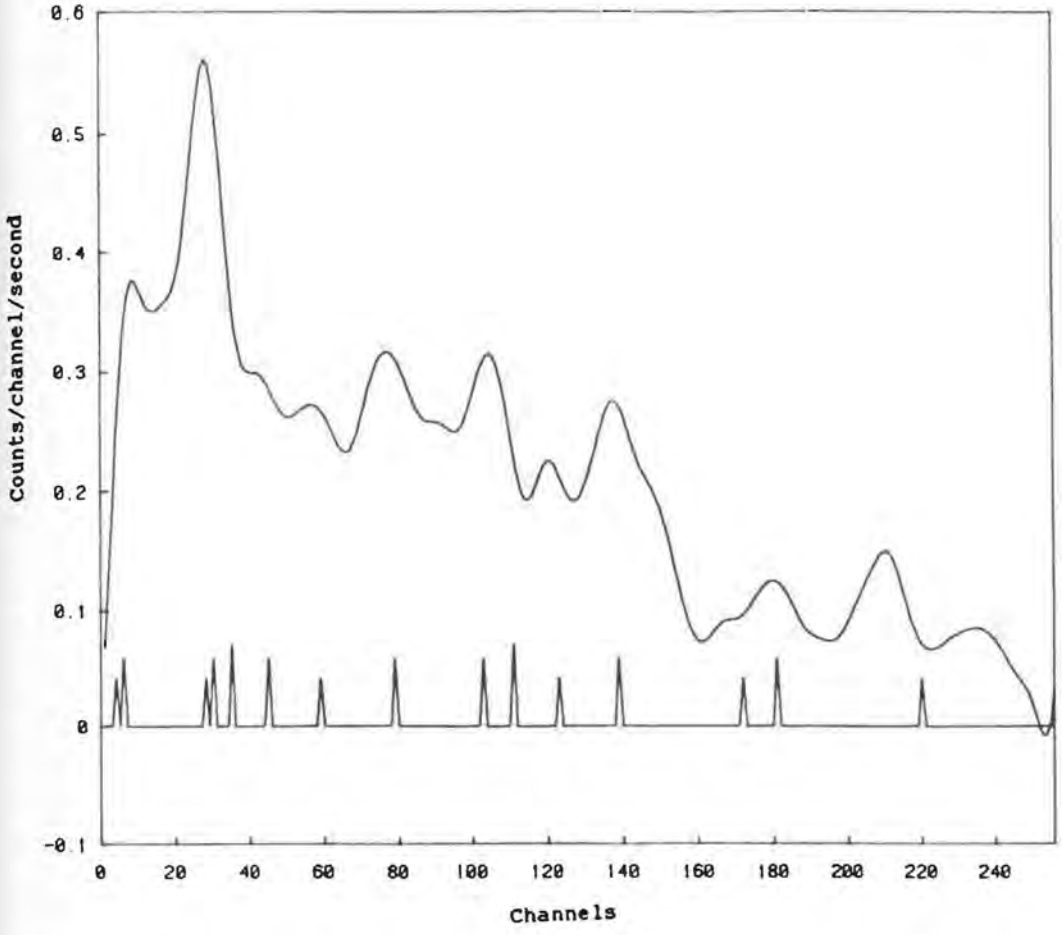

FIGURE 3.6

Smoothed Difference Spectrum

The differences between the channel counts for lines 4013 and 4014 are shown after smoothing with a Hanning function around 16 cycles per spectrum. The result resembles the uranium spectrum. Compare with Figure 3.7 on page 77.

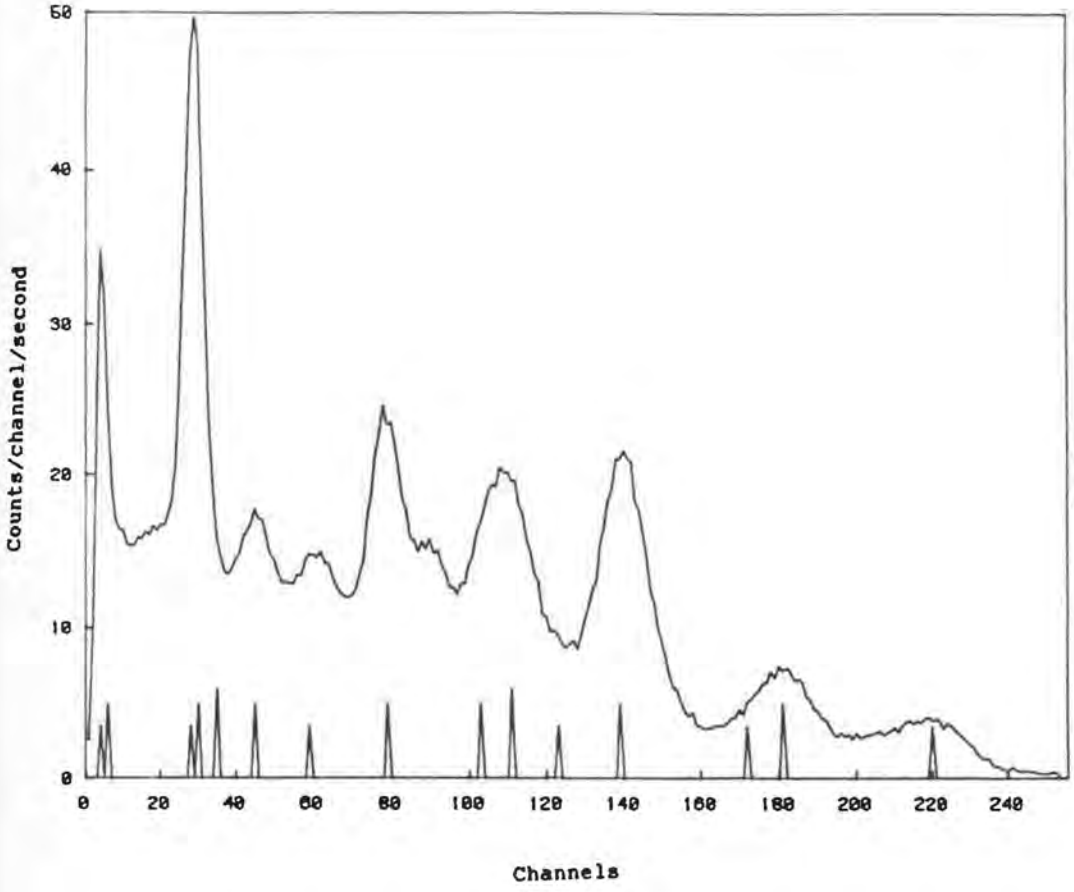

FIGURE 3.7

Uranium Field Calibration Spectrum, Smoothed

The average of a hundred seconds of field readings taken of the uranium calibration sample is shown after smoothing using a Hanning function around 32 cycles per spectrum. The background activity is still evident: the potassium peak and the thorium peaks are seen to intrude in an otherwise uranium dominated profile. Compare with Figure 3.6 on page 76.

The weather at ground level was uneventful in the period around 31 May to 5 June, 1987. The meteorological data for Charters Towers townsite are shown in Table 4 on page 79.

The daily distributed weather maps (The Age,1987) show that the pressure remained constant at 101.6 kPa. The soil gas could not have been displaced from the pores by a drop in atmospheric pressure, a mechanism favoured by some workers.

A temperature drop overnight indicates the growth of a night time inversion. With a clear night sky and an increase in relative humidity to 80% or so, this is strongly suggestive of heavy dew. Dew is likely to have occurred on the nights around 2nd June when line 4013 was collected, but not on the night of the 5th.

The winds at 900 m increased to 30 knots on the evening of the 4th June and persisted, together with an overcast sky. The night-time inversion layer necessary for the formation of dew is unlikely to have formed during that night, the night before the collection of line 4014.

Although the wind reading taken at 3 a.m. in the town suggests otherwise, it is quite likely that turbulent conditions persisted in the field through the morning of the 5th. Conditions would then have been conducive to dispersion of both moisture and radon; and the radon concentration at ground level must have been as low as that of the general air mass.

TABLE 4

Meteorological Data from 26 May to 10 June

The high radon line, 4013 was acquired on the 2nd, the low radon line, 4014, on the 5th. From the Bureau of Meteorology, Brisbane.

DATE	TIME	10M WIND	TEMP.	RELATIVE HUMIDITY	CLOUD	900M WIND
26 May	3 am	110/02	21	73	0	120/18
	9 am	110/02	23	61	0	120/12
	3 pm	VRB/01	29	43	0	230/06
27 May	3 am	VRB/01	18	83	0	170/06
	9 am	VRB/02	21	60	4	180/13
	3 pm	200/05	28	42	6	200/10
28 May	3 am	160/10	16	45	0	160/15
	9 am	150/17	17	39	0	140/20
	3 pm	150/13	23	23	0	165/15
29 May	3 am	140/05	12	44	0	150/15
	9 am	140/18	15	27	0	120/14
	3 pm	130/05	22	50	0	150/10
30 May	3 am	140/02	11	35	0	120/18
	9 am	140/05	14	28	0	100/16
	3 pm	140/05	25	34	0	140/13
31 May	3 am	130/02	11	71	0	120/22
	9 am	140/10	19	43	0	120/22
	3 pm	140/05	26	37	5	140/14
1 June	3 am	130/02	17	77	0	120/26
	9 am	140/05	18	88	8	110/31
	3 pm	140/12	23	61	8	120/26
2 June	3 am	130/02	17	77	0	120/22
	9 am	130/08	21	56	0	110/25
	3 pm	110/10	27	42	7	115/22
3 June	3 am	130/05	18	88	0	110/22
	9 am	120/10	21	69	0	110/23
	3 pm	110/08	27	42	8	115/15
4 June	3 am	110/02	19	83	4	130/08
	9 am	130/07	22	57	0	125/23
	3 pm	120/05	26	42	8	135/19
5 June	3 am	110/01	19	68	6	120/30
	9 am	130/12	20	64	8	115/33
	3 pm	130/10	25	47	8	125/28
6 June	3 am	110/03	19	60	0	120/33
	9 am	110/05	20	53	8	115/30
	3 pm	130/12	22	57	8	120/29
7 June	3 am	110/05	18	83	0	110/31
	9 am	110/12	19	73	8	110/34
	3 pm	100/10	25	50	4	125/29
8 June	3 am	090/01	19	73	6	115/25
	9 am	110/05	17	82	3	120/20
	3 pm	130/05	26	51	7	150/16
9 June	3 am	070/02	18	88	0	115/12
	9 am	130/06	22	60	0	115/18
	3 pm	130/05	28	42	3	165/12
10 June	3 am	090/02	17	88	0	130/26
	9 am	130/05	21	73	0	130/19
	3 pm	130/05	27	37	0	160/14

Darnley et al. (1968) had observed increases in the Bi-214 1.76 MeV counts with the formation of fog and inversion layers. Inversion layers are often associated with fog, mist and dew. It is possible that both their anomaly and the current step are caused by the mechanism -implicitly proposed by Grasty (1973)- of adsorption of radon daughters during the formation of precipitates. However if this was the mechanism, the radon must have been concentrated from a deeper (>200 m) thickness of inversion than the normal detection range of the equipment, which is already of the order of 100 m above and below the aircraft.

There was no precipitation measured at Charters Towers except for 0.2 mm on the 1st June. Since this town is some distance from the survey area, it is possible that a similar amount fell on 2 June after that day's flying without being recorded in the town. In line with the correlations from Clifford et al. (see Section 3.4, page 62) a prediction could have been made that the 0.2 mm precipitation indicates a 1% increase in the radon signal. Yet the figures of Table 2 (page 65) suggest a greater excursion than 1%. Those results of Clifford et al. (1981) were obtained in the winter of the mainland U.S.A., possibly not representative of the dry soil and erratic rain of the area of Charters Towers.

On the basis of the meteorological evidence, it appears that dew or rain brought radioactivity to the ground surface on the second of June 1987, but not on the fifth. The mechanism remains unknown, but it is clear that daughters of airborne radon cause most of the difference between the two lines.

Following these considerations, a working assumption was made; that

the difference between the radiometric data from lines 4013 and 4014 includes a significant contribution due to airborne radon arising from normal atmospheric events.

3.8 Noise

The half-million numbers or so of the data set refer to only 120 km of flight line. Part of that quantity is potentially useful information, part is repeated sensing of the same properties and part is useless noise.

Instrumental noise arises mainly from the gain shift, which alters the relationship between the energy of an incoming gamma ray and the channel number that the instrument allocates to it. From the perspective of quality control, the most likely contribution to gain shift is the drift in temperature of the crystal, which changes the yield rate of scintillation photons. Also the pre-amplifiers which boost the pulse from the photomultiplier are somewhat temperature sensitive. Some authors, including Dickson (1980), refer to gain shift as a drifting energy calibration, others call it gain drift.

Fluctuations in the channel counts are caused by the random variation about the mean count expected at that location for that channel. Such random noise is often suppressed using a simple moving average. This is equivalent to multiplying across a gate or range of N points in the data by 1/N and by zero outside of the gate. The location of the gate is moved repeatedly so that a data set of similar size to the original is obtained.

Detail in the data which is much less than N points across is suppressed, and the features much larger than N are relatively enhanced by the absence of the fine detail.

Since the latter is often dominated by noise, the effect is often a valuable suppression of noise. The use of stationary spectral windows suppresses noise in the same way.

The suppression is highly dependent on the wavelength of the detail concerned. This in turn depends on N. Passing a moving average through the data set is equivalent to convolving it with the gate of size N. Since a convolution of functions is equivalent to inverting the product of their Fourier transforms, it is appropriate to obtain these transforms.

The Fourier cosine transform of the gate of width N is the sync function (see for instance, Spiegel, 1974):

$$F(g(u)) = \int_0^N \cos(wu)/N \, du$$

$$= [\sin(Nu)/Nw]_{0,N}$$

$$= \sin(Nw)/Nw$$

The sync function declines monotonically from $w=0$ to $w=2\pi/N$.
This causes cyclic behaviour in the target data set to be filtered selectively. The average contribution and the slowest cycles are retained but the shorter wavelengths are increasingly suppressed until the Nth wavelength, which is eliminated. Still shorter wavelengths have some little effect, but a characterizing wavelength for this filter is that of the gate length.

A Fourier transform will allow a data set to be laid out in terms of its component wavelengths. Once a characteristic wavelength is recognized for some desired property, the appropriate gate can be chosen for the enhancement of that physical property.

More complex filters than a simple gate may also have characteristic lengths. Their selection can also be made by examining the Fourier transform of the target data. By working in the Fourier domain, the risk of a premature choice of filter can be averted.

The present intention to suppress noise requires some criterion for the noise level in the transform of the data set.

3.9 Synthesis of a Poisson noise set

The proportion of random noise to potentially useful signal in the data set can be estimated if an appropriate noise set is available for reference. For the purpose, a set consisting of Poisson noise was synthesized.

The mean spectrum of line 4013 was taken. Each channel mean in turn was used to calculate a set of 10 000 Poisson distributed counts, a random selection of which was assigned to that channel in 1024 synthetic readings.

The resulting set is equivalent to that obtained by the same aircraft flying at constant height in a constant atmosphere over uniform topography of constant concentrations. The readings differ from the mean spectrum by no more than the Poisson noise due to the

mean. They constitute a noise set. The high number of samples, 1024, was considered sufficient justification to call the noise set representative of the noise on the mean spectrum.

3.10 Two dimensional Fourier cosine transform

In this chapter, the term "spatial frequency" is used in the sense of meaning a number of cycles per line, and "spectral frequency" means a number of cycles per spectrum. Similarly, the "spatial wavelength" refers to a number of values per cycle.

The Fourier cosine transform was then taken for the synthetic noise set. Firstly, for each channel, the transform was taken along the line, returning a new set that contained the amplitude of the component harmonic frequencies, laid out in sequence. Then for each of these spatial frequencies, the cosine transform was taken across the channels, delivering the amplitudes of each of the harmonics along the spectrum.

The value at each point in the Fourier domain is the amplitude of the noise at that pair of frequencies. Along the zero of spatial frequency the transform includes the amplitudes due to the mean spectrum as well as its noise.

It may be expected that a direct Fourier transform be used here, as its squared amplitude is usually used to display the power of a signal, (see for instance Figure 3.8 on page 85) whereas the phase is preserved in a cosine transform and is of little interest in a

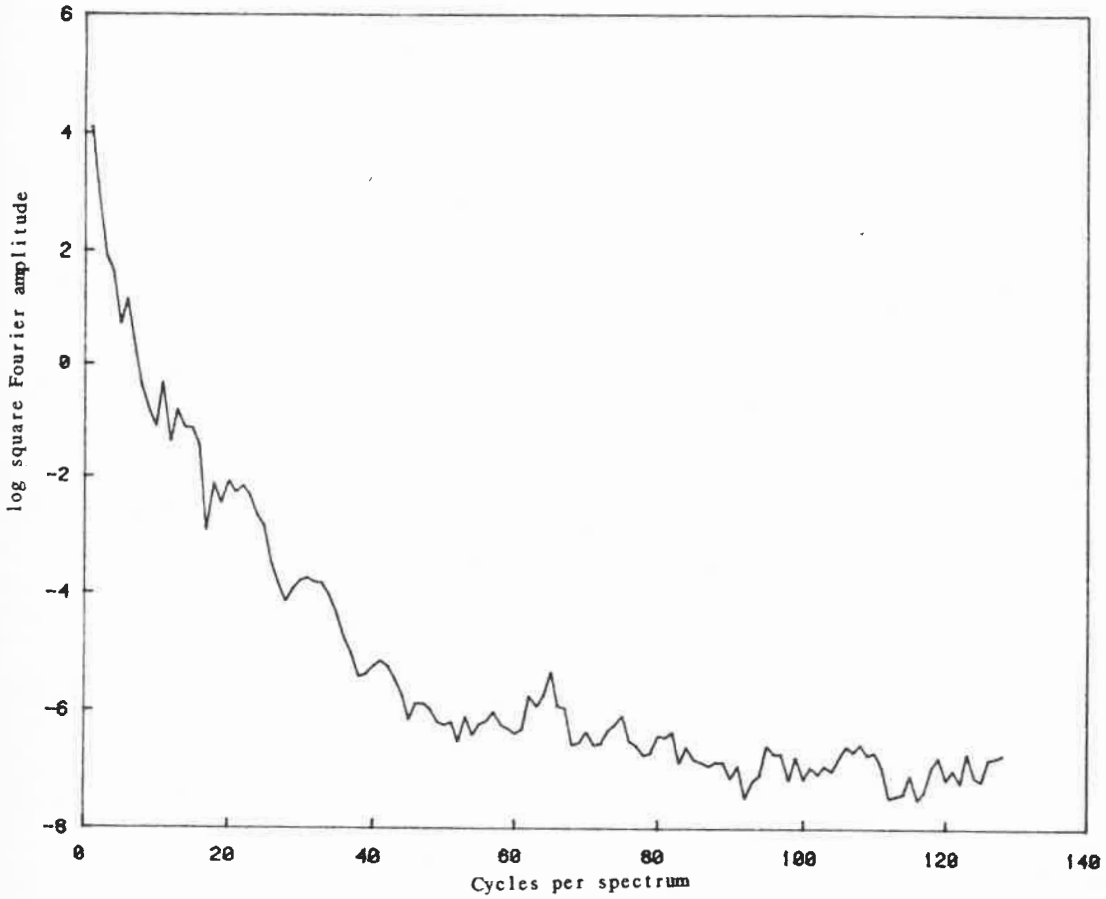

FIGURE 3.8

Power Spectrum of Mean of Line 4014

The scale is logarithmic to keep the noise and signal within the same diagram. Noise is low when the mean is taken over more than a thousand readings, as occurred here. Even so, it is clear that there is little hope of recovering signal from the general noise level above frequencies of 40 cycles per spectrum and higher.

comparison of signal strengths. However the phase is relevant to some of the arguments that follow, so the cosine transform is used instead.

3.11 Fourier interpolation of line 4013

The channel data of line 4013 were interpolated from 1044 samples to 1024 by padding with zeroes to 2048, then taking the Fourier transform, padding that with zeroes (see for instance, Bose, 1985) sixteenfold, reinverting to the sampling domain with the sixteenfold interpolation and resampling the 1024 data points.

Aliasing of the highest frequencies is expected in such a procedure. However, the characteristic wavelengths of the transfer function are of the order of the footprint size, several times the sample spacing at 60 m. Only the highest noise frequencies could be affected significantly, and only minor effect need be expected on the shortest of the ground signal wavelengths.

The two-dimensional Fourier cosine transform was then taken of the interpolated set for line 4013.

3.12 Estimation of the signal-to-noise ratios

The point-by-point ratios of the transforms of line 4013 and the synthetic noise set were taken. An image of the values is shown in Figure 3.9 on page 87. The complete transforms run across 1024

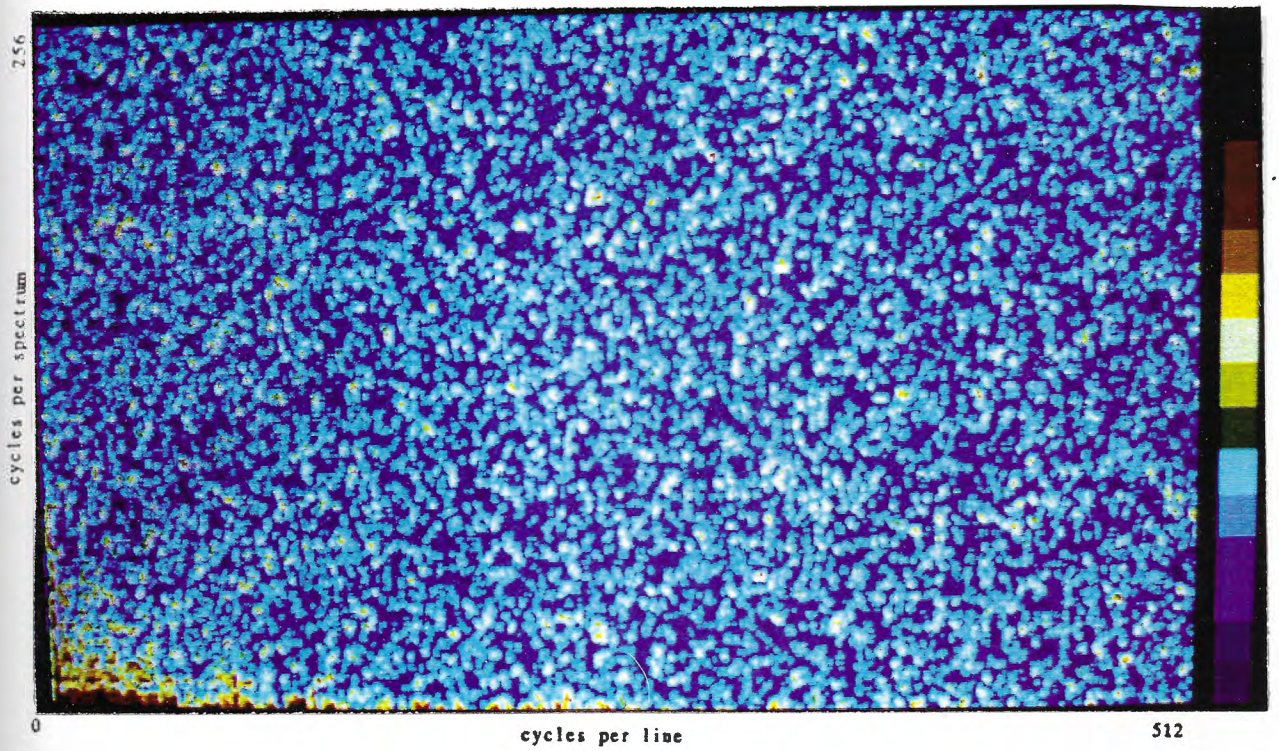

FIGURE 3.9

Signal-to-noise Ratios by Frequency for Line 4013

Smoothed image of the ratios of the two dimensional Fourier transforms, of the spectral data of line 4013 and of the synthetic noise set, taken point by point in the frequency domain. The zeroth spatial frequency is expected to contribute a bright line to the left hand side. Only 512 of the 1024 spatial frequencies are shown. The values in the image are shown logarithmically and are distinguished only between 2 and 200. See Figure 3.10, page 90.

spatial frequencies, twice the capacity of the image processor, so the Figure shows only the lower-frequencies of the ratio set.

The zero spatial frequency is the mean noise of the mean spectrum plus the mean spectrum itself, so the respective S/N values are absent from the diagram although they would be expected to contribute a bright line to the left hand edge, so enhancing a swallowtail appearance.

Insofar as the noise set approximates the Poisson noise of line 4013, the image may be presented as the ratio of total signal to random noise amplitudes, (S+N)/N, in frequency detail. The image of the ratios is itself noisy since the frequent, random low values in the noise set also cause spurious high ratios.

However, the noise set is not exactly the noise due to the counting errors of the observations along the flight line; it represents the counting errors taken in uniform conditions over uniform ground of the average concentration. In that the observations will differ by up to an order of magnitude or so from the average, and the Poisson noise goes as the square root of the expectation, the ratio (S+N)/N' will sometimes differ up to threefold from (S+N)/N.

Moreover, the ratio can only be significant over some two-dimensional range of frequencies. It follows that when the Figure shows a high density, the source data set has a high information content. Examination of the Figure allows a crude division to be drawn between areas of low and high signal content on line 4013. A high density area can be seen in Figure 3.9 on page 87 to trail along both the lowest spectral and spatial frequencies.

Categorizing Figure 3.9 on page 87, into high and low information-content areas separates the high information area as a rough swallowtail shape near the lowest frequencies in either direction, as shown in Figure 3.10 on page 90.

It is possible to use such a shape as a template criterion for retaining or rejecting the frequency data of lines such as 4013. Following zeroizing of the unwanted data, application of the inverse transformations will yield a cleaned data set with more than half the Poisson noise eliminated.

Selection of this rather arbitrary shape is difficult to justify, except in the qualitative terms above. If the information content or noise dropped to zero along some line, the choice would be unequivocal, but there is noise on either side of any realistic cut and potentially useful information, albeit diminishing in amplitude, is also discarded by any cut. It is appropriate to select a cut with the application of the data in mind, in effect making a further distinction between presently-useful information and elsewhere-useful information.

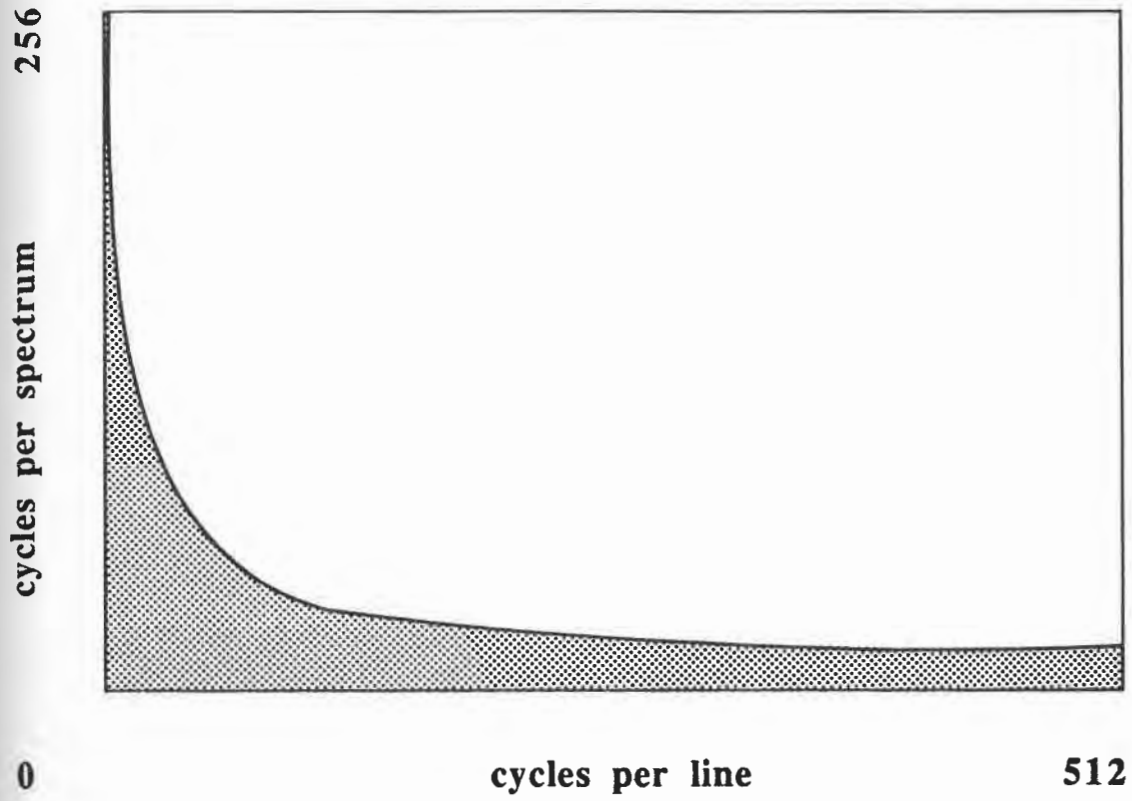

FIGURE 3.10

High Information Zone in Fourier Domain

Categorizing the signal-to-noise ratio for line 4013 separates the high information area as a rough swallowtail shape near the lowest frequencies in either dimension. The shape was inferred from a processed image, a print of which is seen in Figure 3.9 on page 87.

3.13 Smoothing functions

The high frequency end of a Fourier transform of a spectrum (see for example, Figure 3.8 on page 85) includes the amplitudes of many similar frequencies. Usually of little meaning, each frequency contributes an oscillation which is partly cancelled by the neighbouring frequencies. When a cut is made, the signal and noise left surviving near the cut will be seen to oscillate unbalanced by its missing counterparts from the other side of the cut.

This oscillation proved particularly troublesome in these data, and various gradual cuts were introduced to suppress the oscillation due to the cut. A ramp cut was tried but found ineffective.

A Hanning function (Bloomfield, 1975), or Hann, was found to be successful. This tapers the cut to a full-width cosine function. That is, the lowest frequency was multiplied by unity, and thereafter the multiplier dropped by the cosine of an increasing argument. The function used here was-

$$H(k) = \tfrac{1}{2} (1 - \cos(\pi\, k/M)) \qquad k=0,1..M$$

$$= 0 \qquad \text{elsewhere}$$

although Bloomfield (1975) used $k+\tfrac{1}{2}$ rather than k. The parameter k is the sequence number in the set being tapered and M/2 is the centre of the taper. The function is sketched in Figure 3.11 on page 92.

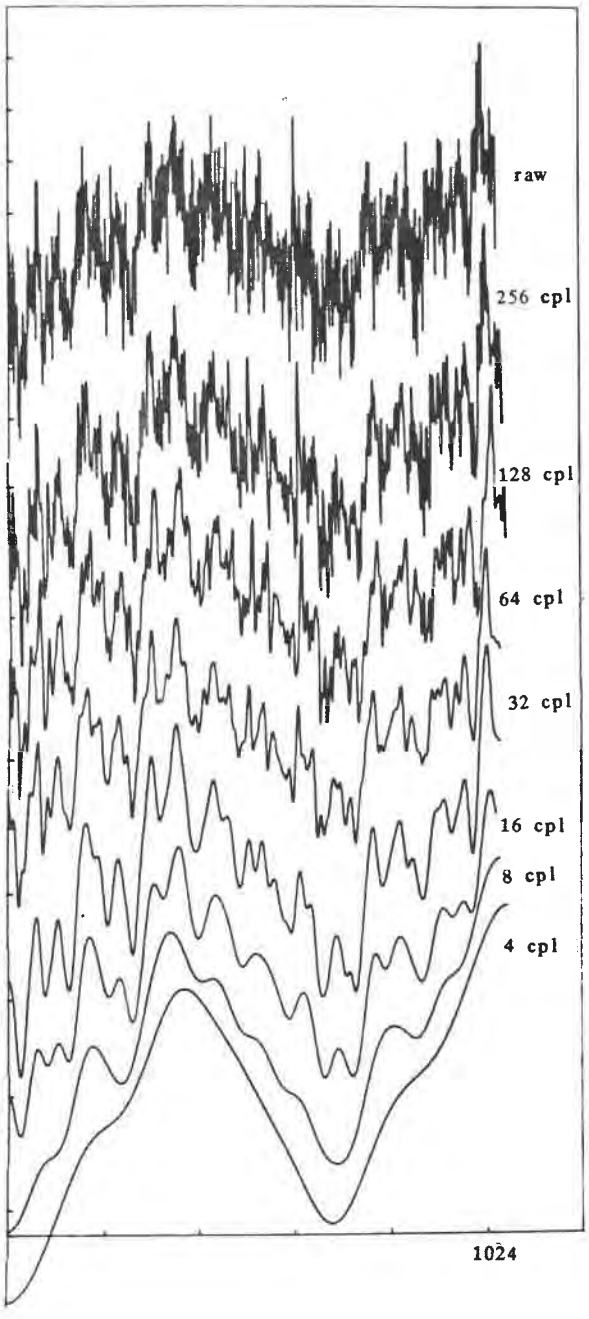

FIGURE 3.11

Smoothing by Hanning Function

The effect of Hanning functions applied in the Fourier domain with centres at 256, 128, 64, 32, 16, 8, 4 cycles per set of 1024 samples. The data set is the difference in the uranium window counts between the two lines, without height correction.

In subsequent text, the phrase, "Hanning function around a frequency of..." indicates that the multiplier had dropped to a half by the frequency quoted. There are an equal number (N/2) of non-zero frequencies remaining but these contribute diminishing value to the
In subsequent text, the phrase, "Hanning function around a frequency of..." indicates that the multiplier had dropped to a half by the frequency quoted. There are an equal number (N/2) of non-zero frequencies remaining but these contribute diminishing value to the result. If subsequent processing has procedures which require the order of N^2 operations, the Hanning function can be seen to be wasteful, consuming up to four (2^2) times the computing load required of a sharp cut data set.

When preparing a map of effective concentrations, all but the shortest of the spatial wavelengths are of high value, so most of the smoothing must occur in the spectral dimension. This implies working in the top section of the high information zone in Figure 3.10 on page 90. Hanns were applied successfully near this area, around 16 and 32 cycles per spectrum, during the deconvolution work. Compare Figures 3.5 and 3.6 on pages 75 and 76.

In radon studies, the shorter and even the medium spatial wavelengths are likely to be discarded and so spatial smoothing must be applied. Correspondingly less smoothing is needed in the spectral dimension for a similar amount of noise suppression, equivalent to working in the high information zone on the left of Figure 3.10, page 90.

The spatial average of a data set is represented fully in the Fourier domain by the lowest spatial frequency. In graphing of

means such as the average of line 4013 (Figure 2.9, page 27), high spectral resolution was achieved since averaging is equivalent to the most severe spatial smoothing. Such information is found along the left edge of Figure 3.10 on page 90.

Residuals of subtraction such as the difference between the lines (Figure 3.5, page 75), will inevitably have an increased noise content and need correspondingly severe smoothing. The result in Figure 3.6 on page 76, required a Hann around 16 cycles per spectrum.

A very wide range of spectral frequencies was needed for tapering to suppress the fine detail spectral oscillations. Although often the range required was found to be less, the range actually used was almost always a full-width Hanning function. Since the inclusion of these extra frequencies is most costly in computer time, and possibly costly of storage, it is recommended that subsequent workers construct more confident, economical tapering functions.

The Relationship between Radon and Altitude

The following Sections examine the spectral relationship between attenuation and radioactivity due to airborne radon. A re-examination of the height correction procedure is found necessary.

3.14 Attenuation coefficients

It is normal procedure to correct the uranium window data for height after correcting for radon (Wilkes, 1988). Some workers such as Darnley (1971) deprecate any height correction at all in noisy conditions. However, if the spectral expression of radon is to be extracted, the spectra must be well corrected for height, and beforehand, rather than subsequently.

The height dependence approximation of Godby et al. (1952) has the form,

$$\exp(-\mu\ h^2) \quad \text{or} \quad \exp(-\mu\ y)$$

Where h is the ground clearance, y is a function of h and μ is an appropriate attenuation coefficient for the window concerned.

The term above refers to a single window. The quantity μ is more generally a function of energy and height for each element. The multichannel equivalent of this approximate coefficient for the vicinity of height h_0 becomes:

$$\mu(E) = \{\ \mu_i\ \} \qquad \text{-for each radioelement}$$

So that the ith channel count $c_i(h)$ due to that element can be corrected to a nominal height h_0 thus:

$$c_i(h_0) = c_i(h)\ \exp(-\mu_i(h-h_0))$$

where h is the ground clearance, y is a function of h and μ_i is the appropriate attenuation coefficient for the channel concerned.

Such a set $\{\mu_i\}$ is only available in principle to correct each

element separately. In the first instance, the μ_i quantify the amount of absorption of the gamma rays from any source, but at all energies below the photopeaks there will also be corresponding reductions in the μ_i peculiar to each element, due to build-up of the photons that have been Compton scattered from each peak.

The differences between the elements' attenuation in each channel, $\mu_{i/K,U,Th}$ are due to the different positions of the peaks; the Compton spectrum below each peak is functionally common to each of the elements, but is nevertheless peculiar to the configuration of the acquisition equipment being used. If this Compton function could be determined for the installation, including any change with the position of the different peak being scattered, the counts could be migrated back up the spectrum to the positions from which they came. The separate $\mu_{i/K,U,Th}$ would not be needed- the counts could be multiplied by a common set $\{\mu_i\}$ as determined for the installation.

Conversely, if the amplitude of the Compton function could be obtained from each reading, the effective height could be obtained for each of the elements. Bailey (1986) effectively seeks the function as a second component spectrum, but must approximate the energy dependence to only two mass attenuation coefficients. Two coefficients are nevertheless an improvement over the one which would be implied by a simple extrapolation of the window method.

Neither the Compton function nor the effective attenuation coefficients $\{\mu_i\}$ are known a priori; the differences between units require separate height calibration.

3.15 Peculiarity of acquisition units

The Seigbahn curve shown in Figure 2.7 on page 21, appears to offer a standard set of attenuation coefficients, but it refers to attenuation out of a parallel beam. It does not include the reappearance of the Compton scattered photons further down the spectrum as collected by the airborne detectors. Having been deflected during the scattering, these photons arrive at the aircraft somewhat off vertical. Consequently upward- or lateral-sensitive detectors receive a softened beam, whereas a downward-looking detector sees a hardened spectrum.

The angular distribution of attenuating mass around each detector varies with the geometry peculiar to that aircraft and configuration. This angular sensitivity gives each installation a particular character which frustrates the application of universal correction. Calibration of the individual installations is necessary.

The calibration of a window installation includes a series of flights of increasing altitude (Wilkes, 1988). The changing counts in each window are treated as though the change were due to absorption alone. Yet they are not; the arrival of the Compton scattered photons in the lower energies gives rise to a discrepancy. The discrepancy is sometimes described, accurately, as being due to a change of the stripping ratios with height.

The change of shape of the spectrum due to the Compton scattered

photons has more severe implications for multichannel acquisition. Interpolation of each channel count between flights of significantly different altitudes is no longer appropriate. The flight paths must be within a few metres of each other vertically, that is, within the reasonable minimum flying variation of the survey, so that any distortion due to the Compton scattering is representative of normal effects.

The implied increase in demand for precision flying may be unattainable. Since in the first instance, only the rate of change with height is needed, it may be possible to obtain an approximate correction from a deliberate variation around nominal height, a requirement which is readily met. However the spill of one element's counts across the spectrum of another is still not accounted for.

Dickson et al. (1981) were able to calibrate for height using ground experiments with airport pads. This may be the most accurate height calibration procedure for multichannel systems.

3.16 The spectral form of the factors

A distinction is to be made between the spectra due to the airborne and ground sources, so it is important to obtain the spectrum of uranium in the ground as would be obtained by an aircraft flying at standard operating height. Another spectrum expressing the effect of a height variation - the height factor - is also sought.

The "airborne radon spectrum" is a spectrum of the radon daughters

at some arbitrary closeness to the detector and the "uranium spectrum" is a more attenuated version of the same emissions. As such, two reference spectra which span these two can be defined in terms of the physics of the attenuation, as has been done by Bailey (1986). Nevertheless, the reference spectra do not have to be physically based, but can be any pair which adequately expresses the differences due to height.

An appropriate method of obtaining the reference spectra is to apply controlled attenuation, and seek the spectrum which expresses the change due to increasing attenuation. Such a method is described by Dickson et al. (1981). It uses successively increasing numbers of plywood sheets inserted between source and detector and applies a covariance analysis. This provides the two reference spectra as uncorrelated (or orthogonal) spectra. These can now be used in linear combination to define the spectra for the two physical factors.

As the radioelements in the two sources of airborne radon and ground uranium are related, their spectra are particularly strongly correlated. Consequently the amplitude of the radon factor in the survey data will generally correlate with the amplitude of the uranium factor. The radon factor will be used in a procedure to suppress the stripes; the uranium factor will be applied subsequently and may use some of the same signal strength, so the correlation is inoffensive.

When convenient access to airport pads becomes convenient for Australian operators, the procedure of Dickson et al. (1981) should be applied, but with the added intention of obtaining spectral

resolution for the effect of airborne radon through the attenuation of the daughters in the pads. Radon in the air during these pad calibrations may give rise to spurious results and so must be minimized. It may be necessary to use a coastal airstrip and delay the activity to weather conditions which deliver an oceanic (i.e. radon-depleted) air mass to ground level.

At the lower energies which are being put to use for the radon factor, all three radioelements contribute to each channel. Dickson's procedure yields a height factor spectrum for uranium which is only independent of the uranium standard spectrum, and remains quite strongly correlated with the spectra of thorium and potassium.

The two uranium spectra obtained from the pads then could be combined to define the factors for ground uranium and airborne radon. These in turn could be fitted to the survey data after height correction and the stripping of the other two elements. The amplitudes resulting characterize the behaviour of the two factors across the survey, the map of the ground uranium amplitude being of particular interest. The sensitivity of the radon factor to the other elements remains so a map of the amplitude of the radon factor itself would have limited value.

3.17 The radon factor from the anomalous height

The work of Bailey (1986) and others treats the effect of airborne radon as an anomalous effective altitude in the uranium spectrum. Such methods require two spectra for each element to obtain the comparison between high and low effective altitudes.

The procedure of Dickson et al. (1981) allows for the preparation of a secondary spectrum that expresses the change of shape due to attenuation for each element. This spectrum is then to be added to the primary spectrum weighted by a function of the radar altitude. Dickson et al. model a simple exponential weight of the form

$$a(h) = A \exp(-\alpha h) + C$$

where A, α, and C are constants that differ for each of potassium, thorium and uranium. The height corrected spectra resulting are then fitted to the data to provide the effective count rates on the ground.

In principle, the secondary spectra could be fitted again to the data to extract the effective altitudes for each element (Dickson, 1980). In that capacity, the secondary spectra constitute height factors.

The extraction from the data of the amplitude of a potassium height factor is equivalent to obtaining a potassium effective height. Such a procedure using a uranium height factor would give a deviant result due to the airborne radon. This led Bailey (1986) to propose the estimation of radon as an anomalous effective height.

Dickson (1980) obtained effective altitudes in each of the elements including uranium, with particularly useful results in the potassium. However, he did need considerable length of flight line for moving averages to obtain these results. The choice of size of gate might more easily have been done by studying the characteristic wavelengths (see Section 3.8, page 85) in a Fourier transform of the spatial amplitude of the uranium height factor.

3.18 Proposal to establish a height correction

The pilot is normally under instructions to maintain a constant ground clearance, a requirement that cannot be completely met. There will always be some variation about the mean, if only because the pilot tends to respond partly to the currently known height discrepancy as well as the oncoming. This inevitable variation suggests a procedure for the extraction of a height correction from data taken during the survey.

Window data are height corrected using three attenuation coefficients, $\{\mu_j\}$; (j=K,U,Th), each being applied exponentially to the respective window count –

$$c_j(h_0) = c_j(h) \exp(\mu_j.(h-h_0)) \qquad (j=K,U,Th)$$

Multichannel height correction might be achieved using an approximate attenuation function $\mu(E)$ or $\{\mu_i\}$ such that the channel count rates at standard height $c_i(h_0)$ may be estimated from the acquired counts $c_i(h)$ and the indicated ground clearance h –

$$c_i(h_0) = c_i(h) \exp(\mu_i.(h-h_0)) \qquad (i=1,2,..N)$$

Such a function $\{\mu_i\}$ might be derived from the correlation $\{r_i\}$ of counts with ground clearance above flat ground in data taken under conditions representative of the survey data to be corrected. It would be dominated by a negative exponential sweeping up from the lower left rather like the estimates of Seigbahn (1965) of the attenuation coefficients for a parallel beam, Figure 2.7 on page 21.

In principle, there is further information contained in a randomization of the height against the distributions of the radioelements below the aircraft. Because the radioelement distributions are also varying separately during the test flight, the spectral height behaviour of each element should be separable – in principle. The possibility may be worth investigating if the above method yields a fair representation of the height behaviour of the average spectrum.

The proposed height sensitivity curve might be more pragmatically obtained when the clean air requirement is approximated by the arrival of a fresh maritime air mass in the survey area. Here a sufficiently long line above a road or watercourse and a regular porpoising of the aircraft a few metres around standard flying height, as sketched in Figure 3.12 on page 104, would allow the randomization of the geological pattern. In these circumstances the covariance must reflect the average variation of the spectral signal with relative ground clearance.

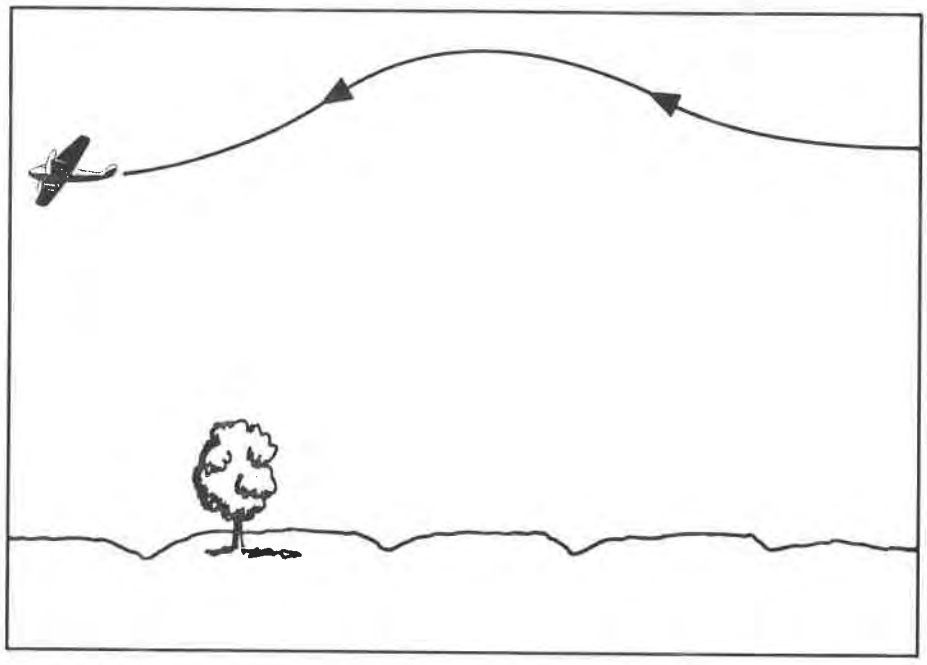

FIGURE 3.12

Accumulation of a Multichannel Height Correction

With suitable choice of ground of low relief, a flight path with a height variation greater than the relief can accumulate the covariance of height and multichannel signal.

It is proposed that a height correction data set be obtained by the procedure described here. From this set a crude mean attenuation function may be derived. Since the procedure takes account of the height dependence and reception characteristics peculiar to the system, it readily presents an option for height calibration.

3.19 Summary

The behaviour and atmospheric distribution of radon have been examined. A likely mechanism to explain its erratic emergence has been brought forward.

A step in radon concentration in a survey has been isolated as a data set for reference. The associated meteorology has been discussed and the likelihood of radon effects differing between the lines has been estimated.

A significant problem has been identified in the correction for height or effective attenuation. A correction function and its calibration has also been proposed.

CHAPTER IV

SOME POSSIBLE APPROACHES TO RADON CORRECTION

4.1 Introduction - Avenues of approach

Multichannel acquisition of a survey area provides a data set which has two spatial and 256 spectral dimensions. Each dimension allows the data to vary independently, and so represents an extra degree of freedom for any variable to be expressed. The implied dimensionality of the data is so high that direct reduction to the element concentrations is not considered. Instead the data are reduced in stages.

The approaches divide into spectral and spatial methods. As the spectral methods divide into window and multichannel, the spatial methods divide into along-line and cross-line.

Window methods are simple in that they refer to a few numbers at each point in the survey yet they are limited because they have so few degrees of freedom. The multichannel data have many degrees of freedom. There are correspondingly many approaches, only some of which are practical. Most of these cannot be applied to the window data at all.

Fourier analysis of the spectrum forms the basis of many spectral techniques which cannot be applied to window data. Principal

component analysis too, is more suited to the multichannel data. The mathematics is standard. Such techniques reduce the dimensionality of the data: once the data are reduced to a few values at each point along a line, the line itself can be processed.

Across-line methods address the steps in the data, including those caused by airborne radon. Hence the data along each line are compressed in some way, so that in each analysis each line is reduced to a few values. If one value is obtained then each line may be represented as a point on a profiled cross-section of the line data.

When the data are assembled in two-dimensional form, standard image processing techniques come into use. Only here can the radon processing become fully two-dimensional.

This chapter provides an overview of the spatial and spectral techniques. A change of processing sequence and a new data form are proposed. Later chapters expand on selected spectral methods.

Spatial Approaches

In the previous chapter the radon effects are shown to be closely related to uranium height effects. When a Fourier transform of the spatial extent is taken, some sort of height correction must have already been performed. In the following Sections, the correction is presumed to have been made beforehand.

4.2 Regression of line means

One published spatial method which is useful when the radon effects are uniformly distributed is that of Green (1987).

He took the regressions of the flight line means of a survey of 150 m nominal flying height. (The reader is referred to the original for the mathematics used.) In his model, he attributed the average deviations of the uranium window counts from the other elements to a background in those counts which stayed constant as each line was flown and shifted between the flight lines. The residuals were then subtracted from the lines, successfully removing the stripes from the image. The survey used appears to have had predominantly uniform radon.

The technique is an image processing technique in that an improvement in the visual quality is achieved. However some customers for the data may be concerned that the zero for uranium has been shifted across the map by the taking of a residual. Such a customer might be reassured by the intervention of a processing operator making an experienced choice of zero from the U:Th and U:K cross-plots.

The data Green (1987) used were restricted to the three element estimations, which he effectively converted to a basis of the ratios of the mean uranium to the other elements. When multichannel data are available, a quantity should be constructed for the ratios' numerator which is less sensitive to the effects of airborne radon than the uranium window count.

If he had taken a profile across the survey with this chosen quantity, a similar baseline could be inferred by the operator, with the residual for each line used for radon correction.

4.3 Comparison of spatial wavelengths

Green's approximation of constancy in the lithology across the lines and constancy of radon along the lines might similarly be made when addressing the first terms in a two-dimensional Fourier series taken over the two spatial dimensions of the data.

When the radon appears in pockets of air it has short spatial wavelengths, and is even more transient than the uniform radon. The correlations between the radioelements expected in the intermediate wavelengths of the lithology are likely to persist to some degree in the shorter wavelengths. Where the assumption can be made that the radon has little correlation with the lithology on the shortest scales, Green's method might be applied to the shorter wavelengths in the line data: the amplitude of a short wavelength component in the uranium may be reduced in proportion to the residual of a longer wavelength. An added danger, beyond the creation of spurious lows as in Green's method as presented, is the creation of spurious highs when the component waves are adjusted.

Smoothing to suppress the short wavelengths is routinely done with a travelling filter before contouring. If the smoothing is done using a Fourier transform the amplitudes of the spatial harmonics are readily derived as a by-product.

The output of this process might be made a display for each element

of line number versus spatial wavelength. It is likely to be flat at the longest wavelengths, with along-line ridges or islands extending into the higher wavelengths. It may be useful to the processing operator to examine the amplitude of those short wavelengths, to compare them with those of the neighbouring lines. When an amplitude shows a jump between lines or between flights, the opportunity arises for the operator to introduce a human judgement, with skill based on experience, of how much of that amplitude was due to transient radon effects and how much to ground uranium. The occasion may arise when the amplitudes between lines are too noisy and the operator decides to remove most of the short wavelength component. Although smoother than desired, the remaining information is presented cleanly.

Spectral Approaches

A semi-quantitative method of finding the whereabouts of the airborne radon is introduced in Sections 4.4 and 4.5. All the spectral techniques reported in the remainder of the Chapter use the reduced attenuation due to the emitters being airborne or exposed above the soil.

4.4 Interpreter's tool from the covariance with height

In terrain where the elevations change faster than the aircraft changes its altitude, there will be a negative covariance between the ground clearance and the sources in the high ground (see Figure

in the high ground (see Figure 4.1 on page 112). Correspondingly there can be a positive covariance between ground clearance and signal from sources in low ground if the clearance increases when the aircraft passes over that low ground.

Randomly distributed sources in the ground surface will give a negative correlation function rather like the Seigbahn (1965) curve of Figure 2.7 on page 21. This would be a smooth exponential curve if the attenuation were simply absorption, but Compton scattering builds up the count in some channels at the same time as it decreases the counts in others, putting ripples on the curve. These curves must differ somewhat between the elements as each ripple reflects the presence of a characteristic emission higher up the spectrum.

The covariance shows much more detail than the correlation and reflects the spectrum of the source being tracked. (See Figure 4.1 on page 112.) The familiar shapes allow identification of the elements concerned in their apparent proportions and the sign of their contribution to the covariance.

Figures 4.1 and 4.2 on pages 112 and 113 show the covariance of ground clearance against counts versus channel number along lines 4013 and 4014 respectively. The positive potassium is interpreted as implying that most of the potassium is low-lying in a relationship with the relief like that of claypans. Comparison with the map of the potassium window concentrations in Figure 4.3 on page 114 shows that the potassium is occurring in a floodway, a length of low ground. The negative amplitude of the uranium and thorium spectral

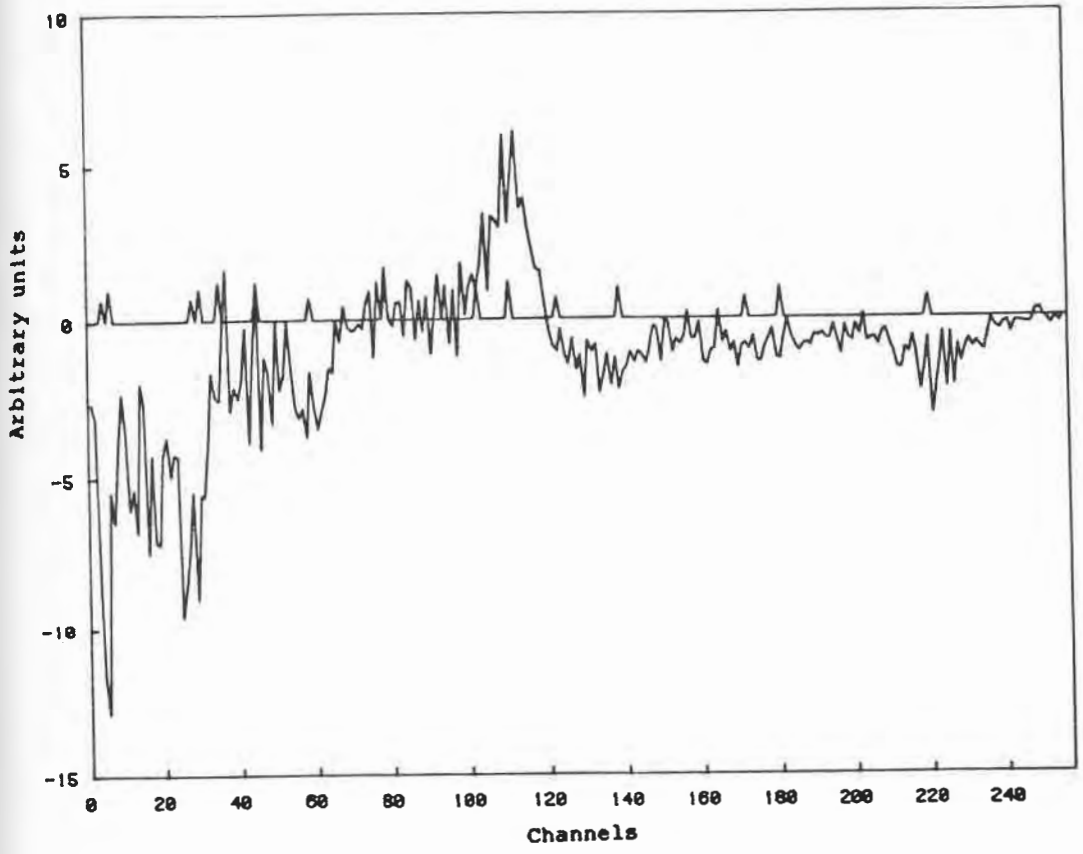

FIGURE 4.1

Spectral covariance with ground clearance, line 4013

In terrain where the elevations change faster than the aircraft changes its altitude, there will be a negative covariance between the ground clearance and the sources in the high ground and a positive covariance between ground clearance and signal from sources in low ground. Uniformly active ground gives an intermediate negative covariance. Note the spectral shapes of the radioelements are still apparent.

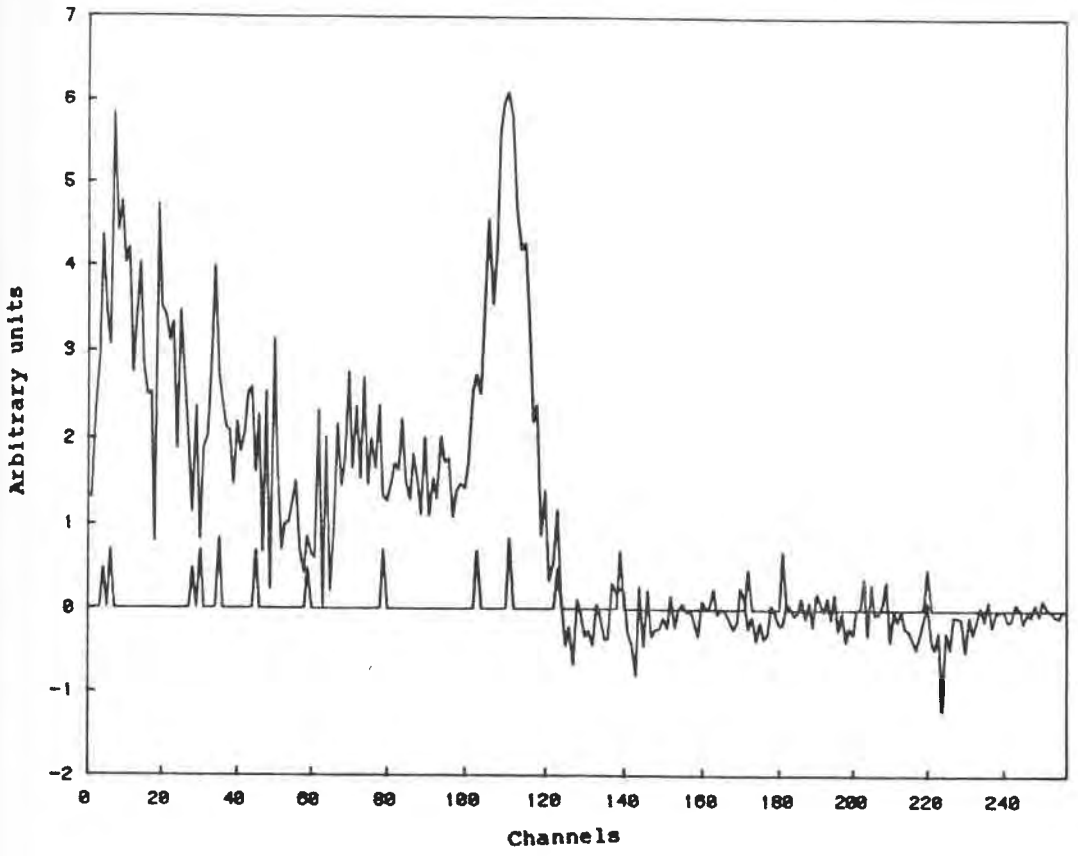

FIGURE 4.2

Spectral covariance with ground clearance, line 4014

The covariance of each channel count against the radar height is shown graphed against the channel number. The uranium spectrum has made a distinctly different contribution compared to the covariance on Figure 4.1 on page 112, and now appears to originate mainly from the lower ground, as though there has been a reduction in the atmospheric radon.

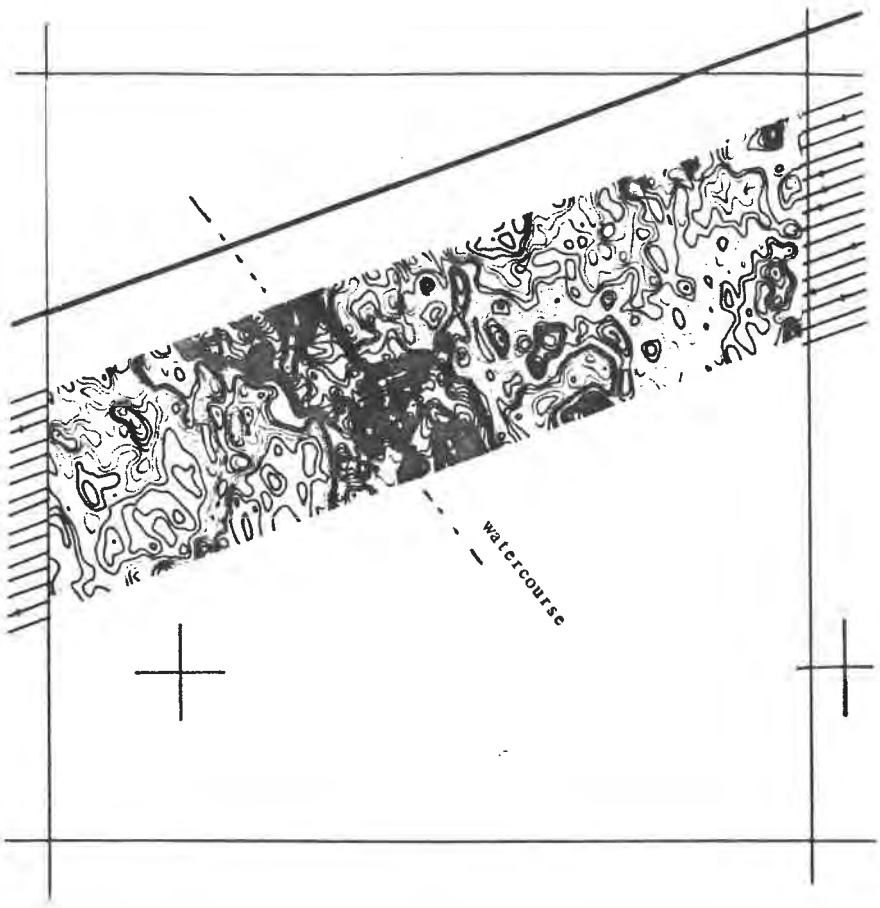

FIGURE 4.3

Part of the raw image for potassium

The same area is shown as in Figure 3.4 on page 72. Here the potassium estimate is shown. Further image processing would be performed before commercial release, but most of the corrections have been made already.

profiles on Figure 4.1 on page 112 indicates that the occurrence of thorium or total radon may be either biased toward the high ground or spread over ground of relief less than that of the aircraft's line of flight.

There is a further possibility in the case of the total radon. Ground-hugging layers of radon-containing air may be lifting off the steeper slopes associated with the higher ground.

This interpretation finds some confirmation in the height covariance of the adjacent line, which is believed to be lower in radon, see Figure 4.2 on page 113. In this Figure the low-energy contribution of the total radon is seen to be positive. This signal can be attributed to a uranium distribution which tends to the low ground. If this is the case, the difference between the two Figures is readily attributed to the presence of airborne radon.

The weak covariance near channel 140, in the conventional uranium window around 1.76 MeV, may indicate that the behaviour here is still airborne, since the normally highly attenuated low-energy channels have a strong covariance. This too indicates that the signal is due to nearby, airborne radon.

The height covariance forms an interpreter's tool for the whereabouts of radon. In Figure 4.1 on page 112, the low energy (where all sources contribute) covariance on line 4014 is seen to be positive despite a negative thorium covariance in the high energy thorium channels near channel 220. The positive low energy covariance can then attributed to uranium being low lying. This distribution has been observed by Butt Horwitz and Mann (1977), but

the point of interest there was the formation of calcretes rather than the occasional presence of radon.

However on the other, high-radon line 4013, the negative covariance of the low energies indicates a signal from the uranium series to be distinctly "nearby". It is reasonable to attribute the difference to the products of airborne radon.

The covariance with the ground clearance has been used in these calculations rather than the true terrain altitude, because the barometric heights of the aircraft were not available in the data. Normally readily obtained from the barometric and radar altitude channels of these instruments, the true height allows for more direct inferences to be made about the covariance relationships between the terrain and the radiometric signal.

These covariance plots will be found useful by interpreters for confirming terrain related distributions. Further study may reveal other properties that may tracked using these plots.

4.5 Interpreter's tool from the correlation with height

The correlation of radar altitude against the channels of lines 4013 and 4014 is shown in Figures 4.4 and 4.5 on pages 117 and 118. Where the ground contains the only sources of radiation and the radar altitude measures only minor variations around a mean height above the ground, these curves should approximate the proportionate rate of change of signal strength with height above the ground.

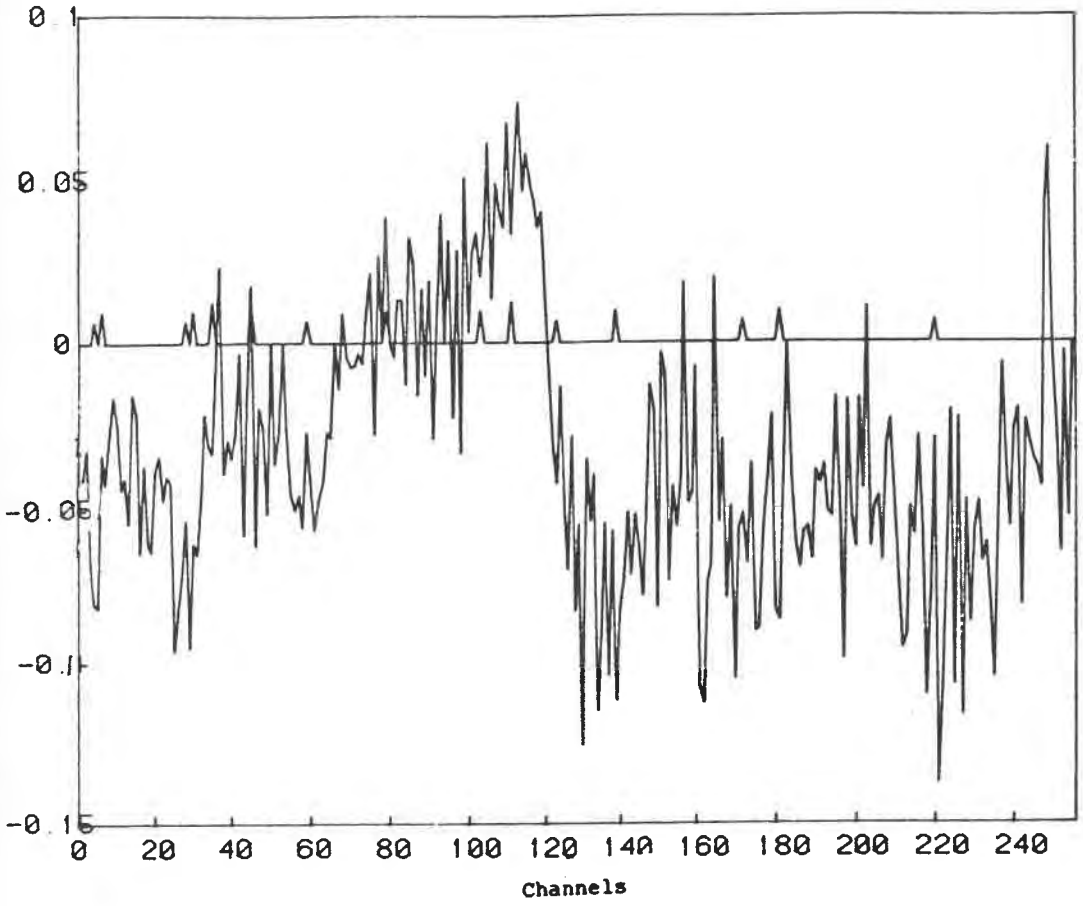

FIGURE 4.4

Correlation with ground clearance, line 4013

Compare with Figure 4.5 on page 118.

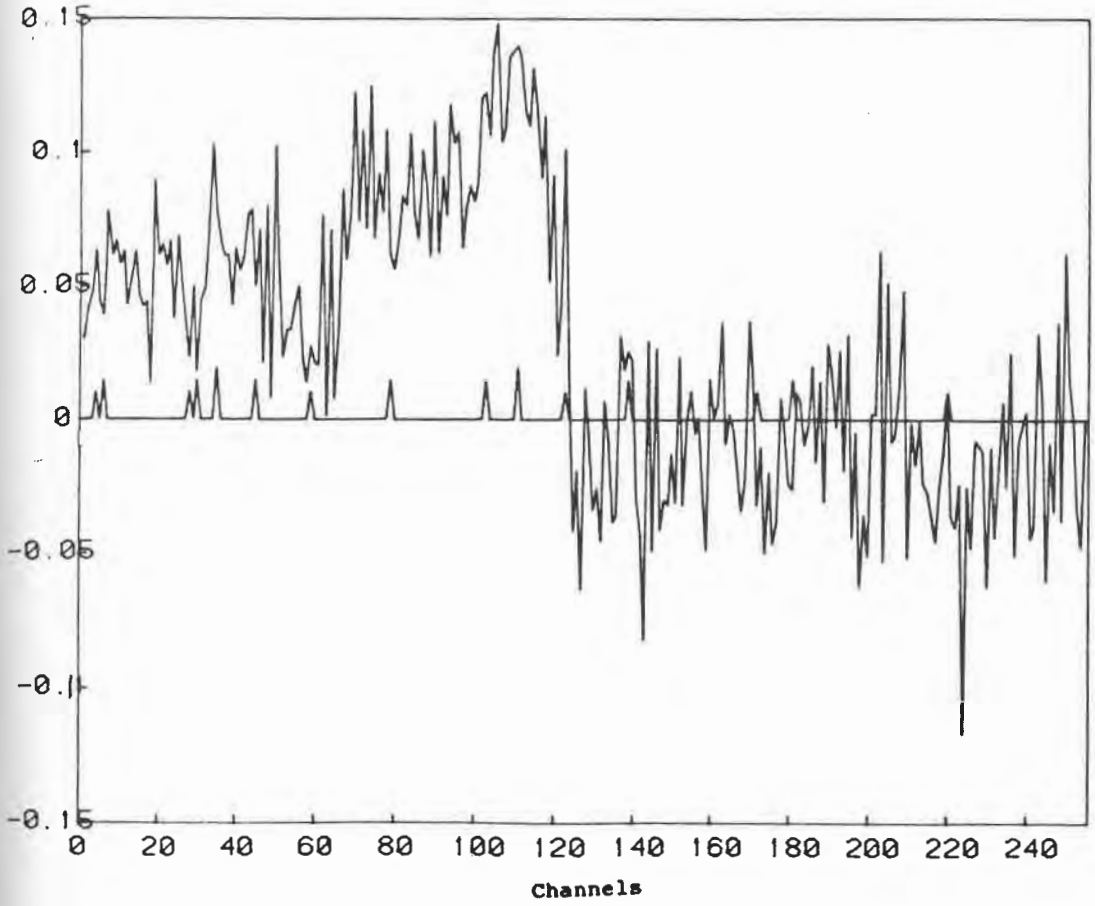

FIGURE 4.5

Correlation with ground clearance, line 4014

Compare with Figure 4.4 on page 117.

Without the knowledge of the correlation of uniform ground with arbitrary ground clearance, an interpreter would have to sketch in a line based on his experience. The curves shown in the Figures 4.4 and 4.5 are noisy, but the shapes of the three spectra are recognizable, reflecting systematic correlations of the radioelement distributions with the ground clearance. Interpretation may then give the correlation of the lithology with the topography.

Since the correlation of uniform ground is definitely negative yet the potassium covariance is seen to go positive on Figures 4.1 and 4.2, it is clear that the potassium is distributed remotely from the aircraft rather than uniformly. Such a distribution would be shown by sources following the hollow or low-lying ground such as claypans or saltpans.

The two lines were flown by different pilots on different days, which may explain the different values of the potassium and thorium correlations and covariances between the lines. Once the interpreter has become familiar with the effects of the flying styles and with the positions of the curves of the correlations expected of uniform ground, more confident statements about topographic distributions can be made.

4.6 Use of Pb-214 peak as quantifier

A window was sought that was more sensitive to airborne radon than to uranium. This discrimination can be achieved by making use of the higher attenuation at low energies.

The 352 keV peak has been studied by Grasty (1982b) with spectral

data corrected for local background using three channels on either side to establish a local background. These channels are shown on Figure 4.6 on page 121. Grasty flew a sufficient length of line, some kilometres, to obtain enough counts to reliably collect the spectrum on either side of the peak. The use of the adjacent spectrum to some extent removes the effect of the ground emitters, but some interference must be caused by the sharp thorium peak (see Figure 2.5 on page 16) also near 350 keV.

An attempt was made to deconvolve the peaks along the spectrum with the intention of sharpening the peaks until they no longer overlapped, and then of comparing the amplitudes of the 352 keV peak thus isolated with other sharpened peaks of the uranium series. The approach was found unsatisfactory partly because the peak, being approximately proportional to its energy, was much sharper than the other uranium peaks with several times the energy of the 352 keV peak.

In the data set used in this study, spurious variation around the 352 keV energy was encountered during deconvolution studies. Later this variation was found to be due to the low energy cut-off of the acquisition equipment drifting across the low channels. The investigation was eventually abandoned. The cut-off is visible at the far left of Figure 2.9 on page 27.

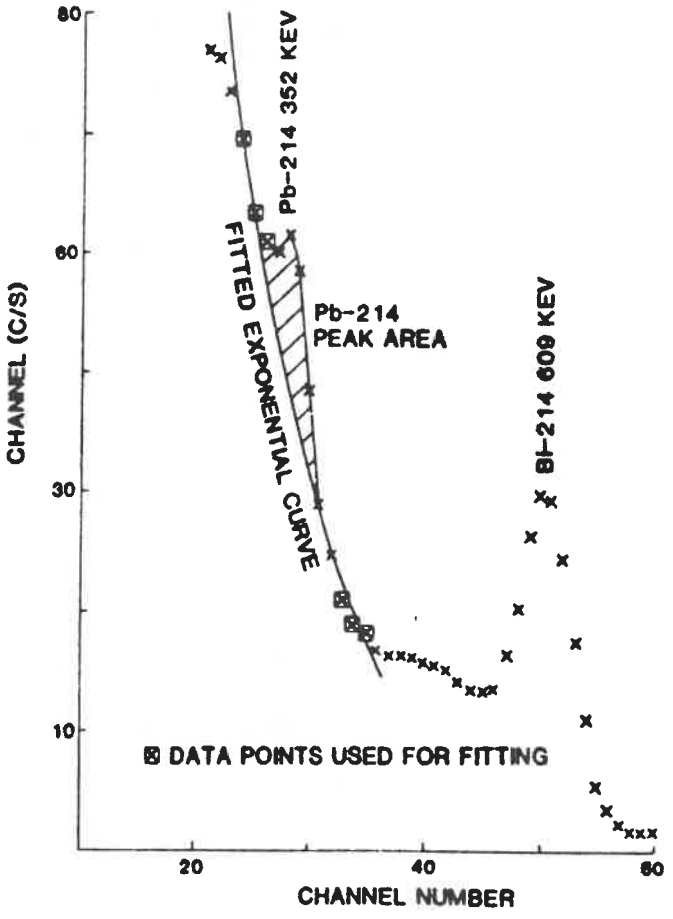

FIGURE 4.6

Low energy uranium peaks

The uranium series peaks at 352 keV due to Pb-214 and at 609 keV due to Bi-214 are shown. The exponential fit for isolating the Pb-214 counts used by Grasty (1982b) is also visible. After Grasty (1982b).

Clearly any possibility that this part of the spectrum will ever be used in the future of a survey data set requires the field worker to ensure a level of quality control which is appropriate to the possible uses rather than the currently planned uses.

4.7 Window at 609 keV

For the establishment of a low energy window, the peak at 609 keV offers an advantage over the 352 keV peak in that it receives considerably fewer of the twice-scattered secondary photons from the higher-energy peaks.

Bailey (1986) estimates that a scattering typically halves the energy of a photon, so that the 609 keV vicinity includes some twice-scattered signal from the thorium peak at 2.67 MeV, but relatively little of the much stronger potassium peak at 1.46 MeV. The vicinity of 352 keV receives both.

Both areas, however, are obscured by the once-scattered photons from all three radioelements. The 609 keV energy has a thorium peak close by, too close for exclusion, so that peak must be stripped out as well. The other contributions requiring calibration and stripping are the broad spectrum gamma rays from the Compton scattering of thorium and potassium, and also the photons associated with their beta decays. (See Figure 4.7 on page 123.) In the sense that ground uranium is independent from airborne radon, so also does the contribution from ground uranium at the operating altitude need separate calibration so it can be stripped out.

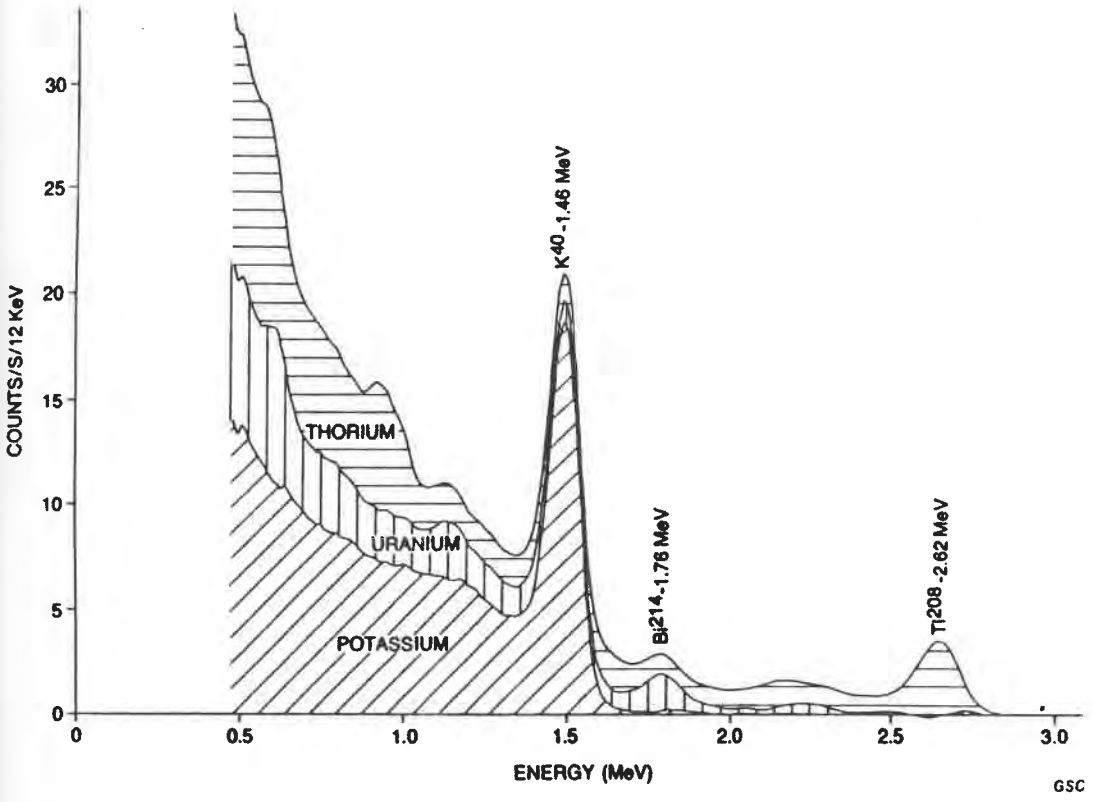

FIGURE 4.7

Composite spectrum

The relative contributions to the gamma-ray spectrum due to typical crustal material, as estimated by Grasty et al. (1985). From Grasty et al. (1985).

The sensitivity matrix for a four-window method is estimated from procedures appropriately adapted from the calibration procedures outlined in Section 2.13. Its inverse has 16 (4^2) elements, or stripping ratios. The matrix of the conventional three-window method has only nine elements, several of them zero. The extra row and column will add several non-zero elements since potassium, thorium and ground uranium all add signal to the new window.

Whereas the most accurate stripping can reduce the expected contributions of the ground concentrations it cannot remove the contribution due to their spectral noise. However, the high count rate of the exposed Bi-214 at 609 keV reduces the relative contribution of this form of noise. This peak is seen to stand above the noise in Figure 3.5 on page 75, the difference between the mean spectra of the two lines 4013 and 4014. It is clear that the signal is swamped by noise everywhere except in the vicinity of 609 keV.

Moreover the interest in the radon effects is usually on a longer scale than the detail in the lithology. Advantage can then be taken of the reduction of statistical noise on the longer spatial wavelengths (see Section 3.12) in the inferred radon estimate.

Grasty et al. (1985) had rejected the 609 keV peak as an aid to determining uranium in airborne surveys due primarily to the overlapping peak of cesium-137 at 662 keV which had been found to be so prominent in the Canadian studies as to invalidate the use of the line. Their argument refers primarily to North America where much of the nuclear weapon testing occurred.

During the scanning of the flight line means of the survey data used here, little evidence of this cesium peak was seen, however the small hump near 662 keV on Figure 3.6 on page 76 invites scrutiny. The British nuclear weapon tests did contaminate some of the Australian inland (Connor, 1984) but we do not know how far this or other fallout remains distributed.

For that reason, a special monitoring routine would be required as part of the regular field quality control. This routine would require specifying an appropriately long count for the background, long enough for the convergence of the counts in the vicinity of the cesium peak. Clearly the discovery that an area or period has cesium contamination would dictate resorting to other processing methods, an option available only with multichannel acquisition.

4.8 Fourier domain processing

The lowest spectral frequencies (1 to 4 cycles/spectrum) have only a modest relationship with the photopeak shape, but nevertheless were found to correlate well: they contain significant amounts of signal from the three radio-elements. This effect appears to be due to the Compton scattering spreading the emissions across the spectra.

At the same time the signal-to-noise ratio is relatively high at these low frequencies. (See for instance,Figure 3.9 on page 87.) On this basis, the Fourier cosine coefficients of the readings in line 4013 were taken, and satisfactory correlation with the radioelement estimates were obtained at the lowest frequencies. (See Table 5.)

TABLE 5

Correlation of Spectral Cycles with the Elements

Tabulated here are the correlations of the Fourier cosine coefficients against the element concentrations obtained by the conventional window method. Half-cycles per spectrum appear because of the use of the cosine transform, chosen to avoid problems with the phase drifts common in spectral data. The similarity between the results for the two lines is some reassurance of the repeatability of the correlations.

	Line 4013			Line 4014		
Freq.	K	U	Th	K	U	Th
0.0	0.890	0.497	0.766	0.889	0.442	0.790
0.5	0.948	0.457	0.609	0.944	0.415	0.637
1.0	-0.695	-0.193	0.184	-0.606	-0.124	0.243
1.5	-0.944	-0.178	-0.310	-0.934	-0.106	-0.339
2.0	0.680	0.436	0.150	0.667	0.425	0.163
2.5	0.963	0.273	0.591	0.963	0.222	0.624
3.0	-0.439	-0.435	-0.812	-0.441	-0.401	-0.803
3.5	-0.926	-0.166	-0.193	-0.911	-0.113	-0.202
4.0	-0.714	-0.178	-0.670	-0.723	-0.089	-0.686
4.5	0.938	0.253	0.592	0.930	0.188	0.639
5.0	0.825	0.062	0.222	0.816	0.033	0.228
5.5	-0.900	-0.179	-0.485	-0.904	-0.139	-0.511
6.0	-0.929	-0.299	-0.409	-0.928	-0.224	-0.431
6.5	0.177	-0.292	-0.438	0.144	-0.338	-0.420
7.0	0.931	0.295	0.496	0.925	0.231	0.553
7.5	-0.039	-0.001	-0.366	-0.098	0.045	-0.412
8.0	-0.902	-0.271	-0.342	-0.896	-0.217	-0.385
8.5	-0.758	-0.327	-0.385	-0.742	-0.248	-0.435
9.0	0.790	0.323	0.484	0.777	0.257	0.463
9.5	0.814	0.349	0.424	0.814	0.297	0.482

Only the first 20 coefficients are shown correlated in Table 5 on page 126 although the full set of 256 Fourier cosine coefficients is required to completely describe the readings. Most of the higher coefficients have trivial correlation values. That is, they add little information compared to their noise, so it is of interest to see how many of these components can be discarded along with their shares of the noise.

If there is sufficient linear independence between the lowest Fourier coefficients, as few as three coefficients may be sufficient to estimate the concentrations of the three elements. At least one more is needed to estimate radon. Linear independence may be inferred in Table 5 where the correlations are distinctly different between the elements. It is apparent that there is a redundancy of choice of frequencies.

The possibility of using a reduced data subset is particularly attractive because of its convenience in acquisition. The unit may collect 256 channels per reading, take a Fourier transform -in flight- in a dedicated chip such as are currently available, and only have to store a selected few numbers.

Alternatively, the redundancy might be used to obtain a linear combination with improved significance. This possibility was pursued successfully to obtain greatly improved "principal components". These results are reported in the following Chapter.

The project did not allow time to fully investigate the subset proposition. There is interest in obtaining improved subsets of the spectrum: Grasty et al. (1985) tested the convergence of the

International Atomic Energy Authority's (1976) subset of possible windows with a well-controlled multichannel data set. It is recommended that a similar study be undertaken to select the subset frequencies which best describe the useful information.

4.9 Reduction of dimensionality

Two representations of the data are the channel counts and the Fourier coefficients. The counts or coefficients are the independent variables for the information content. When there are more independent variables in the data than physical properties to be estimated, it is appropriate to seek a smaller set of linear combinations of the variables. The chosen combinations must show good linear independence amongst themselves to best span the variation in the data.

Since there is always some statistical noise associated with each degree of freedom, it is spread across the independent variables and is partly left behind in this reduction of dimensionality. Dickson (1980) found he could reduce the 256 channels to 50 without loss of information. Presumably there were signal losses, but they were offset by the truncation of noise.

Grasty et al. (1985) recommended discarding a fourth low energy uranium window to improve the estimation of the three radioelements. In order to allow the extraction of other factors, particularly the effective altitudes, the same group recommended ten windows as a desirable, powerful minimum. Inevitably, they would have had to prejudge the nature and value of the unknowns that their choice no

longer spans.

One way to delimit the physically realizable dimensions while spanning the maximum physical possibilities is by matching the resolution of the detector, which cannot resolve detail finer than the gaussian characteristic of the NaI crystal. In this division the excluded detail is known not to contain useful information.

Successive tests in the current work showed that the signal of individual readings could be satisfactorily reconstructed using 32 cycles per spectrum. Higher terms showed higher noise than signal content. In the line means, some detail was lost at this truncation, but the value of this information is not as great as that in the individual readings. There will always be some remnant of signal accessible to meticulous extraction, but its retention will always be under question in environments of commercial production.

In order to maintain a maximum span of physically significant variables, it is proposed that any reduction consist of taking the early Fourier cosine coefficients, perhaps the first 64.

4.10 Statistical methods of reduction

Any physical quantity which can be expressed as a spectrum defines a functional expression or "factor" among the observables, the channels. The inner product of this function with the reading provides an amplitude to the physical quantity.

The subspace spanned by the factors of interest can be determined by factor analysis. This area of applied mathematics is described by texts such as Joreskog et al. (1976).

In general, these factors are not orthogonal. A purely statistical method, principal component analysis (see Appendix A) does provide orthogonal functions which are linear combinations of the observables which best describe the variation in the data.

These functions, principal components, or PCs, are mathematically independent and so there are only as many PCs as there are dimensions in the data. Preferably, the data provide more dimensions than there are factors of interest.

Thus a four-window data set can provide four PCs so that a subspace of three lithological degrees of freedom can be approximately spanned by three of them, leaving the remaining PC to express all the minor factors put together. The presence of these minor factors is likely to inhibit the extraction of a fourth factor such as the radon.

Further study may show that such a procedure can be successfully applied to the ten windows of Grasty et al. (1985) to yield the subspaces of the lithological factors, the height factors and possibly a radon factor. Biasing may be necessary.

In Chapter V, the 256-channel data set will be manipulated with principal components and Fourier cosine coefficients. Chapter VI includes an attempt at obtaining a radon factor.

4.11 Summary

Various methods of data reduction and radon suppression have been discussed. An emphasis has been placed on techniques using Fourier analysis. Methods of achieving savings in computing time and acquisition costs have been proposed, including in-flight processing to reduce the volume of data.

CHAPTER V

PRINCIPAL COMPONENTS ANALYSIS

5.1 Introduction

Multichannel processing is simplified by giving the all the channel counts equal status as variables. This can be achieved by defining a vector space in which each independent degree of freedom is represented by an orthogonal vector. In this chapter each reading is treated as a single point or vector in a 256 dimensional vector space. The terminology is not necessary to the mathematics of the treatment but it aids visualization and description.

A set of readings is then a collection of points in this vector space. Principal components analysis allows the behaviour of this collection to be characterized in terms of a set of orthogonal principal components of decreasing significance. An immediately valuable result is the isolation of significant behaviour into a subspace defined by the first few principal components.

Factors, which in this thesis are the spectral evidence of some physically identifiable cause, are also vectors in this space and so can be characterized in terms of the principal components. This must include any radon factor.

5.2 Linear dependence in the data

Potassium, uranium and thorium are physically independent quantities as radionuclides and as chemical elements. However it is found that their distributions are well correlated in igneous rocks (Serra, 1984, p129-131) and to a certain extent in the sedimentary rocks (Adams and Weaver, 1958). It is probably on the first grounds that the three are explicitly separated in modern radiometric work. The radiometric maps then mimic geochemical soil maps, and are consequently the starting point for the interpreter to infer the lithology.

To arrive at that form, the data have been rather harshly processed. In the process of separating the element estimates from the correlated data, the noise associated with each prints the behaviour of one element onto the estimate of the next. Over and above the geological correlation between the elements which is already present, there is a spurious correlation due to that noise.

The calibrations used for the transformation are also prone to statistical noise and systematic drifts. The extrapolation of the attenuation relationships during calibration to acquisition conditions introduces further spurious correlations.

These effects may be partly avoided by seeking combinations of the element concentrations which will be less correlated than the element concentrations themselves. These combinations are quantifiable and are similar to the quantities studied in geological factor analysis, a field led by Joreskog et al.(1976). Moreover, it

can be shown that there will always be a set of linear combinations of the element concentrations which are completely uncorrelated. These do not require calibrations at all, but may be sought directly from the data, by principal components analysis. This technique, often abbreviated as "PCA", is described in texts such as Chatfield and Collins (1980) and has been applied in the current work.

5.3 Spectral vector spaces

It is appropriate to summarize the mathematical model used in PCA as applied to radiometric data reduction by workers such as Dickson (1980) or Grasty et al. (1985).

The application of the stripping ratios to the cleaned window data described in Chapters II and IV is equivalent to a matrix inversion applied to a set of simultaneous equations. The equations express the contributions of each of the three elements to each of the three windows. This relationship closely resembles that of three vectors to their basis vectors.

Consider the three independent window count rates as independent vectors. In vectors terms, their independence is expressed as orthogonality. The three vectors span the vector space of all readings which consist of three window counts. Any vector in that space can be described by some linear combination of the base vectors, and any reading of the windows will be a vector in this space.

The reading can be equivalently considered as a three dimensional

vector or as a three point spectrum. A pure radioelement's spectrum gives a vector whose components are the stripping ratios for that element, so the three elements are represented by three vectors inclined together in the positive sector. The elements' counts can also be considered as independent variables so they also can span the space of the readings. The matrix inversion transforms the space, so that the counts of each element appear as the components of the (vector) reading on the new basis vectors.

It is reasonable to assume that the concentration of each element is proportional to the counts. As long as the spectral contributions of the elements in range of the detector remain constant in shape but vary in amplitude, the inversion remains effective, and the concentrations of the radioelements can be extracted cleanly from the data.

However there is random variation in the shape of the spectra. Statistical uncertainty is inevitable, both in the survey readings and the calibration readings used in defining the stripping ratios for the inversion. Consider that this noise is apportioned according the amplitude of each of the element concentrations. Then the component of the reading which is due to the element contains a noise part which is not expressed by the stripping ratios used for the inversion. When that reading is inverted, the noise will be partly delivered into each of the other element estimates. Consequently the variation of one element estimate will be printed through into the others.

Moreover, as the elements are frequently correlated in the lithology, so they have a true dependence on each other. If one

varies, so also are the others likely to vary at the same time. The separation of variation implied by the matrix inversion is greater than the reality it is modelling, the geochemical variation of the lithology. For these reasons it can be argued that the inversion is an excessive operation, causing more damage than necessary.

The vector space description can be extended to the multichannel data, and the inversion now becomes restrictive, condensing the data from 256 or so dimensions into the three (Crossley and Reid, 1982) dimensional space with the element concentrations being delivered as before as the amplitudes of the orthogonal base vectors. However, this condensation may not be necessary if a means of description in the original vector space can be constructed.

5.4 Principal components analysis

Each window or multichannel reading is a set of numbers, forming a vector, so a survey data set then forms a cloud of vectors with the same origin, all falling in the positive sector. Insofar as each count approximates a normally distributed variable, the tips of the vectors form an ellipsoidal distribution in this space. The approximation is discussed by Dickson (1980).

The mean of the data set falls close to the centre of symmetry, and those readings with a variance near unity are described by vectors falling on a (hyper-) ellipsoidal shell with the mean at its centre and one extremity near the origin. The more correct Poisson description would have the extremity at the origin since the mean

equals variance, but the approximation to the normal distribution is used in this work.

The principal axes of such an ellipsoid are all orthogonal. Each is also a vector; and as a set of counts represents the spectrum of a physically definable quantity. Since the vectors are orthogonal, so also are these quantities uncorrelated. Since the shape of the ellipsoid describes the behaviour of the counts, these quantities span the vector space. Thus these new basis vectors can be used to completely describe the data with independent amplitudes. They are known as the principal components.

The extraction requires assembling the covariance matrix and a diagonalization then provides the principal components as eigenvectors. (See for instance, Chatfield and Collins, 1980, or Campbell and Atchley, 1981.) In some biological literature it is called "empirical orthogonal analysis" (Dong-ping and Walsh, 1976).

These new, principal axes point in the directions of maximum variance. The principal components express the data in the most concise expression of uncorrelated variance. The variance of each principal component is the maximum possible after removal of the previous principal component. Conventionally, the principal components are numbered in order of decreasing variance.

The random noise is approximately equally distributed across the different directions in the vector space. Accordingly it tends to appear equally across the principal components ("PCs") whereas the lithological variance has been separated into the first few PCs. This amounts to a separation of signal from noise, especially when

there are many dimensions and as many PCs for the noise to spread over.

A three window data set is not particularly amenable to principal component analysis. The first two have value, but they can only express two degrees of freedom when the interpreter is likely to be requiring three. The third PC must contain all the remaining variance of window data, with all the minor contributions including the weakest lithological variation. It is likely to include much of the radon signal together with much of the ground uranium signal.

An immediate advantage is presented by multichannel data, for the noise can now be divided across the 256 degrees of freedom, of which only the most significant need be retained. Further, other variations in the data than the three elements find expression in the spare degrees of freedom and can in principle be extracted.

Dickson (1980) did perform multichannel principal component analyses on a set of calibration data, obtaining two components of value for height correction and a third which showed the gain shift. Duval (1977) applied factor analysis to a survey with window data. It would appear that nobody has published a successfully applied principal component analysis of multichannel survey data. This application of PCA is achieved later in this chapter.

5.5 Truncation of noise by smoothing

The channel covariance matrix of an arbitrarily chosen test line, 2608, is represented in Figure 5.1 on page 140. The variance appears faintly as a diagonal fin up to two orders of magnitude higher than the covariance, indicating a high proportion of random noise. The variance is more visible as the diagonal on the covariance matrix of the Fourier cosine components, in Figure 5.2 on page 141.

Following the signal-to-noise studies reported earlier it was concluded that the shortest spectral wavelengths are dominated by noise and can be discarded. The fine detail across the covariance field (seen as salt-and-pepper noise in the covariance matrix in Figure 5.1 on page 140) was taken to be predominantly due to Poisson noise and was accordingly smoothed from the covariance matrix with a Hanning function around 32 cycles per spectrum in the Fourier domain.

Whereas a meaning can be assigned for the smoothing of a reading or spectrum, a mathematical justification could not be obtained for the smoothing of a covariance matrix. This procedure will be seen to have worked, so it may be that a legitimation can theoretically be found. A legitimated procedure was later found (reported in Section 5.9, page 148) which produced superior results.

Because some variance has been truncated away, the variances of the PCs are quoted on the axes of the figures in percentages of the total remaining variance.

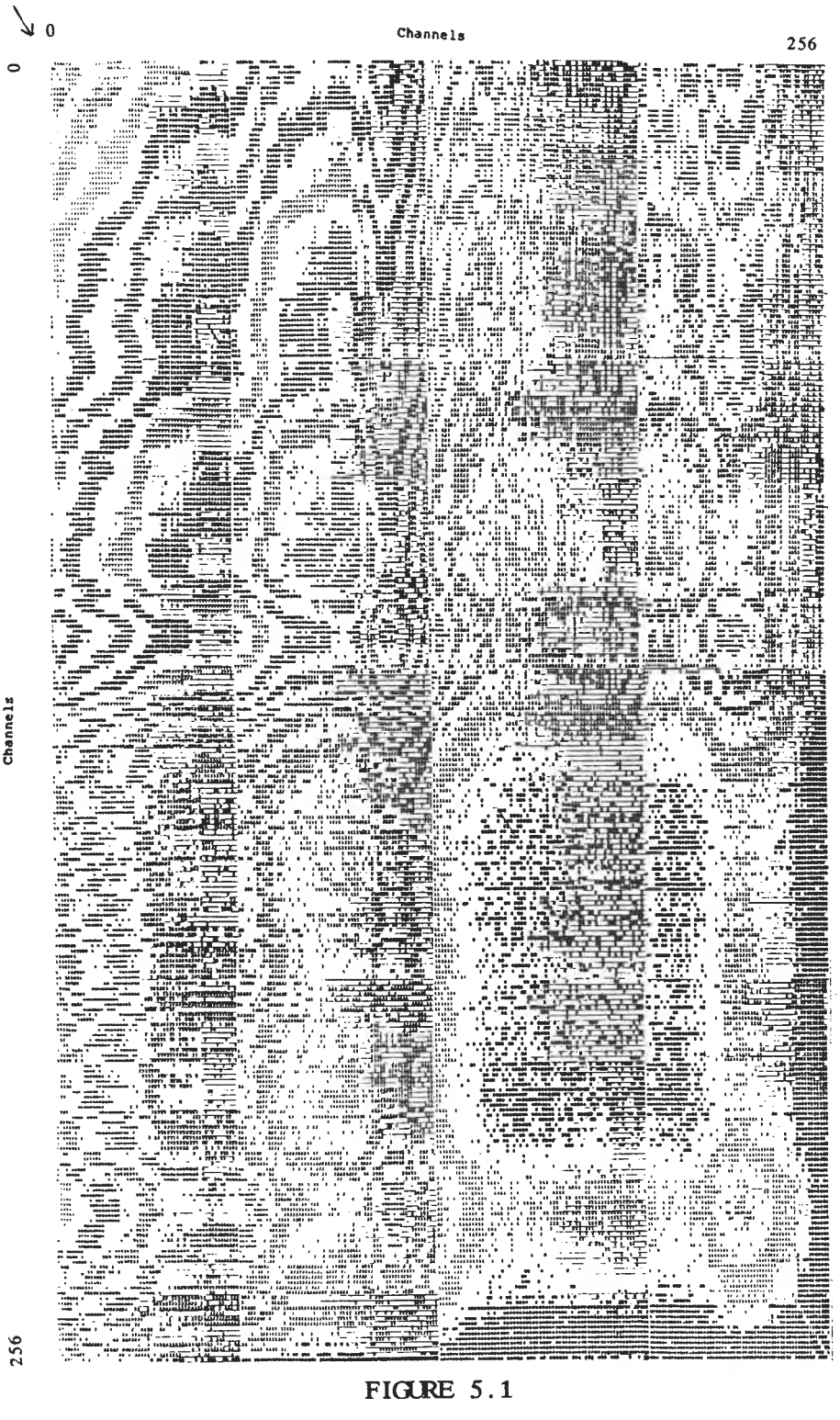

FIGURE 5.1

Covariance Matrix, Channel

The covariance matrix derived from the channel counts of line 2608. The steps are logarithmic, each 2.5x on the previous step.

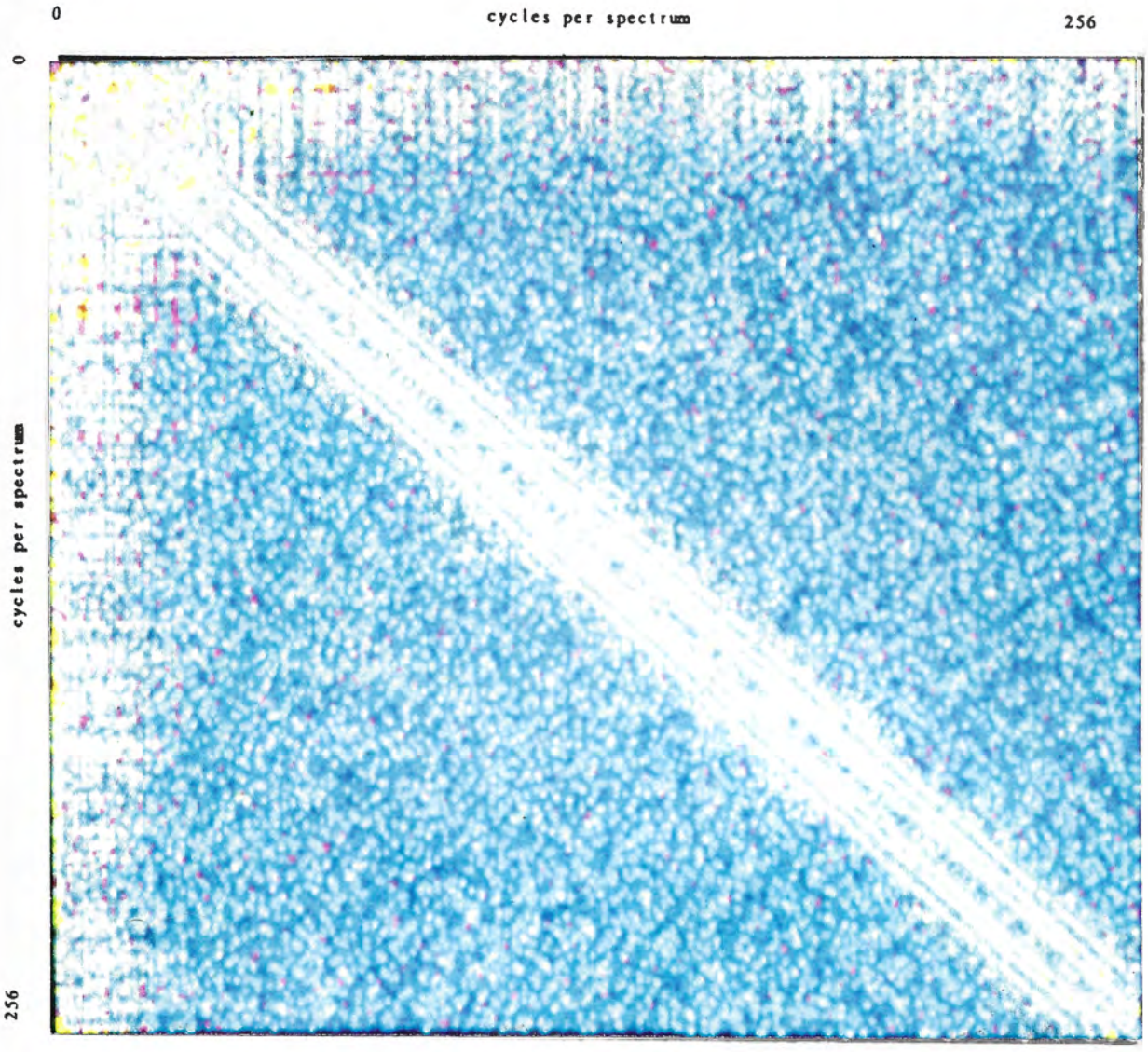

FIGURE 5.2

Covariance of the Fourier Cosine Components

The Fourier components of the readings, biased to intensity, were used in the calculation of the covariance (of line 4013) rather than the channel values. The top left corner, having the lowest spectral frequencies, contains most of the useful information. The Poisson noise is again evident as the diagonal.

5.6 Taking principal components

The principal components of a test line 2608 were taken by the conventional procedure of diagonalizing the channel covariance,

$$C_{ij} = \Sigma_{\text{data set}} (x_i - \mu_i) * (x_j - \mu_j) / N$$

where $\{x_i\}$ are the channel counts, $\{\mu_i\}$ are the channel means and N is the number of readings in the data set.

The diagonalization of the covariance delivers a complete set of principal components in order of decreasing variance. Figure 5.3 (page 143) shows the most significant principal components of line 2608, represented as channel count spectra.

Figure 5.3iii shows the third PC from line 2608. Appearing at the left hand end is a Poisson oscillation. Such fluctuations, described in Section 3.8 (page 81), worsen in the higher PCs to the point that the PCs' composition becomes dominated by the variance contributed by these meaningless fluctuations of the low energies. Accordingly, a bias must be applied.

5.7 Spectrum biases, bias to intensities

Poisson fluctuations in the long spectral wavelengths are statistically indistinguishable from variation due to surges in the spectrum due to concentration changes in the radioelements. They tend to occur when the counts are consistently high, that is, at the low energy high count end of the spectrum. Their variance is then

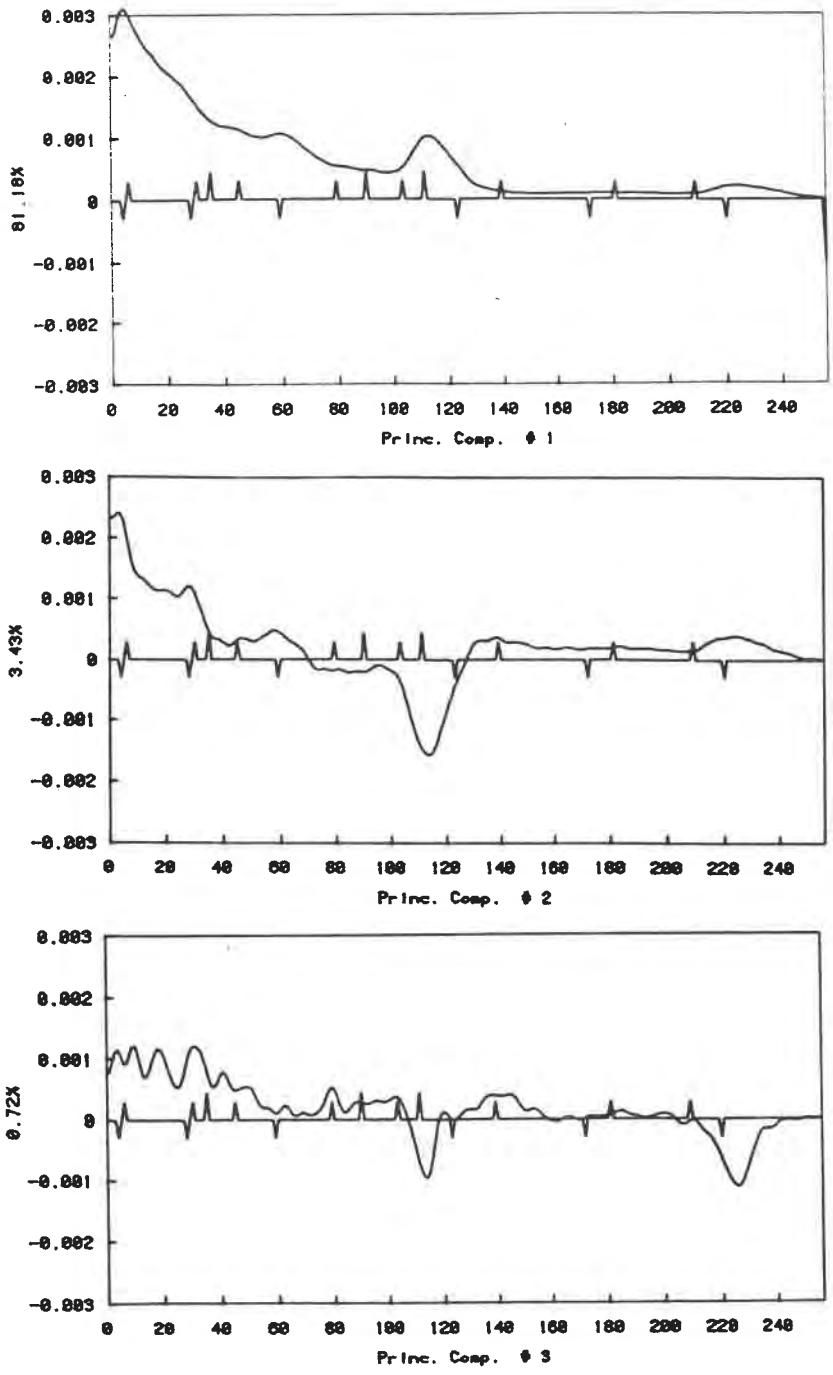

FIGURE 5.3

Principal Components, Line 2608, Unbiased Channels

The principal components of line 2608, were taken by smoothing and diagonalizing the covariance matrix shown in Figure 5.1 (page 140). The axes are channel numbers and normalized counts. The percentages of total remaining variance are also shown.

concentrated in that (low energy) subspace of the larger vector space containing the data. It is appropriate to use weighting to suppress the contribution of the spurious Poisson fluctuations.

Smoothing was always found necessary during principal component analysis. Smoothing amounts to a bias in favour of the long wavelength component shapes of the spectrum. Since these component waves are also member vectors of the vector space, it follows that smoothing also weights the components of the data in favour of a significant subspace.

The least squares minimization fit for the element concentrations by Crossley and Reid (1982) assumed that the variances are equal. Grasty et al. proposed a generalized weighted least-squares solution which accounted for the changing variances:

$$c_i = (A^T V^{-1} A)^{-1} A^T V^{-1} x_j$$

This formula gives the contribution of the jth channel count to the ith concentration, where **A** is the calibrated sensitivity matrix and **V** is the covariance matrix.

In effect, the different dimensions of the vector space are accorded different degrees of significance. The conceptual simplicity of a vector space with dimensions of similar status is somewhat eroded. An alternative is proposed.

Whereas Dickson (1980) used the covariance of the channel counts to obtain his principal components, the channel intensities have been used henceforth. These are simply the product of the channel energy and the counts in that channel. This amounts to a bias which

suppresses the lower energy end of the counts spectrum, where there are high mean counts and a correspondingly high variance in the long spectral wavelength Poisson fluctuations. The latter would otherwise swamp the principal components. Neither the variances nor the calibration data are needed to apply the bias, unlike either of the weighting methods above.

5.8 PCA of the intensities

Principal component analysis was performed on the unsmoothed intensity covariance matrix, yielding only a satisfactory first PC and a weak second PC. Successful PCA on the intensities required smoothing.

Accordingly, principal component analyses were performed on the weighted, smoothed covariances. The first three principal components from line 4013 are shown in Figure 5.4 on page 146, and the first six from line 4014 in Figure 5.5 on page 147. The principal components had been taken of their intensities and have been left in that form for display. Comparison of the two lines shows their PCs to be very similar.

The Figures 5.4 and 5.5 on pages 146 and 147 are using a true physical quantity, the intensity. Although the appearance may be unfamiliar to the reader, it is the form in which the PCs are normalized and orthogonal, due to the bias (see Section 5.7, page 142) which has been applied to them. Properly, they should only be

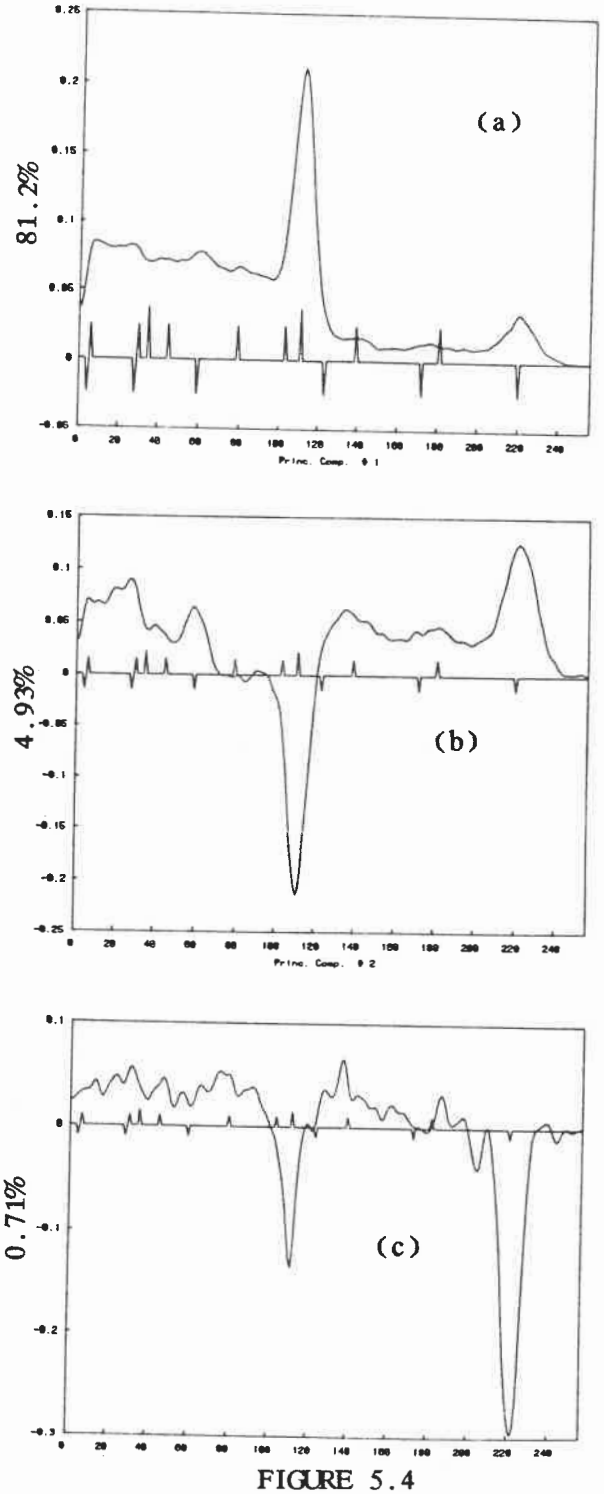

FIGURE 5.4

Principal Components, Line 4013, Intensity

The first three principal components of line 4013, obtained by diagonalizing the smoothed covariance matrix of the channel intensities. The axes are channel number and normalized intensity units. The share of remaining variance is also shown.

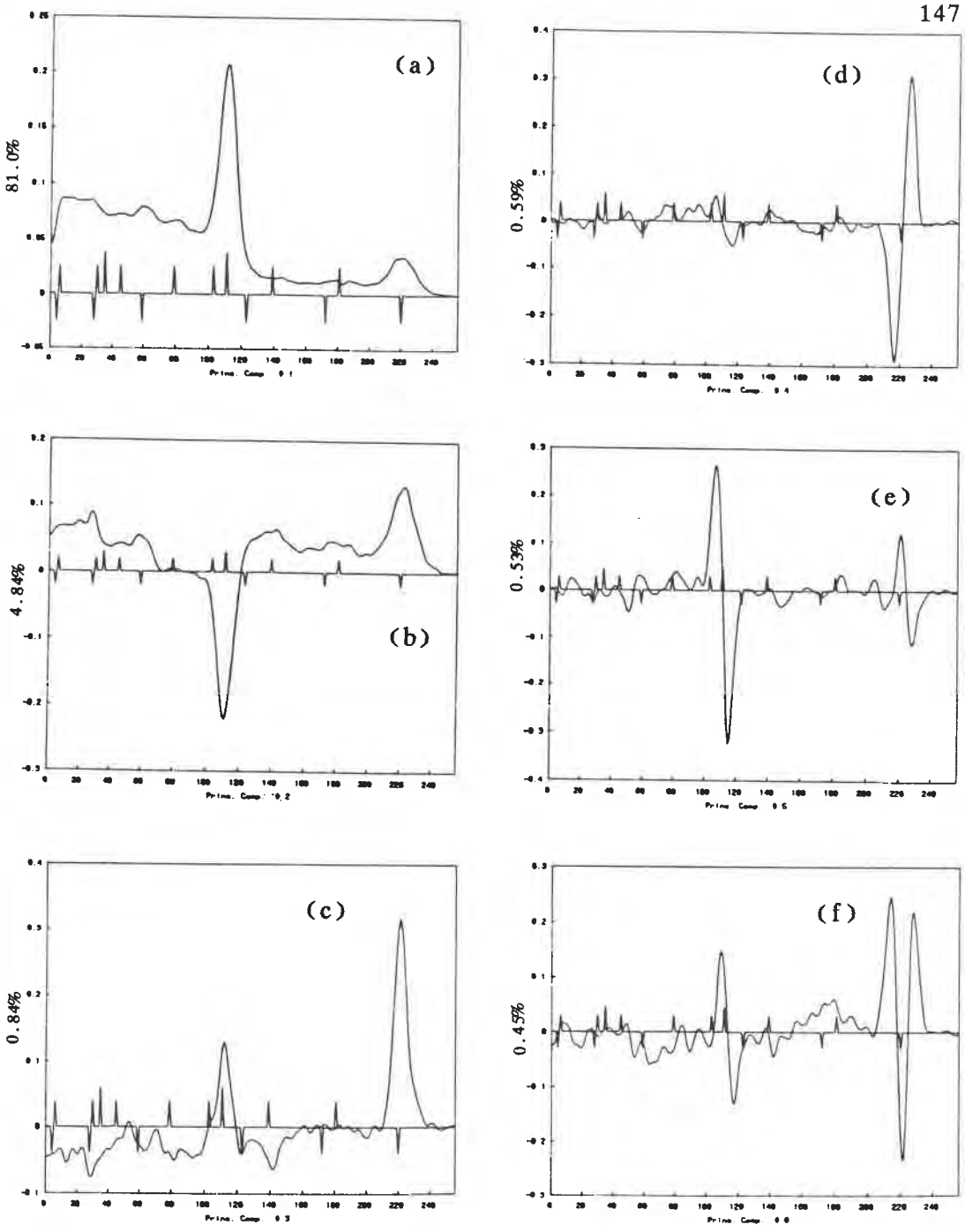

FIGURE 5.5

Principal Components, Line 4014, Intensity

The first six principal components of line 4013, obtained by diagonalizing the smoothed covariance matrix of the channel intensities. The axes are channel number and normalized intensity units. The share of remaining variance is also shown.

used in the intensity form, since the diagonalization was done on them when in that form.

Despite the weighting and smoothing, the matrix itself remained 256x256 in size, so its diagonalization remained noticeably slow on the VAX 8600 computer, taking several minutes running the NAG software package F02ABE. Optimization is desirable.

5.9 PCA in the Fourier domain

Other representations can be used for constructing the covariance, and the representation in the Fourier domain is conveniently achieved using a fast Fourier transform. Since the patterns of variation in the data are not affected by the representation used, the principal components can also be extracted in the Fourier domain.

Extraction of the PCs in the Fourier domain is attractive particularly in that it gives rise to a considerable computing time saving. The significant frequencies are the lowest and so occupy the low numbered corner of the covariance matrix (Figure 5.2, page 141). The higher frequencies have decreasing signal, (see Figure 3.6, page 76) compared to the noise, and so can be suppressed or discarded. The number of frequencies involved can be reduced immediately in order to smooth the covariance. Since this simultaneously reduces the size of the matrix, it also reduces the computing time taken in the diagonalization. Further reduction of the maximum frequency, the cut, can be made at run time to optimize computing time against the degree of smoothing implied by the cut.

Smoothing again consists of a Hanning function multiplied across the frequencies. The previous smoothing of the channel covariance was an ad hoc procedure without theoretical justification - it was used because the PCs obtained were much better than those obtained without smoothing. When extracting PCs in the Fourier domain however, the smoothing of the frequency covariance can be justified algebraically:

Consider the Hanning function as a set $\{R_i\}$, and
express each reading as a set of spectral frequencies $\{f_i\}$
with ϕ_i as the mean ith frequency,

then the covariance becomes-

Covariance matrix

$$C_{ij} = \Sigma_{\text{data set}} (f_i - \phi_i) * (f_j - \phi_j) / N$$

On smoothing the covariance matrix a new form is obtained:

$$= \Sigma (f_i - \phi_i) * (f_j - \phi_j) * R_i * R_j / N$$

$$= \Sigma (f_i - \phi_i) * R_i * (f_j - \phi_j) * R_j / N$$

$$= \Sigma (f_i' - \phi_i') * (f_j' - \phi_j') / N$$

$$= C'_{ij} \quad \text{-the covariance of the smoothed readings.}$$

The above argument shows that the smoothed covariance matrix is the covariance of the smoothed data set. This constitutes a legitimation that was not done and perhaps could not be done when extracting PCs in the channel domain.

5.10 Comparison of PCs from the Fourier domain

Principal components were extracted in the Fourier domain, with bias to intensity, from flight lines 4013 and 4014. Several seconds of computing time were taken by the software, very much less than taken by the previous method. The results are shown in Figures 5.6 and 5.7 on pages 151 and 152.

When compared to the PCs obtained conventionally from the covariance of the channel intensities, shown in Figures 5.4 and 5.5 on pages 146 and 147, the similarities are evident. Two distinct procedures have arrived at essentially the same result, confirming both. On that basis, it is recommended that smoothing be applied before taking principal components by either method.

The theoretical and practical advantages gained by taking the principal components in the Fourier domain make that procedure distinctly more attractive than the conventional method. The former method was established too late to apply it usefully in the current project.

5.11 Examination of the first PC

The first PC, with about 80% of the variance, is everywhere positive and includes positive photopeaks from all three spectra. (See Figure 5.5(a) on page 147.)

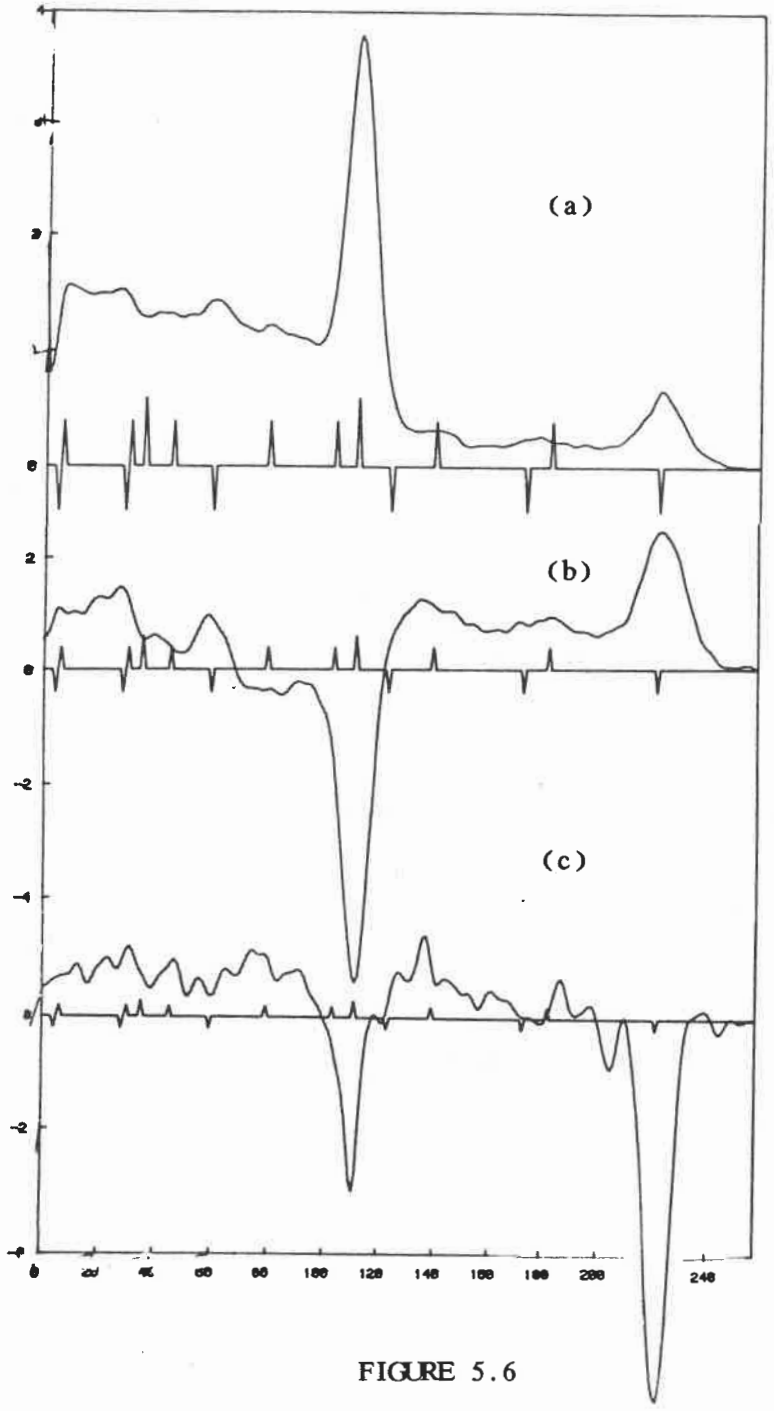

FIGURE 5.6

Fourier principal components of line 4013

The PCs shown have been obtained from the covariance of the cosine coefficients of the data set intensities. The vertical axis is in arbitrary intensity units, the horizontal axis gives the channel sequence. Still in the intensity form, these PCs are orthogonal. Compare to Fig 5.7, following.

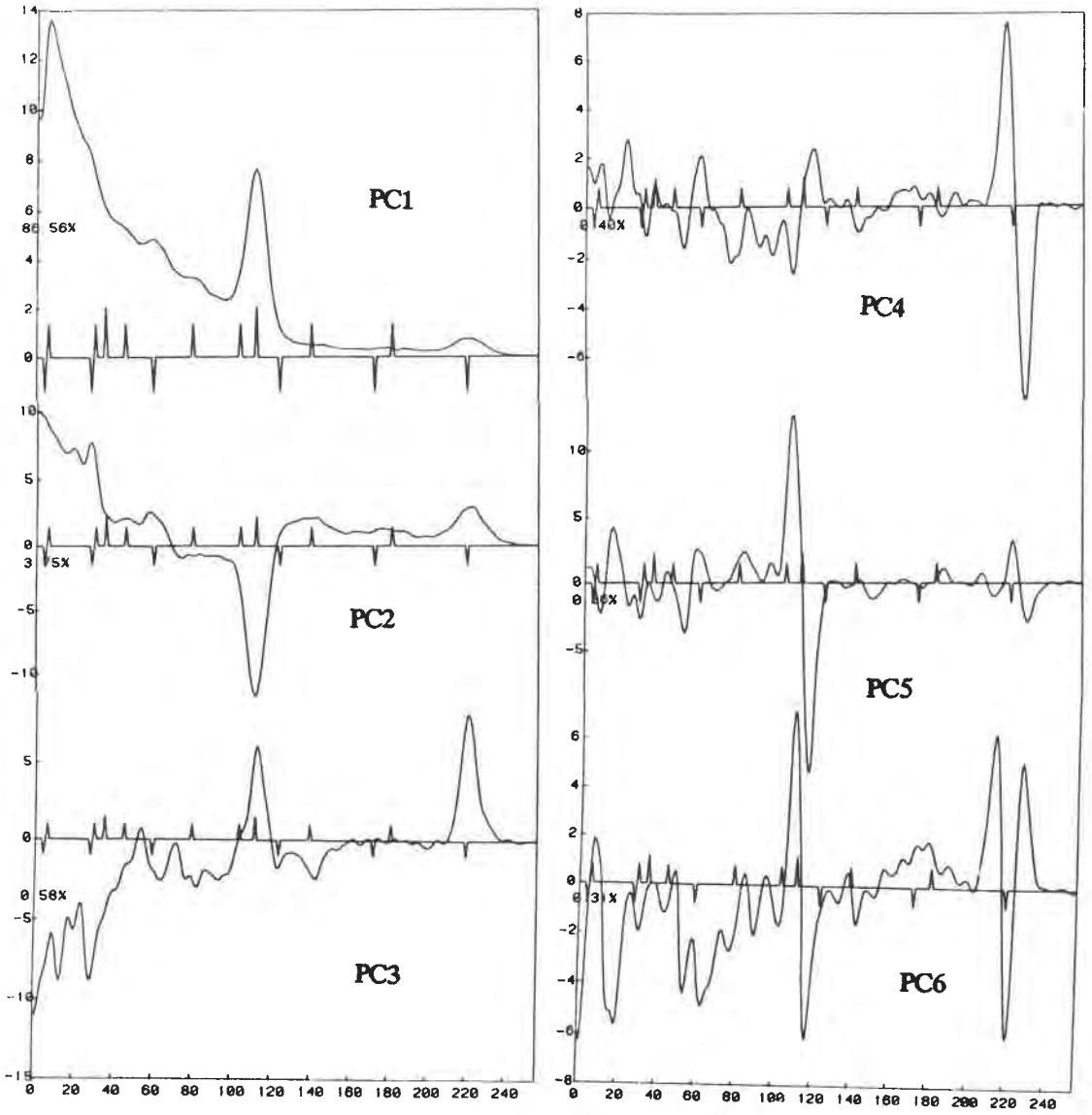

FIGURE 5.7

Fourier principal components of line 4014

These PCs have been obtained from the covariance of the cosine coefficients of the data set intensities and reduced to the counts form for display. They are only normalized and orthogonal when the bias is returned to them. The variance fraction is included. The vertical axis is marked in normalized counts and the horizontal axis gives the channel sequence.

Any radioactive source will give a reading which is everywhere positive along the channels. For that reason alone, there will always be a positive amplitude to the first PC wherever there is radioactivity. This cannot amount to 80% of the variance, however, as the lithology alone must vary by more than 20%.

Serra (1984) demonstrates that the concentrations of the three elements tend to vary together as the ground changes from basic to acidic. The resulting positive covariation would be expressed here as positive peaks on a positive spectrum, and Figure 5.5(a) on page 147 shows the first PC having that shape. The first PC expresses the geological variation between basic to acidic rock types.

Duval (1977) attempted to obtain the first principal factor – equivalent to a first PC here– using various combinations of some window data. It is possible that his results may have benefitted from the availability of multichannel data for a more effective first PC. If the data have been acquired with a minimum of external signal, the first PC must express the main lithological contribution to the variance.

A major way that the three element estimates vary together is through the variation of the ground clearance below the aircraft. In the absence of a multichannel height correction (see Section 3.14, page 95), this variation had not been removed, so the height effect remained in the data. The standard deviation of the ground clearance as given by the radar altitude data on lines 4013 and 4014 was 10 m and 5 m respectively. Since radiometric signal varies exponentially with distance, the altitude induced radiometric variation contributes at least proportionally to the variance of the

first PC. Comparison of the variances of the first four PCs on the two lines showed them to increase by 10%, 14%, -6%, 14% respectively on the line with strongly varying altitude, with little effect on their proportions to each other within each line. It was concluded that although height affects the variance it does not affect the spectral character of at least the early PCs.

Radon is not expected to show a variance distinctly separate from the lithology, especially if it had largely remained near the ground from which it had emerged. Part of its variance is then likely to appear in the first PC as well as subsequent PCs. The image of the first PC amplitude is then likely to be striped to some degree.

The significant behaviour of the first PC is the sensitivity to the acid-base changes in rock type. If the amplitude of the first principal component were taken through the data set, corrected for height and displayed as a grey-scale image, it would express the distribution of the more radioactive rock types. Because other independent sources of variance are excluded by the analysis, this image would have less noise than the conventional total-count maps currently used for the purpose.

5.12 The second and third principal components

The second PC can be considered as the main variation from the first PC. In Figure 5.5(b) on page 147 it seen to be dominated by potassium contravarying against uranium and thorium, to a share of about 5% of the variance.

A comparison of the second PC of the high radon line, 4013, in Figure 5.4(b) on the page 146, with that of line 4014 in Figure 5.5(b) shows it to be higher at the uranium peaks than the other peaks. Since the two lines are separated by only 200 m yet share 60 km of lithology, it is unlikely that the ground uranium differs sufficiently between the lines to show this much effect without a similar change in the potassium or thorium. The difference in the uranium peaks is more likely to have been caused by the known difference in airborne radon effects between the lines. It is apparent that some of the radon factor will be expressed in the second PC.

The third PC (Figure 5.4(c)) shows uranium - or radon - peaks contravarying against the other two spectra, with less than 1% of the total variance. The low variance indicates that this may indeed be due to ground uranium, or at least, uranium activity varying independently of the uranium behaviour of the second PC.

The above ratio of -6% for the two variances of the third PC appears anomalous. In Section 4.4 (page 110) it was concluded that airborne radon contributed a positive covariance with height on line 4013, whereas the ground uranium had a negative covariance with height on both lines. It would appear that the net covariance was less on the high radon line. If the first four PCs -as quoted above- include most of the survey's mappable variance, then it seems that the third PC is dominated by, or has a significant proportion of, the radon and uranium signals.

It is highly probable that most of the lithological variance is

already expressed in the first three PCs. If they were displayed together in distinct colours on the same image, the lithology is likely to be largely expressed. The radon stripes would still be apparent since the variance due to the radon factor has not yet been removed.

Linear combinations of the three PCs are expected to adequately express both the ground uranium and airborne radon factors. The coefficients of the combinations are needed.

5.13 Higher PCs

During his extraction of a third principal component of the potassium attenuation data set, Dickson obtained (1980) an N-shaped function, see Figure 5.8(a) on page 157, like that apparent on Figure 5.5(d) on page 146. After calibration of the energy scale and repeating the analysis, the feature was replaced by a W-shaped function -see Figures 5.8(b) and 5.4(d) - of much lower amplitude. He attributed the N-shape behaviour to the spurious variance due to the gain shifts, and proposed that the N-shaped component be used to test the energy calibration, that is, testing the gain shift.

It might similarly be argued that the W-shaped function is a second-order expression of the gain shift. Since there were four independent gain devices (Dickson et al., 1981) contributing to his (1980) data, it is inevitable that their drifts will contribute independent variation to the data. However it is not necessary to require that the shapes were caused by gain shift for them to be

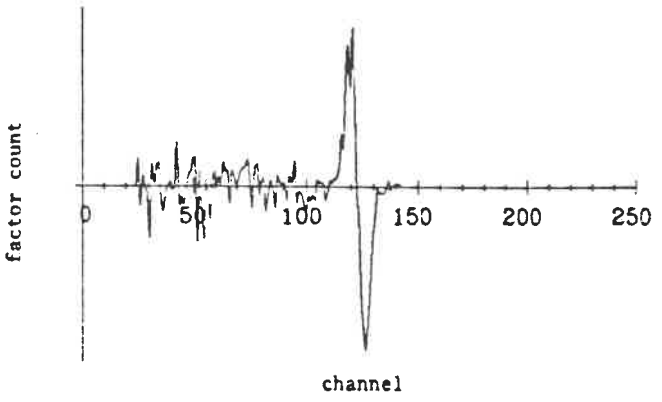

(a) Potassium factor 3 before energy calibration

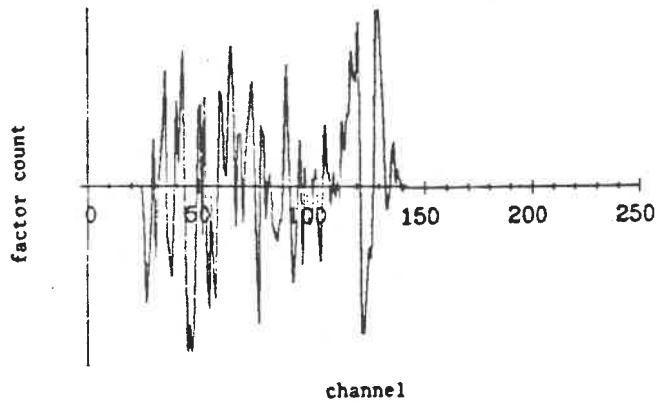

(b) Potassium factor 3 after energy calibration

FIGURE 5.8

Tentative Gain Shift Factor

B H Dickson's third principal component of his potassium attenuation data set, before and after energy calibration. The N-shaped feature is replaced by a W-shaped function of much lower amplitude. From Dickson (1980).

used as appropriate measures of the shift.

More generally it can be said that PCs may be useful templates without them having to have any physical significance of their own. From the considerations of Section 3.9 (page 83), it can be argued that the noise at a wavelength of a few cycles per spectrum will express itself in proportion to the amplitude of the expected signal at each part of the spectrum. The shapes of the higher PCs, for instance the sixth and higher in Figure 5.5 on page 147, may signify nothing more than random orthogonal functions of decreasing representation in the smoothed data. To that extent, even their sequence may be an artifact of the smoothing.

5.14 Principal components of statistical noise

Inspection of higher PCs such as those on Figure 5.5 on page 147 show more of the higher spectral frequencies as the variance slowly declines. Since the signal passed by the smoothing also slowly declined as the Hann progressed over the higher frequencies, (see Section 3.13 on page 91) the question arose as to whether the entire PC set could be mimicked using random noise as a source data set.

The noise data set presented in Section 3.9 (page 83) underwent principal component analysis in the Fourier domain with the same bias to intensity and the same smoothing function as used to construct the PCs on Figure 5.6 on page 151. Both refer to line 4013, but the noise data set contains only the information implied by the mean spectrum of the line, whereas the full set contains all

the physical effects detected.

The PCs resulting are shown in Figure 5.9 on page 160. The differences between them can only reflect the meaningless variations due to Poisson noise on the mean spectrum. It may be found surprising that similar shapes to those of the survey data PCs are obtained. However it might also be said that these are the selections of the eigenvectors with the highest frequency content under the smoothing constraint used. The sequence of the PCs is expressing the choice of smoothing function.

It is tempting to see in Figure 5.9 the rising frequencies of the Fourier trigonometric functions modulated by the envelope of the mean spectrum, however their wavelengths elude satisfactory measurement for orthogonality. Similarly the orthogonal gaussian derivatives are resembled in the vicinity of the peaks. It is possible that useful analytic approximations can be made, based on either model.

The variances of the noise PCs are shown compared to those of line 4013 in Table 6 on page 161. The variances of the noise follow a fairly even decline across the first ten PCs. Since the Hann smoothing function is decreasing slower than this, the decline must reflect a simple statistical tendency. It is reasonable to expect a peak to vary with or contravary against another as likely forms of random fluctuation. It is convenient that the variation of the geochemicals also is firstly to vary together and then to contravary in turn.

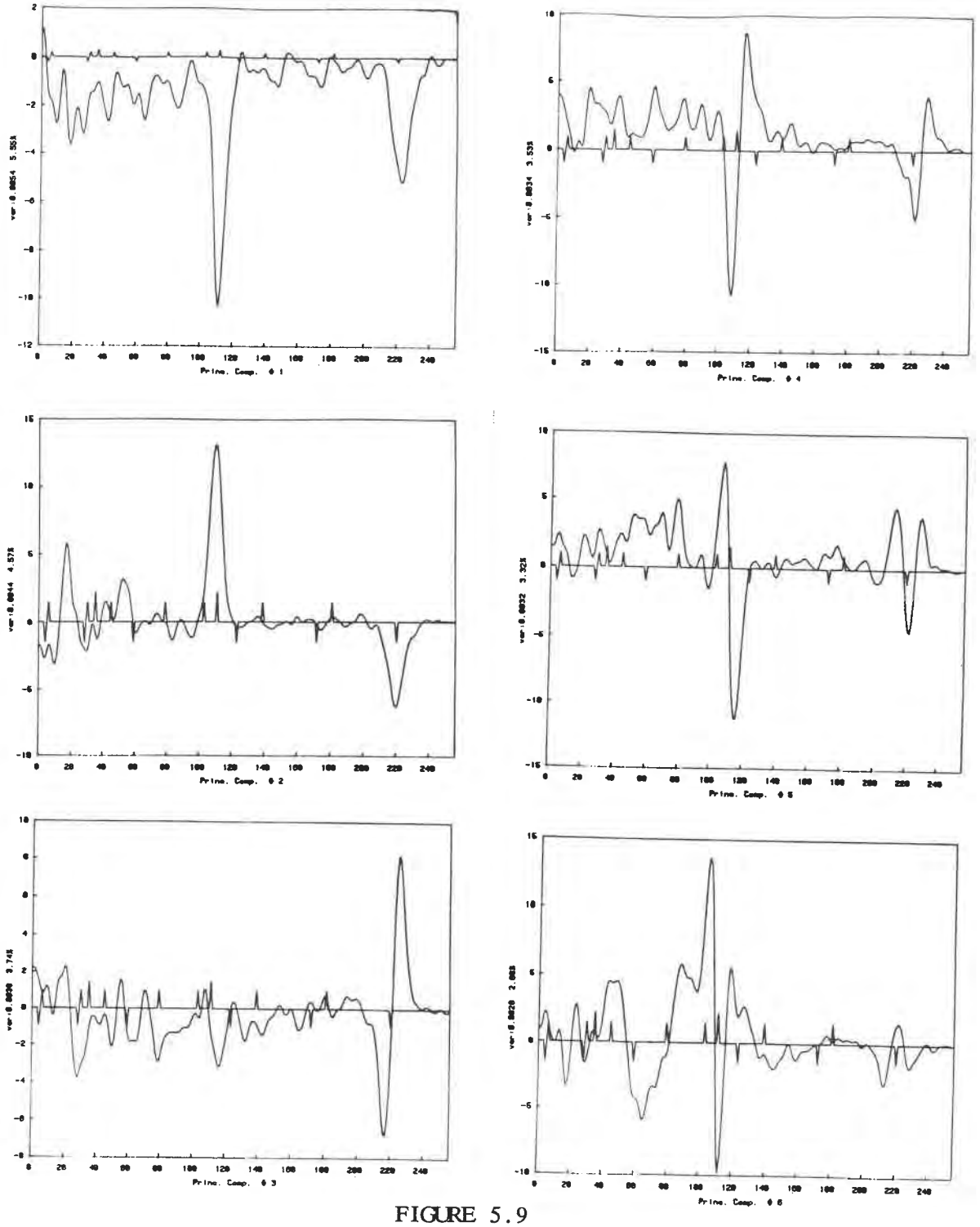

FIGURE 5.9

Fourier Principal Components, Poisson Noise

These PCs have been obtained from the covariance of the cosine coefficients of the noise data set intensities. They are normalized and orthogonal when the bias is returned to them. The variance fraction is marked beside the vertical axis which is marked in normalized counts and the horizontal axis is the channel sequence.

TABLE 6

Variance of PCs of Line 4013 and its Noise

The variance units used here are arbitrarily based on intensity squared. Note that the signal-to-noise ratio for the (spectrally smoothed) data set is near 10, but for the first PC it is more than 150. The S/N ratios of the other PCs may improve with spatial smoothing since the variance of the noise in the denominator tends to come from the shortest spatial wavelengths. The "≈" indicates that the shapes of the corresponding PCs are similar but not perfectly matched for the variance comparison.

Principal component	σ^2 4013	σ^2 Noise	S/N Ratio
1	0.8261	0.0054	153
2	0.0370	0.0044	8.5
3	0.0047	0.0036	≈1.3
4	0.0040	0.0034	≈1.2
5	0.0034	0.0032	≈1.1
6	0.0031	0.0028	≈1.1
7	0.0027	0.0026	≈1.0
8	0.0027	0.0024	≈1.0
9	0.0025	0.0023	≈1.0
10	0.0022	0.0022	≈1.0
Total	0.9543	0.0973	9.8

The signal-to-noise ratio indicated by the table shows a very much more rapid decline. Only two PCs are seen to be of certain value on this scale, with ratios of variance of 153 and 8.5. The next few PCs with ratios near unity will need careful manipulation; possibly spatial smoothing may have to be invoked to suppress the noise further.

The total variances on Table 6 are worth noting. Apparently only 10% of the total variance on line 4013 passing the smoothing function was due to Poisson noise.

Clearly the choice of smoothing function is particularly important to maximize the passing of physical effects and suppression of noise effects.

5.15 Conclusion

Principal components have been successfully obtained for a survey data set. Several problems have been addressed and solutions have been tested satisfactorily.

A procedure has been proven for obtaining principal components in the Fourier domain. The PCs resulting are cleaner than those from the more conventional method and are obtained with more practical computation times. Not seen before in the literature, this procedure may be a new contribution to the field.

The specification of procedures for principal components analysis provides a means for the reduction of dimensionality of multichannel data. The separation of the lithological signal from most of the

Poisson noise is made possible. Reduction of the multichannel readings set to a smaller set of amplitudes of the significant PCs allows further, more sophisticated algebraic manipulation than was conveniently done before.

The principal components of noise characteristic to this installation in this survey area have been obtained and have been found to be functionally the same as those taken from the data. It can be concluded that good approximations to the PCs of a survey can be found before the survey begins. This allows of the use of the PCs during acquisition, to enable real-time condensing of data for storage. Preprocessing is also facilitated.

It has been demonstrated that at least three and possibly six PCs are readily achieved to span most of the geologically significant subspace. This must include the effects of airborne radon.

CHAPTER VI

FACTOR ANALYSIS FOR RADON

6.1 Introduction

As any spectral vector can be expressed in terms of the PCs, so also can any physical behaviour which has a spectral expression, that is, a factor. The definition of factors in terms of PCs lies in the area of factor analysis.

The application of factor analysis to multichannel survey data is shown to be feasible; a first approximation to the thorium and potassium factors was readily obtained. The uranium estimation requires the removal of radon, so it is of interest to obtain a factor specifically for the clearing of radon effects.

Accordingly, a demonstration extraction of a radon factor was performed. An analysis of an application follows. Although the factor is rather arbitrarily constructed for the sake of the demonstration, some useful conclusions about the data set are drawn.

6.2 Factors for potassium and thorium

The model spectra for the elements themselves form factors and can be expressed in terms of PCs such as those from line 4013, shown on Figure 5.6 on page 151.

In Figure 6.1 on page 166 the second PC from line 4013 is subtracted from the first in the simple proportion of 11:-3. The Figure shows the difference in the intensity representation. The result strongly resembles the spectrum of potassium. Comparison with the laboratory spectrum for potassium in Figures 2.1 on page 11 confirms that an approximate potassium factor has been obtained. Minor improvement is obtained by adjusting the proportions and including other PCs.

Similarly the second PC was added to the first in proportions of one is to two. The result is seen to resemble the spectrum of thorium: compare Figure 6.2 on page 167 with Figure 2.3 on page 14. The second lithological factor has been approximated, the thorium factor.

These two factor spectra represent two directions spanning the strongest variance in the data set. The conclusion is readily drawn that potassium and thorium dominate the radiometric signal.

6.3 A radon factor independent of the uranium signal

The considerations of Section 5.12 prohibit the extraction of either the ground uranium or the airborne radon factor from the third PC alone. Other considerations must be invoked to construct the candidate factors. The approach chosen is that suggested by the apparent spread of the radon factor over the early PCs. It was expected that part of the radon factor still in the image would be

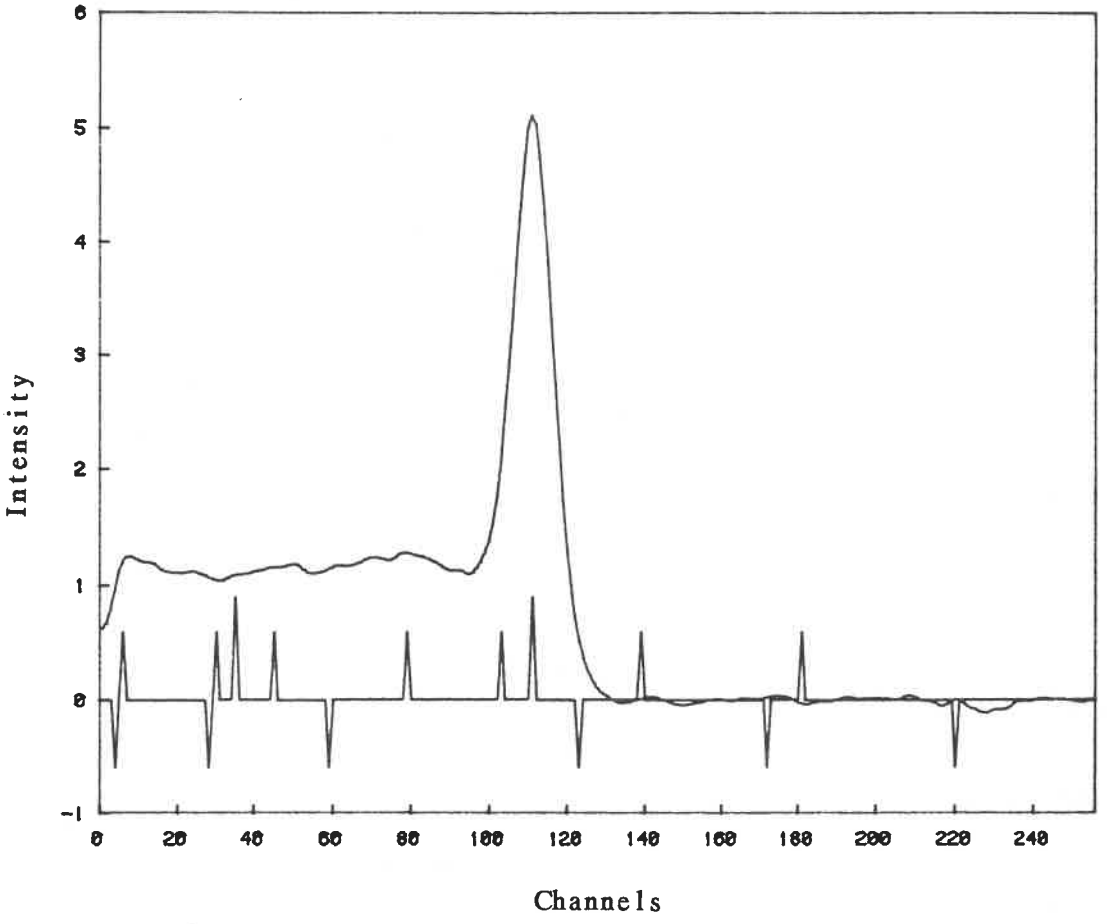

FIGURE 6.1

Potassium Factor extracted from the First Two PCs

Obtained by subtracting three parts of the second PC of line 4013 from eleven parts of the first PC. It is shown as a spectrum of intensities. Obtained in a purely statistical procedure, this factor approximates the influence due to potassium, isolated without reference to a standard calibration. Compare to the laboratory potassium spectrum (counts) in Figure 2.1 on page 11. (See also Figure 6.2, on the following page.)

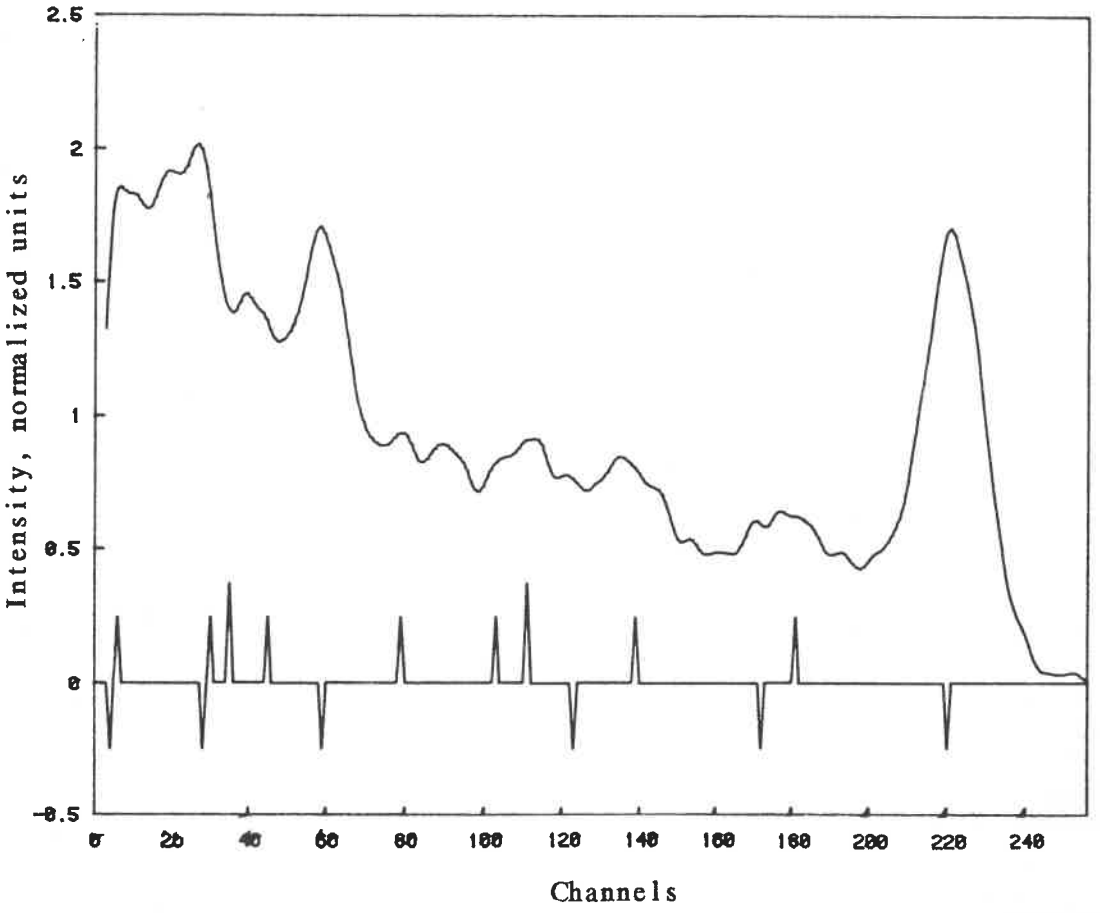

FIGURE 6.2

A weighted sum of the first two PCs of line 4013 reveals the radiometric contribution to the line data due to the thorium series, the thorium factor. The proportions used here are simply 2:1, and would benefit from refinement and the addition of some of the third PC. It is shown as a normalized intensity spectrum. The factor has been obtained without reference to a calibration: compare to the field calibration spectrum for thorium, seen in counts form in Figure 2.3, page 14. (See also Figure 6.1 on page 166.)

traced by that part outside of the subspace spanned by the first three PCs.

Construction of a radon factor orthogonal to the first three PCs can be achieved by subtracting their contribution from a total uranium factor. An expression of total uranium which was available was the uranium field calibration reading set, seen in Figure 3.7 on page 77.

Described in Section 2.13, the field calibration procedure accumulates a spectrum from the Pb-214 and Bi-214 in the uraninite sample nearby. There is less attenuation effect in this spectrum than the airborne radon is ever likely to show, there being only a few millimetres of sample and a metre of air between the sample and the aircraft skin. As the lithological contribution has more attenuation than the airborne radon, it is clear that much of the uraninite calibration spectrum lies outside the subspace spanned by the first three PCs.

After a least-squares removal of the first three PCs, a radon factor orthogonal to all of them is obtained. The resulting partial radon factor is shown in Figure 6.3 on page 169. It is "partial" in the sense that it lacks an unknown fraction of the radon signal which is still in the three-PC image, but its remaining presence in the data set was hoped to coincide sufficiently with the radon presence in the image.

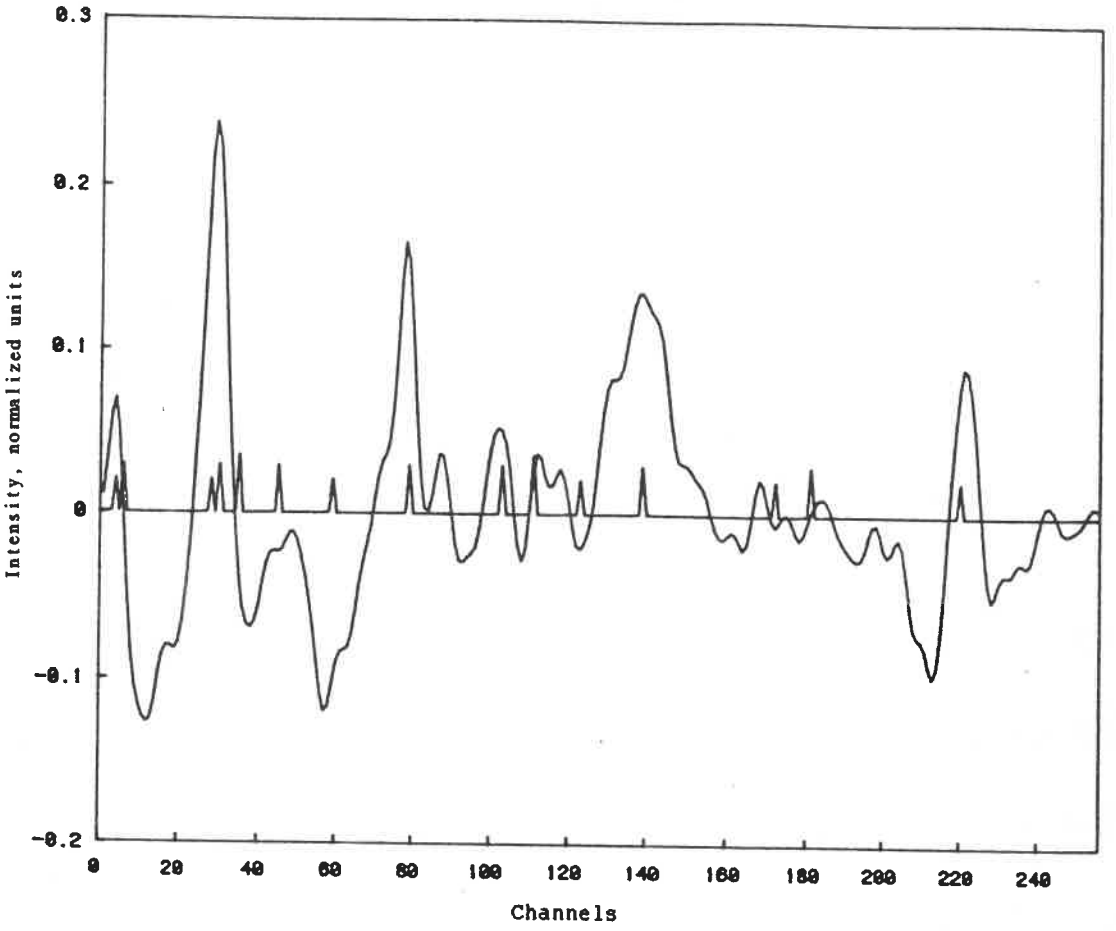

FIGURE 6.3

Partial radon factor

Obtained by removing least-squares fits of the first three PCs from the field calibration uranium sample. This minimizes the capacity of this factor to fit the lithologically-sourced information in the data. Some of its capacity to fit the airborne-sourced signal remains, albeit weakly.

6.4 Spatial behaviour of the partial radon factor

The least-squares amplitude of a factor in a reading can be obtained by taking the dot product of the vector representations of the two quantities. A justification is found in the Appendix.

Accordingly the amplitude of the partial radon factor was taken along the lines 4013 and 4014. The two amplitude sets were then subtracted one-for-one so that the difference in the partial factor amplitude was obtained. The subtraction further reduces its signal content, leaving a very noisy data set. Its profile is shown in Figure 6.4 on page 171, and after smoothing, in Figure 6.5 on page 172.

It was considered that the variance in the raw uranium count rate would be dominated by the height variation and the airborne radon variation in unknown proportions. In that no height correction is available for either the radon content of the window counts nor the amplitude of the current radon factor, it was decided to use the window data as a reference without correcting for height. Accordingly the difference between the lines in the uranium window counts was obtained by subtraction one-for-one along the lines. The profile of the difference is shown included in Figure 6.5 on page 172, where it is superimposed on the difference in the radon factor amplitude.

The Figure shows a fair correlation at the longer wavelengths. However at wavelengths shorter than 1 km contravariance is seen.

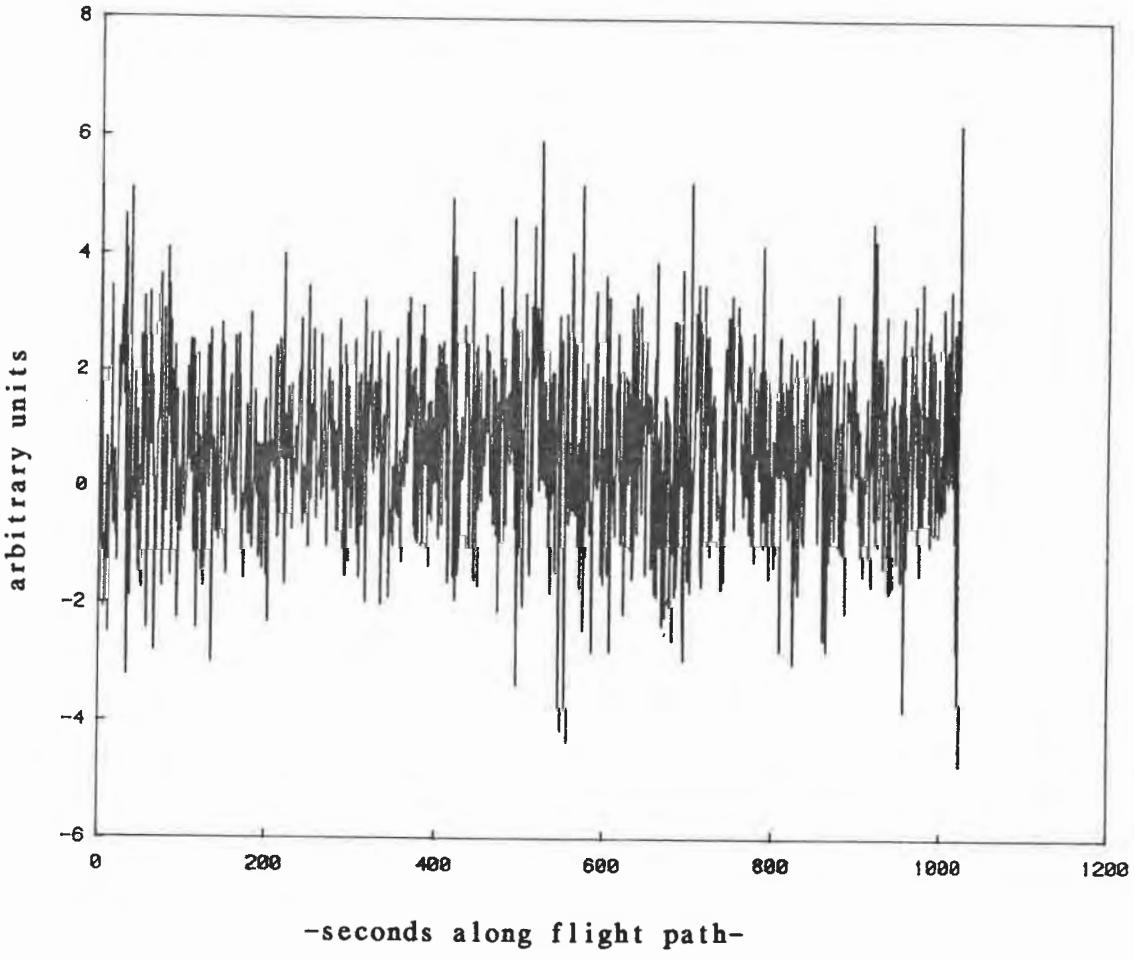

FIGURE 6.4

Amplitude of partial radon factor

The difference in amplitude of a partial radon factor between lines 4013 and 4014, without height correction. The bottom scale spans about 60 km. (See also Figure 6.5 on the next page.) Arbitrary intensity units are used.

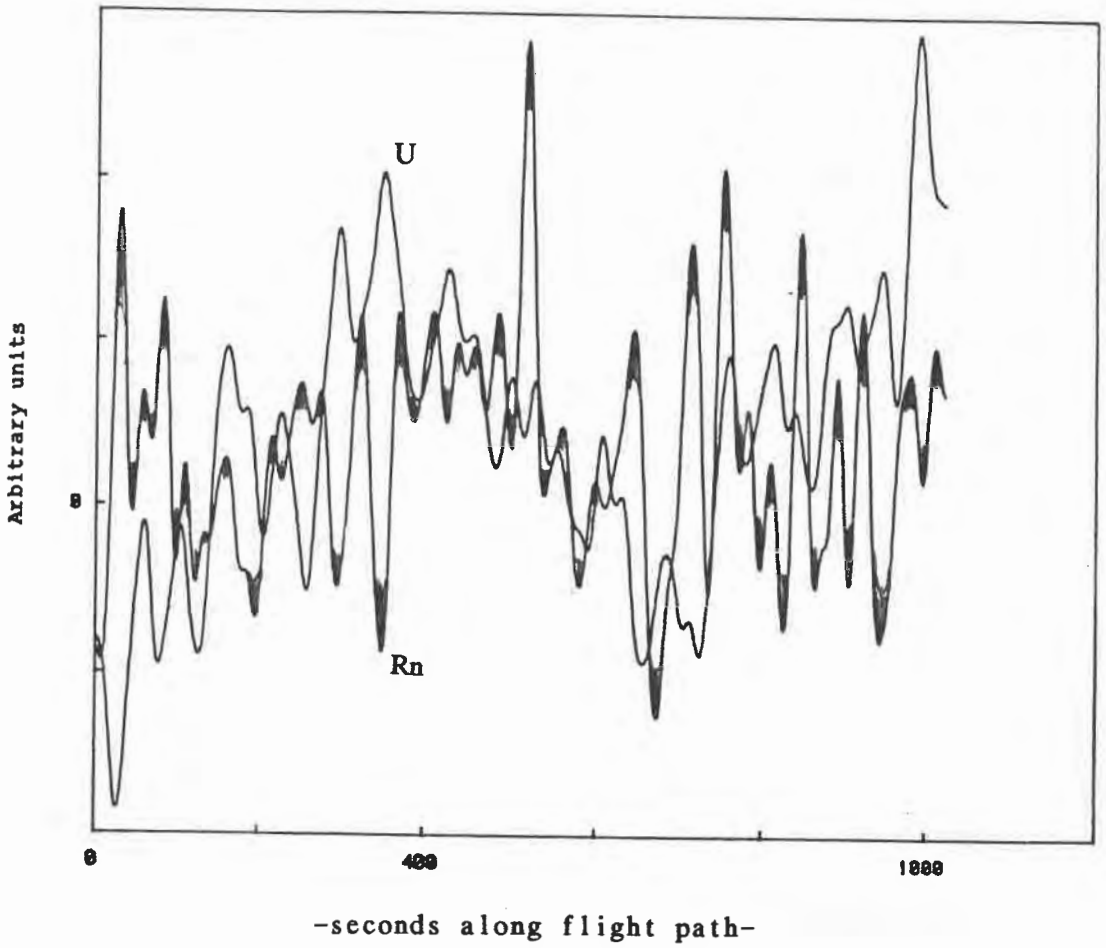

FIGURE 6.5

Smoothed amplitude of partial radon factor

The difference in amplitude of a partial radon factor after smoothing to around 1 km scale. The difference in the uranium window estimate is also shown superimposed. Contravariance on the shorter scale is evident. Neither data set is corrected for height.

Considering that 100-1000 m is both the scale of flight path variation of the aircraft and topographic variation, the implied variation in thickness of the intervening air mass was invoked as the source of the contravariation.

Table 7 on page 174 shows correlations at successive spatial smoothing. The positive correlation emerges again at the shortest spatial wavelengths. Variation less than 200 m does not occur in the absolute height of the fast moving aircraft but it does occur in both in the short scale variations in the topography, and in pockets of air. The covariance of this behaviour has already been investigated in Sections 4.4 and 4.5 on pages 110 to 119. The terrain related distribution proposed and examined there appears to be confirmed here.

The uranium height factor required to make a proper multichannel height correction will resemble the partial radon factor in that both must express the softening due to attenuation. The converse, the apparent spectral hardening or sharpening of the peaks is seen in Figure 2.4, on page 15, of the (nearby) calibration sample, where the relevant peaks are seen to be sharpened. Thus the partial radon factor should be more sensitive to the daughters of radon near the detector, rather than to radon at the ground surface.

TABLE 7

Effect of Smoothing on the Fit of a Radon Factor

A modest correlation occurs at both large and small spatial frequencies, but vanishes around 64 cycles per line, at an implied wavelength of one kilometre. A contravarying quantity has been inferred, but not identified. Its spectral covariance can be inferred from Figures 4.1 and 4.2 on pages 112 and 113.

Position of Hanning function:	Correlation coefficient:
none	r = + 0.12
256 cycles per line	r = + 0.06
128 cycles per line	r = + 0.03
64 cycles per line	r = + 0.01
32 cycles per line	r = + 0.04
16 cycles per line	r = + 0.14
8 cycles per line	r = + 0.23
4 cycles per line	r = + 0.31

6.5 Radon correction using factors

In principle, the removal of the effects of radon from the uranium estimate may be achieved by subtracting the amplitude of a radon factor from the uranium estimate at each point. Several points need consideration.

The uranium and radon factors span a two-dimensional subspace (see Figure 6.6(a) on page 176) of the spectral space described by the multichannel data so there is an essential ambiguity in the choice of the radon -or uranium- factors. The orthogonal radon factor (see Figure 6.6(c)) used in the preceding Sections is convenient in that it is largely independent of the uranium signal. It is "partial" in the sense that some of the radon signal is lost.

An orthogonal uranium factor may be constructed so that it will not correlate with the expected radon signal, but it will have lost much of its capacity to express the the uranium signal. (See Figure 6.6(d).)

As the aircraft moves across the ground the radon may appear in a different relative altitude so that its signal drifts away from the factor used as a working model. Although this damages the estimate of radon quantity it does not greatly affect the estimate of radon effects in the raw uranium signal detected. (See Figure 6.6(e) on page 176, also Section 3.3, page 59.)

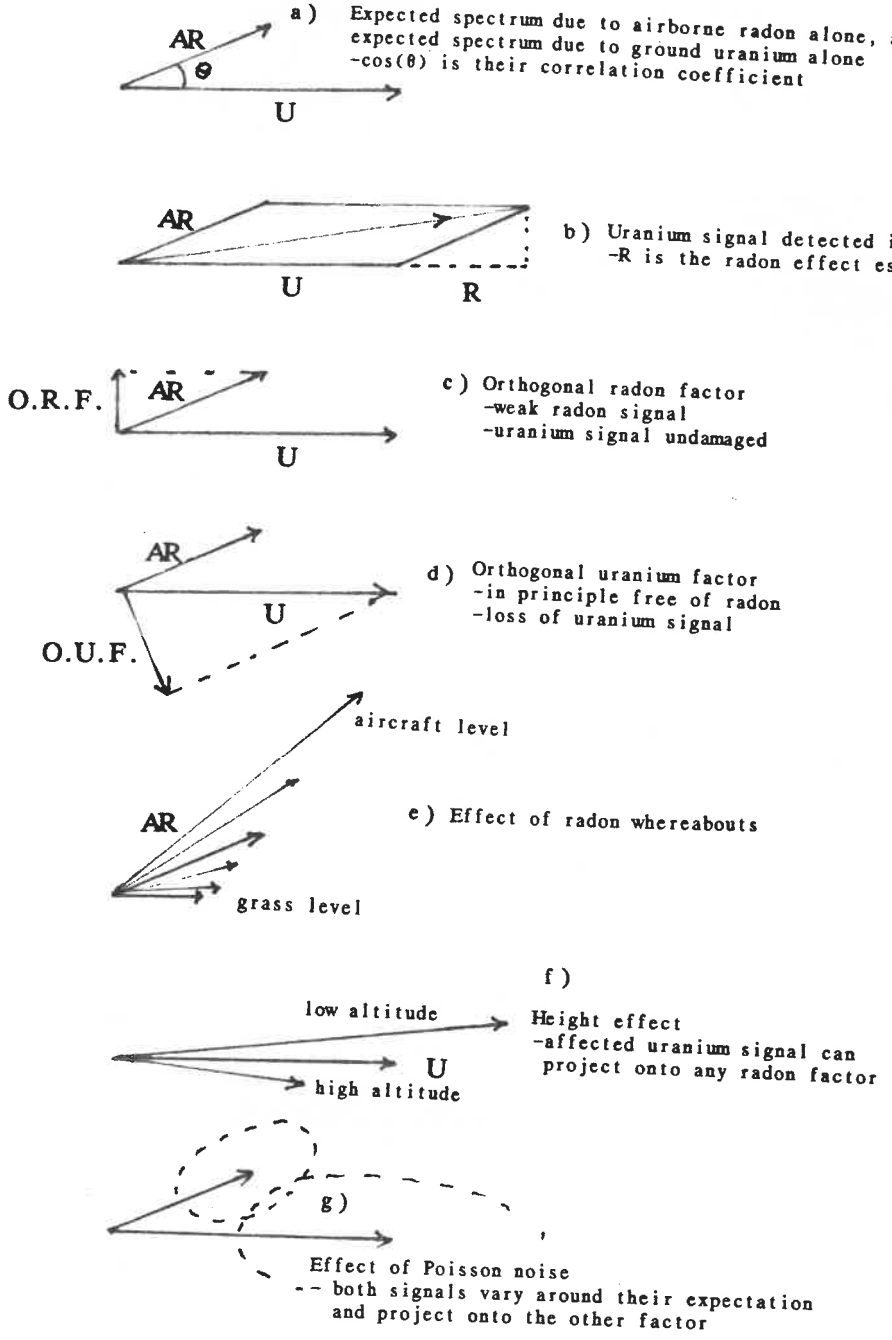

FIGURE 6.6

Radon Correction in Spectral Space

Once a uranium and a radon factor have been obtained, various approaches to reducing R, the effect of the airborne radon on the uranium signal, are possible in the subspace they define. Effects such as height and counting noise may produce errors.

A similar effect -see Figure 6.6(g)- arises when noise occurs in the low channels due to high contributions from each other's sources, or even potassium or thorium. This noise can print through (see Section 5.2, page 133) into the radon signal and to a lesser extent, into the uranium signal, thereby distorting the relationship between the two factors.

Height effects will require particular attention. The attenuation due to the changing air column will affect the low channels more than the high, so they will interfere with the radon estimate. When a uranium height factor (see Section 3.16, page 98) is used, it will be very similar to a orthogonal radon factor. In that case, the radon estimate may be made as an anomalous effective height, (see Section 3.17, page 101). Height correction by any method is likely to leave an imprint on the radon correction.

Considering the number of effects which are expressed in the subspace, it may be seen fit to provide a processing worker with some sort of representation of the subspace, analogous to the wind recording in meteorology. The effects could more easily be monitored and manipulated.

6.6 Application of the radon correction

A hypothetical routine using radon factors would require the worker to select the optimum linear combination of PCs for a radon factor, using a skill based on experience as well as training. The amplitude of the factor would be taken through the data and the result smoothed. The data may have already been corrected for

height in a manner which minimized damage to the evidence of the radon. However, it is also possible that the height correction would be applied after the suppression of radon in the total uranium signal.

The lack of signal level in the radon amplitude means that a pointwise subtraction would be unacceptably noisy. The uranium signal would have to be reduced in proportion to the amplitude of the radon factor smoothed or averaged over some length along the flight line or over some area of the image.

It is not clear, in the absence of evidence of the effects of height correction, how much smoothing of the radon amplitude will be necessary. The raw amplitude (Figure 6.4, page 171) of the partial radon factor is an ostensibly unsmoothed set, yet it already has an effective smoothing length of 50 m, due to its acquisition over one second at 50 m/s groundspeed. Such a short spatial wavelength inevitably has high noise content and longer, perhaps kilometre, smoothing lengths are likely to be required for radon removal.

The smoothing length used in Green's regression method was at least as long as one line, itself perhaps 10 km long. Smoothing lengths longer than a few reading spacings, of the order of 100-200 m, should be avoided if possible to avoid blurring the uranium signal. Between the two extremes, there is much room for run-time optimizing, although to a certain extent the size of the smoothing span depends on the scale length of the interpreter's interest, which may not always be demanding.

6.7 Height correction factors

As discussed above and in Chapter III, height correction of uranium is intimately related to the radon correction.

If height correction has not already been performed on a survey data set, then it may be necessary to derive and use a secondary version for each factor, a new factor that expresses the behaviour of the primary factor as the altitude changes. This is a height factor; its amplitude when taken (see Appendix) throughout the data is a function of the detector's altitude and the amplitude of its primary factor. These pairs of factors are described by Dickson (1980).

After applying the correction through each reading so that it resembles a reading at the standard ground clearance, the data may be fitted for the amplitudes of the factors. However, the fit of the radon factor will have been distorted by the treatment. The consequent radon factor amplitude may require height correction, but it will not necessarily get the same amount of height correction as the lithological elements since the vertical whereabouts of the radon is generally unknown.

Since the greatest radon effect is that due to precipitation bringing the activity to ground level (see Section 3.4, page 62), the most appropriate starting assumption is that the radon is just above the surface and needs a similar height correction to that of the lithological quantities.

6.8 Gain shift factors

Dickson (1980) suggested that a higher PC might be used as a criterion for the presence of gain drift. The possibility has been discussed in Section 5.13, page 156.

If the assumption is made that the first three PCs express the lithology, it follows that a simple gain drift across a survey can be expressed as three gain shift factors, one for each of the first three PCs and orthogonal to it.

Since an orthogonal gain shift factor need only be orthogonal to its primary, it follows that it will be a linear combination of the other PCs. An inspection of the higher PCs in Figure 5.7 on page 152, for instance, shows several with the appropriate shapes, the derivatives of the primary PCs:

$$f(e) - f(e+\delta e) \approx df/de.\delta e$$

Where f is the primary PC, df/de indicates the gain shift factor and e is the logarithm of the energy. Then δe represents the logarithm of the gain shift fraction. A similar quantity to $10^{\delta e}$ is shown in Table 3 on page 73.

In principle, the first three gain shift factors could be obtained by differentiating their primary PCs. These would be used to automatically quantify -as δe above- and correct for gain drifts at some minimum spatial wavelength, a wavelength chosen according to the causes expected for the shift.

The approach assumes that only one variable is needed to describe the drift. One possible difficulty with this approach is the minor freedom of the units to vary against each other, beyond their tendency to vary together. The effect has been approximated by Grasty et al. (1985) as a broadening of the peaks. With gain shift factors resembling the PCs such as those shown in Figure 5.6iv and 5.6v on page 151, however, the effect must appear in a factor analysis as terms with the form of the higher order shapes in Figure 6.7 on page 182.

It will not always be practical to correct for gain shifting in the data. Good practice dictates that it should be averted at the acquisition stage. The improvement in quality control required for true multichannel processing implies a necessity to re-examine existing equipment and procedures.

6.9 Cesium factor

Cesium has not been significant on the scales used in this data set. Its neglect has been discussed in Chapter III.

Although cesium estimation might be achievable on large scales (greater than 10 km), for studies such as regional weathering or land degradation, there is not enough signal for its use as an exploration tool.

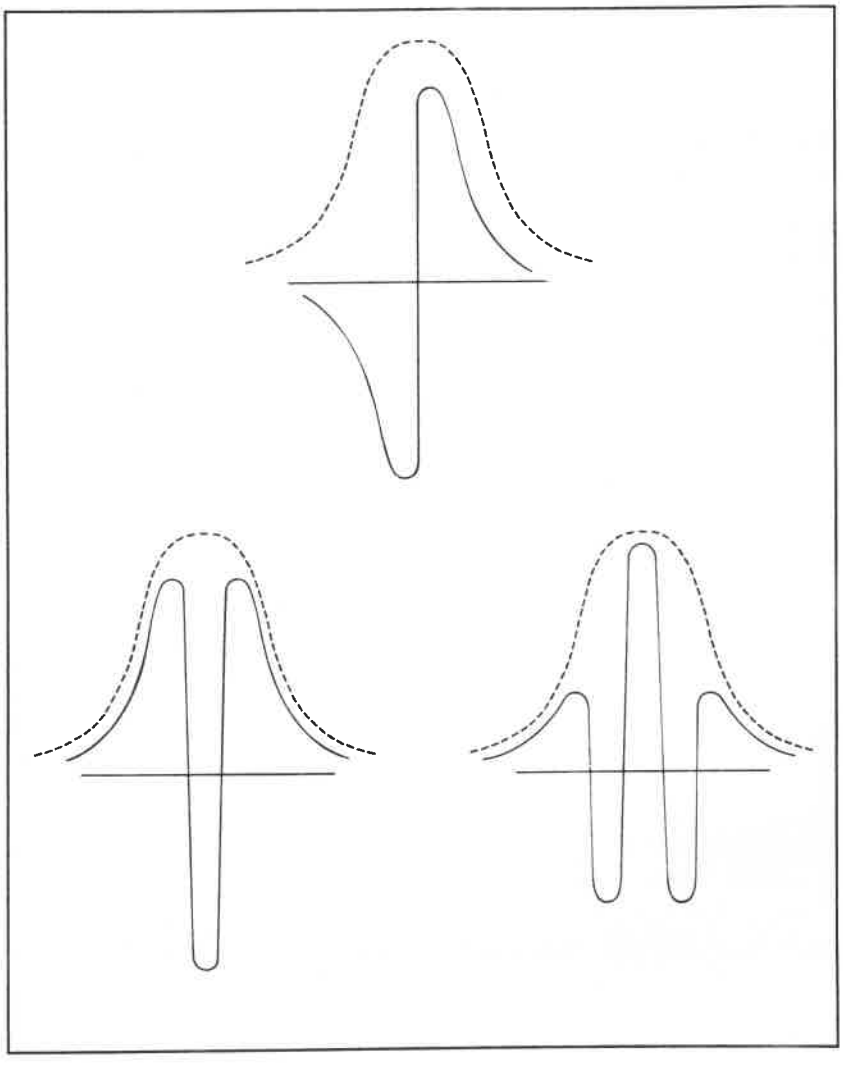

FIGURE 6.7

Functional shapes in the PCs

Patterns in the higher PCs may be inferred; there is a tendency for increasing spectral frequency to appear in the envelope of the mean spectrum. Sketched here are the common patterns appearing under the envelope of the NaI photopeak. Note the similarity to the derivatives of the gaussian shape.

If the methods of this chapter are to reach general usage, procedures would need to be set up for the construction of the cesium factor, or a total "airborne factor" including cesium and radon, must be redetermined for each event. Calibration for cesium would also need to be included in the standard calibration procedures.

6.10 Reprocessing and preprocessing

Years after the original acquisition, construction or reconstruction of the factors can be done, perhaps laboriously, from the raw multichannel data if it has been preserved. The computing time can be protracted and the work with the quality control of the raw data may duplicate that of earlier iterations.

The flexibility of PCs and factors is an argument which can be used to justify multichannel acquisition. Weighed against that is the amount of magnetic media the multichannel counts require for intermediate storage and the computing required to reduce it again in subsequent use.

Such volume storage may be unnecessary. Once a set of standard PCs have been prepared, only their amplitudes in the data need be stored. Even allowing for future developments in constructing useful factors from the PCs, there need only be as many PCs used as have variance above the noise level at the spatial wavelengths of interest. This number will be somewhere between 3 and 20.

Moreover, the construction of the factors could also be done after the extraction of the PCs. Such a sequence allows for

preprocessing, so that a worker need not wait for a computer to complete a task; the body of the work has already been done in an earlier, less urgent circumstance.

Further, the compact form allows the interval between first preparation of the PCs and their last applications to be many years. Re-examination of old data for newly constructed factors is always possible if the less voluminous PC data sets are kept after the raw multichannel data have been thrown out.

Once the behaviour of a particular production team and its equipment is known, it may be possible to use a standard set of PCs and reduce the data in real time. While there is a second's delay between radiometric readings, there is a second available for any dedicated computer on the aircraft to preprocess the previous reading before sending it on to the storage unit. The data compression implied can also reduce the number of times the magnetic tapes need changing.

6.11 Summary

Methods of extracting a radon factor were discussed. The first attempt met with a modest success.

These results are sufficiently encouraging to indicate the need for further work. Regardless of any schedule for a future transition to true multichannel processing, there is some urgency for the industry to tighten the quality control now, particularly of the gain shifts, so that reprocessing in years to come can extract information not presently derived.

CHAPTER VII

CONCLUSION

7.1 Summary

The literature of airborne radiometrics has been reviewed. The window techniques were found to be fully established whereas the multichannel techniques are still in a state of development. Radon effects can be seen to be an outstanding problem.

An instance of radon in a commercial survey has been obtained. Analysis of the weather at the time led to the conclusion that dew had brought the radon to the surface. In general, the whereabouts of the transient radioactivity is unknown, however a covariance procedure allowed some inferences to be made.

The various influences on the problem have been studied. Altitude and other attenuation effects were found to be significant both to the problem and to the possible solutions. Following these considerations, a proposal for the altitude calibration of multichannel systems has been put forward.

Various approaches have been examined, the spectral techniques that addressed the attenuation effects receiving particular attention. Several lines of approach appear profitable, particularly those

based on Fourier transforms.

Principal components analysis was invoked as a means of accessing the degrees of freedom that isolate or characterize the radon effects. Much work was performed to get this method workable in the presence of the high noise levels. Synthesis and analysis of the Poisson noise were performed, to useful conclusions. Smoothing procedures received particular attention, with the full-width Hanning function showing itself to be most effective.

A new, possibly original, method was developed, using the Fourier covariance. These principal components were found to have a much lower noise content than the conventionally obtained principal components. Further, they were found to be readily calculated on currently available computers.

Factor analysis followed logically. Although the topic was addressed late in the project some progress was made. A demonstration radon factor was extracted and its correlations with the radon data set studied. Further work this area is recommended.

7.2 Discussion

As a matured technique, the window processing has left only the most intractable of problems. A generation of equipment and skilled workers has already addressed the radon striping. It is not likely to be resolved with direct attack, neither is the old equipment nor are the old methods likely to yield frequent breakthroughs.

However changes in circumstance are likely to reveal new opportunities. For example, the aircraft have become more reliable, so the flying height has decreased; also the navigation systems have also become more precise, so the grids have become finer. Interactive processing too, has become common, so allowing for more subjective input, and so that the computers are becoming more of a part of the process of judgement rather than just quantity calculation. New technologies such as these will almost certainly allow the resolution of the old problems, including airborne radon corrections.

This thesis has particularly relied on the recent changes in computing power. In particular, it develops the applications of principal component analyses and Fourier decompositions which will involve considerable numerical calculation.

7.3 The future

It is likely that the common hardware of acquisition will change over should the multichannel data collection be proven cost effective. One change underway at the moment is the use of upward-looking crystals. Yet to occur is the use of FFT microprocessor chips. Another possible change is the installation of preprocessing units which reshape the data before storage. Already interactive interpretation has become routine.

However the immediate changes expected are in the software. We can now have confidence in the arrival of raw computing power. It is an appropriate time to write the programs which will bring out the as

yet unused detail in the data.

7.4 Recommendations for future work

The thesis has made some progress and opened up several possible avenues for productive investigation. The body of the text contains many references to work which needs to be followed up.

The procedure (in Section 3.9, page 83 and Section 3.12, page 86), of synthesizing a Poisson noise set and setting up a signal-to-noise study may be found a useful tool for studies of the information content of a radiometric data set.

A height calibration proposal is sketched in Section 3.18 on page 102. The proposal is something of a stopgap measure. The subject of height correction for multichannel processing is a field ready for research projects, at least as big as required for another Masters' thesis. The elucidation of the Compton function (Section 3.114, page 95) would be particularly valuable, as it would allow analytic procedures for height correction.

Terrain correction studies are likely to be fruitful. The covariance and correlation tools developed in Sections 4.4 and 4.5 (pages 110 and 116) deserve application and extension for this purpose.

The lower energies for radon suppression, including 352 and 609 keV (Sections 4.6 and 4.7, pages 119 and 122) deserve further study. Any study here will require experimental investigation of the acquisition unit's response peculiarities, and a review of the

cesium distribution across Australia and other surveyable areas would also be indicated.

Fourier domain processing (Sections 4.8, 4.9, 6.10, pages 125, 128, 183) is likely to increase in importance; the processing houses should be developing the necessary software. This work will naturally involve development of more efficient smoothing functions. Minor research is indicated for the choice of frequencies to optimize the concentration estimates (Section 4.8, page 125).

Such Fourier work would be likely to lead to development of the Fourier domain principal component analysis (Section 5.9 and 5.10, pages 148, 150).

Display of the first three principal components as three coloured maps will certainly be a profitable exercise for interpreters, as the image constitutes a map of the lithological variation (Section 5.12, page 154) Experimentation with the choice of colours on a visual display unit will be necessary to arrive at a set of colours which the eye can use for combinations (See for instance Section 6.2 on page 164) expressing the lithological units of interest. Manipulation of the colours of appropriate spectral components may also allow the radon effects to be visually suppressed without loss of the uranium sub-image.

The satisfactory achievement of principal component analysis in the Fourier domain (see Section 5.9, page 148) should be followed up to explore the possible applications. Optimization of the smoothing functions for PCA is expected to be profitable.

The amplitudes of the Fourier or principal components give a significant reduction in dimensionality (see Section 4.9, page 128, and Section 5.12, page 154) Assessment of the minimum sets of components is indicated. At the same time an opportunity exists to increase the efficiency of acquisition with the design and commissioning of a reliable preprocessing unit on the aircraft (see Section 6.10, page 183). The reduced set of variables presents a fertile area for the construction of factors, including the radon factor.

The thesis has entered a productive area and presented several tools for use in processing. Some progress towards the main target of suppression of radon effects has been achieved. The field remains challenging.

APPENDIX

LEAST SQUARES FIT AS A DOT PRODUCT

Consider that we seek a least square fit of some model spectrum $\{f_i\}$ to a reading spectrum $\{x_i\}$. The requirement is for the minimization of the sum of squares:

$$\text{min.} = \Sigma_i \, (x_i - \emptyset . f_i)^2$$

where $\emptyset$ is the amplitude of the model spectrum.

Applying partial differentiation with respect to $\emptyset$,

$$0 = \Sigma_i \, 2(x_i - \emptyset . f_i)(-f_i)$$

$$= -2\Sigma_i \, x_i . f_i + 2 . \emptyset . \Sigma_i \, f_i^2$$

If we require the model spectrum to be normalized, $\Sigma_i \, f_i^2 = 1$

$$= -2 \, \Sigma_i \, x_i . f_i + 2 \, \emptyset$$

Then–

$$\emptyset = \Sigma_i \, x_i . f_i$$

which is equivalent to saying that the amplitude $\emptyset$ is the projection of the vector $\{x_i\}$ onto the unit vector $\{f_i\}$.

The model of the channel count set as a vector space is convenient, but does not take account of the different amount of useful information given by the different channels. A stricter accounting of the variance is given by Grasty et al. (1985) as a matched filter, or weighted least squares fit:

$$\mathbf{c} = (\underline{A}^T \underline{V}^{-1} \underline{A})^{-1} \underline{A}^T \underline{V}^{-1} \mathbf{x}$$

GLOSSARY OF TERMS

* -indicates a further entry in the Glossary.

Activity: Radioactivity, measured in Becquerels (Bq, events per second). Often each event includes the emission of a gamma ray*.

Airborne data: Data collected from aircraft. Hence "airborne radiometrics".

Airborne radon: Radon* which has escaped into the atmosphere above ground level. Also, the daughters* of radon and their effects.

Alias filter: A removal of frequencies* near half the sampling frequency. Particularly important in time series data collection where it is used to avoid aliasing*.

Aliasing: Frequencies* near half the sampling frequency will be incorrectly sampled. If the amplitudes are not trivial, the effect obscures with correctly sampled, lower frequencies. Should be truncated* with an alias filter* before sampling.

Alpha decay: Decay in which the nucleus loses four units of mass. The daughter* is usually excited and relaxes in turn with the release of a gamma ray*.

Amplitude, spectral: The projection* of a reading* on a unit vector* in spectral space*.

Autocorrelation: The Fourier inverse of a power series*. It is a squared, dephased* version of the original data. Strictly, this is an autocovariance, but the term used is more common and is less confusing in the current context.

Background: All radioactivity* not coming from the ground. Sometimes used in more restricted meanings such as that part of the spectrum not arising from photopeaks*.

Beta decay: When an nucleus emits or takes up an electron, a gamma

ray* of uncertain energy is simultaneously released. A broad exponential spectrum to some maximum energy is formed. Beta decay occurs at the x-ray end* of the spectra of each of the three radioelements*.

Calibration: The acquisition units must be tested periodically to measure the sensitivity* of their response to a known quantity of radionuclides* at some known distance.

Channel: A means of handling an independent stream of data, here the counts detected in an energy range of 10.5 eV or 1.7 aJ.

Compton event: Scattering* of a photon*, with loss of energy.

Counting noise: See Noise*.

Daughter: Nucleus resulting from a decay. Often it is radioactive* in turn, giving rise to a series*.

Dephase: To remove the phase, or suppress the imaginary part from a complex coefficient in a Fourier transform. Any sine functions in the original data are converted to cosines.

Deconvolution: The removal of a repeated function from a data set by division in the Fourier domain*.

Dot product: The sum of the products of the corresponding components of two vectors, such as a factor and a reading. See Appendix.

Equilibrium: See Chapter II.

Factor: The spectral expression of a physical behaviour. Usually has some negative channel values, unlike an observed spectrum which is always positive. Alternatively, the physical behaviour itself, or any identifiable pattern in the variance, depending on author.

Factor analysis: Analysis, including the mathematics, of factors. Some authors may include PCA*.

Fourier domain: The representation of a data set which uses the amplitudes of its frequencies resulting from a Fourier transform*.

Fourier transform: The amplitudes of a set of harmonics when fitted to a set of data. Each frequency* has both a sine and a cosine, in general. The cosine transform lacks the sines but needs twice as many frequencies to describe the original function.

Frequency: Cycles in data apart from time variation are often seen. The terms frequency and wavelength are used in this thesis by analogy, that is, a frequency is expressed in cycles per spectrum, or cycles per flight line.

Gain: Amount of amplification. Determines which channel* an event is to be counted in.

Gain drift, gain shift: Gains* drift as the amplifiers change temperature or reference voltage. Distorts the spectrum.

Gamma ray: Photon* of energy greater than an x-ray.

Gaussian: A bell-shaped figure arising from the exponential of a square.

Gaussian statistics: The Normal distribution.

Grid: Set of parallel flight lines* along which the aircraft is to take samples.

Ground uranium: Part of the uranium* signal which originates in the ground as distinct from the air. The source radionuclide is Bi-214 or Pb-214, but the element of interest to an interpreter is usually the parent, uranium.

Hann: Hanning function*.

Hanning function: $H(x) = 0.5 + 0.5 * \cos(\theta)$ where θ runs over $(0,\pi)$ in the interval to be tapered*.

Image: A two-dimensional analogue representation of a set of data.

Often coloured to allow overlay of three data sets, it may be live on a screen, or hard copy as a map. In remote sensing, the image is usually distance-by-distance, but the method does not require the data to be spatial.

Interactive processing or interpretation: At intermediate stages of processing, the software throws up an image* on screen, requiring a subjective or skilled or otherwise informed judgment to be made before proceeding. The computer and software combination becomes a tool of the worker.

Ill-conditioned: Lacking linear independence. Any uncertainty in the value of a coefficient in a set of simultaneous equations can then give an unstable result.

Line, emission: A radioelement* may make a transition which releases photons of a well-defined energy or line. This forms a photopeak in the NaI spectrum.

Line, flight: Path followed by the aircraft along the grid*.

Linear independence: Of a set, occurs when a change in one member does not imply any change in the others.

Model spectrum: The average spectrum which would be obtained when flying in clean air over ground containing only that radioelement.

Multichannel: Each reading* has many numbers, each being the count in one channel*.

Multispectral: Collected using more than three windows. More than three significant images* can be formed from multispectral data. Remote sensing data is increasingly multispectral.

NaI(Tl): Sodium iodide with thallium doping, used in crystal scintillators*.

Noise: Variation in the data which is of unknown or irrelevant

cause. Interference. May be systematic as in gain* drift, or random as in-

Noise, statistical: Caused by the measurement of a quantity of probabilistic origin, such as the counting of random events. Inevitable but meaningless. Counting noise, or Poisson noise falls into this category.

Normal statistics: Gaussian statistics. The study of random events of a high rate of occurrence. The mathematics is well developed.

Overflight range: A length of ground of known activity*. A detector is flown over at a known height for calibration*.

PC: Principal component*.

Pads: Concrete blocks of known high activity* are laid out at an airfield and the plane is parked on the resulting pad for calibration*.

PCA: Principal component analysis*

Peak: Photopeak*, or crest of photopeak.

Photon: Elementary particle of light. Here, a gamma ray*.

Photopeak: An emission line* seen spread out on a spectrum after acquisition.

Poisson statistics: The study of random events of low rate of occurrence. The correct statistics for gamma ray counting, but the mathematics becomes intricate. Gaussian statistics* is used instead.

Preprocessing: Much of the work which slows down the computation does not require operator intervention. It thus can be done before the data reaches an interactive* session.

Principal component analysis: The extraction and study of principal components.

Principal component: See Chapter V.

Projection: The dot product of a vector on a unit vector of a specified direction.

Radioactivity: Frequent nuclear decays. Activity*.

Radioelement: An element whose nuclei decay.

Radionuclide: Those isotopes of an element which may decay. Not always all, e.g. K-39 does not decay, but K-40 does.

Radium: Precursor to radon*. Chemically active, may travel in the ground water. Ra-226 has a half-life* of 1600 years.

Radon: Inert gas with a large massive atom. Tends to diffuse out of the host material. Rn-222, in the uranium series*, has a half-life* of 3.82 days. In lithology mapping by radiometrics, the term is often used to mean any transient radioactivity other than cosmic radiation, since it is predominantly the daughters of radon which contribute to the transient effects on the surveys.

Range factor: A height factor* which is being used to determine the distance to a source.

Reading: The accumulated counts in each channel are stored once each second, or at some chosen interval. The resulting set of counts is a reading.

Regridding: The transfer of the information from the flight lines to a rectangular grid drawn on the survey area.

Reprocessing: After initial use, the raw data may be stored for possible later processing in some different way.

Residence time: The characteristic time for an added material to leave a natural system, such as radon leaving the air.

Scattering: Photons may recoil from collision rather than be absorbed. See Compton*.

Scintillator: Material such as sodium iodide or polymethyl methacrylate which gives off visible light as it stops a gamma ray*.

Sensitivity: The degree of response of the acquisition system to the presence of a quantity of radioelement*.

Series: The product of a radioactive* decay may itself be radioactive, and give rise in turn to a further decay.

Signal: Useful information in the readings*.

Signal-to-noise ratio: The amplitude of the signal* compared to the amplitude of the noise*. The variance, or intensity or energy may be used for the ratio. Often used qualitatively.

Skyshine: Photons* coming from above the horizontal. Includes the cosmic* rays, backscattered photons*, and at energies below about 600 keV, the twice-scattered photons. See Bailey (1986) or Beck and de Planque (1968).

Softening: Some photons are scattered and reappear further down the spectrum. This tends to fill in the areas between the peaks, hence softening the spectrum.

Spectral space: Considering the channels as independent axes, each reading scan be seen as a vector in a multi-dimensional space. The model applies equally to 3-window data and multichannel.

Spectrum: A set of counts of gamma ray detections, sorted according to energy.

Station: Position along the flight line* to which the reading is assigned.

Stripping: The removal of one spectrum from another. Once a graphical method, it is now computed.

Striping: Stripes appear on maps of processed data, particularly due to airborne radon being more prevalent at the time of that

particular flight than that of its neighbour.

Tapering: A Fourier transform* of a function may be truncated* gradually, usually as its signal-to-noise ratio* declines in the high frequencies*. This is done by multiplying the amplitude of these frequencies by a set of numbers which change from unity to zero as they are applied, such as a Hanning* function.

Terrain: Any character of a ground surface which can be expected to repeat itself, often has characteristic topography, and may reflect the lithology.

Thorium: Often the entire thorium series* is being referred to, sometimes the signal of just one of the daughters*. The signal received is mainly that of Tl-208, but also that of Pb-208* (Beck, 1972) and Ac-228 (Adams and Dams, 1970).

Transform: A set of numbers which express the information of another set in a different form. See Fourier*.

Upward-looking crystal: Upward-looking detector shielded from below, where most of the lithological signal* comes. Later a subtraction is made to enhance the latter.

Uranium: Often the entire uranium series* is being referred to, sometimes the signal of just one of the daughters*. The signal received is mainly that of the radionuclide* Bi-214, also Pb-214.

Vector: An ordered set of numbers obeying certain rules. Here a multichannel reading obeys the rules sufficiently to apply PCA, in particular, the numbers are ostensibly independent, have the same units and have similar status.

Window: A range of energies over which the counts are averaged.

X-ray end: Low energies of the gamma-ray* spectrum.

REFERENCES

Adams J A S, 1954, Uranium and thorium contents of volcanic rocks. In: Nuclear Geology, New York: John Wiley and Sons.

Adams F and Dams R, 1970, Applied Gamma-ray Spectroscopy, second edition, Oxford: Pergamon Press.

Adams J A S and Weaver C E, 1958, Thorium-to-uranium ratios as indicators of sedimentary processes: example of concept of geochemical facies, Bull. Am. Ass. Pet. Geol. (AAPG) 42(2) (1958).

Aerodata Holdings P.L., 1987, Multiclient survey of Charters Towers.

Ahrens L H, 1965, Distribution of the Elements in our Planet, New York: McGraw-Hill.

Bailey R C, 1986, The altitude dependence of terrestrial gamma-ray spectra: a simple model, Geophysics, 51(11) (November, 1986) p2108.

Beck H and de Planque G, 1968, The Radiation Field in Air due to Distributed Gamma-ray Sources in the Ground, United States Atomic Energy Commission.

Beck H L, 1972, The Absolute Intensities of Gamma-rays from the Decay of U-238 and Th-232, United States Atomic Energy Commission.

Bloomfield P, 1975, Fourier Analysis of Time Series: An Introduction, New York: John Wiley and Sons.

Bose N K, 1985, Digital Filters, Theory and Applications, New York: North-Holland Publ. Co.

Butt C R M, 1981, The Nature and Origin of the Lateritic Weathering Mantle, with particular reference to Western Australia, in Doyle (1981).

Butt C R M, Horwitz R C and Mann A W, 1977, Uranium Occurrences in Calcrete and Associated Sediments in Western Australia, CSIRO Division of Mineralogy Report FP16.

Campbell N A and Atchley W R, 1981, The geometry of canonical variate analysis, Syst. Zool., 30(3) 1981 pp 268-280.

Charbonneau B W and Darnley A G, 1970, A Test Strip for Calibration of Airborne Gamma-ray Spectrometers, Geological Survey of Canada Paper 70-1, part B. (quoted in Wilkes, 1976)

Chatfield C and Collins A J, 1980, Introduction to Multivariate Analysis, London: Chapman and Hall.

Clark R B, 1971, Computer simulation and a simple approach to some topological problems, Rice University, Project themis report, p82-88. Quoted in Duval (1977).

Clifford C E, Rubin R M and Wells M B, 1981, A Study of the Distribution of Radon in the Atmosphere to a Height of 457 Meters, U. S. Dept of Energy, Grand Junction Office, Colorado.

Conaway J G and Killeen P G, 1978, Quantitative uranium determinations for gamma-ray logs by application of digital time series analysis, Geophysics, 43(6) (October 1978) p1204.

Connor S, 1984, The blast that Britain kept secret, New Scientist, 24 May 1984.

Cooper M J, 1977, Deconvolution: if in doubt, don't do it. Physics Bulletin, October 1977.

Cooper M J, 1985, Compton scattering and electron momentum determination, Reports on Progress in Physics, 48(4) (April 1985).

Cordell L and Knepper D H, 1987, Aeromagnetic images: Fresh insight to the buried basement, Rolla quadrangle, southeast Missouri, Geophysics, 52(2) (February 1987) p218.

Cowan D R and Crabb T N, 1981, Airborne magnetic and radiometric surveys in sequential exploration, in Doyle (1981).

Crossley D J and Reid A B, 1982, Inversion of gamma-ray data for element abundances, Geophysics, 47 p117.

Darnley, A G, Bristow Q and Donhoffer D K, 1968, Airborne Gamma-ray Spectrometer Experiments over the Canadian Shield, in: Nuclear techniques and mineral resources, p163, I.A.E.A.

Darnley A G, 1971, Aeroradiometric Survey Techniques, Nato Advanced Study Institute on methods of prospecting for uranium minerals.

Demnati A and Naudy H, 1975, Gamma-ray spectrometry in central Morocco, Geophysics, 40(2) (April 1975) p331.

Dickson B L, Clark G J and McGregor B J, 1979, Technique for correcting for overburden effects in ground level radiometric surveys of uranium ore bodies, Geophysics, 44(1) (January 1979), p89-98.

Dickson B H, 1980, Analytic methods for multichannel analysis of airborne radiometrics, M.Sc. thesis, University of Toronto.

Dickson B H, Bailey R C and Grasty R L, 1981, Utilizing multi-channel airborne gamma-ray spectra, Can. J. Earth Sci. 18 p1793.

Dmitriev A V, Kogan R M, Nikiforov M V and Fridman Sh D, 1973, The

experience and practical use of aircraft gamma-ray survey of snow cover in the USSR. WMO Symposium on measurement and forecasting, Banff, Alberta, 1973, quoted in Grasty (1976d).

Dong-ping W and Walsh J J, 1976, Objective analysis of the upwelling ecosystem off Baja California, Journal of Marine Research, 34(1) (1976) p43.

Doyle H A, Glover J E and Groves D I, (Eds) 1981, Geophysical Prospecting in Weathered Terrains, Perth: University of Western Australia.

Dunn P, 1987, Personal communication, Geological Survey of Western Australia, Perth.

Duval J S, 1971, Circle of investigation of an airborne gamma-ray spectrometer, Journal of Geophysical Research, 76 p8466.

Duval J S, 1977, High sensitivity gamma-ray spectrometry- state of the art and trial application of factor analysis, Geophysics 42(3) (April 1977) p549.

Fischer D, 1988, Letter to the editor, New Scientist, No 1598 (4 February 1988).

Foote R S, 1968, Improvement in Airborne Gamma Radiation Data Analysis for Anomalous Radiation by removal of Environmental and Pedologic Radiation Changes, Nuclear techniques and mineral resources, I.A.E.A. production series, quoted in Grasty et al. 1985.

Godby E A, Connock S H G, Stelje J F, Cowper G and Carmichael M, 1952, Aerial Prospecting for Radioactive Minerals, National Research Council Laboratories, Report A.E.C.L. 13, quoted in Wilkes (1976).

Grasty R L, 1973, Snow-water equivalent measurement using natural gamma-ray emission, Nordic Hydrology, 4 p1.

Grasty R L, Loijens H S and Ferguson H L, 1973, An Experimental Gamma-ray Snow Survey over Southern Ontario, US/IHD Interdisciplinary symposium on advanced concepts and techniques in the study of snow and ice resources, Monterey, California.

Grasty R L, 1976a, The Circle of Investigation of Gamma-ray Detectors, Geological Survey of Canada paper 76-1B.

Grasty R L, 1976b, A Calibration Procedure for an Airborne Gamma-ray Spectrometer, Geological Survey of Canada paper 76-16.

Grasty R L, 1976c, The reduction of statistical noise in airborne radiometric data, Can. J. Earth Sci., 13(10) (October, 1976)

Grasty R L, 1976d, The applications of gamma radiation in remote sensing, from: Methods in Remote Sensing, Springer Verlag.

Grasty R L, 1982a, Direct snow-water equivalent measurement by airborne gamma-ray spectroscopy, Journal of Hydrology, 55 p213

Grasty R L, 1982b, Utilizing experimentally derived multi-channel gamma-ray spectra for the analysis of airborne data, Symposium on Uranium Exploration Methods, Review of the Nuclear Energy Agency/International Atomic Energy Authority R&D Programme, Paris, 1st-4th June 1982.

Grasty R L, Glynn J E and Grant J E, 1985, The analysis of multichannel airborne gamma-ray spectra, Geophysics, 50(12) (December, 1985) p2611.

Green A A, 1987, Leveling airborne gamma-ray data using between-channel correlation information, Geophysics 52(11) (November 1987) p1557.

Hansson C B, 1972, Physical Data Book in SI Units, Oxford: Pergamon Press.

Harshaw 1988, Advertisement, Physics Today, 41(11) November 1988.

Hurlbut C R, 1985, Plastic Scintillators a Survey, Bicron Corp., American Nuclear Society Winter Meeting.

International Atomic Energy Authority, 1976, Radiometric Reporting Methods and Calibration in Uranium Exploration, Technical Report 174, I.A.E.A., Vienna, p57.

International Atomic Energy Authority, 1987, Nuclear Spectrum, 3(2).

Joreskog K G, Klovan J E and Reyment R A, 1976, Geological Factor Analysis, New York: Elsevier.

Kerrigan G C and O'Connor B H, 1989, Thorium disequilibrium in Monazite, submitted to Health Physics.

Killeen P G and Carmichael C M, 1970, Gamma-ray spectrometer Calibration for field analysis of thorium, uranium and potassium, Can. J. Earth Sci., 7 p1093 (1970).

Killeen P G and Cameron G W, 1977, Computation of In Situ Potassium, Uranium and Thorium Concentrations from Portable Gamma-ray Spectrometer Data, Geological Survey of Canada paper 77-1A.

Kogan R M, Nazarov I M and Fridman S D, 1969, Gamma Spectroscopy of natural environments and formations, Israel Program for Scientific Translation, No 5778, Jerusalem, 1971, quoted in Grasty et al., 1973.

Lapp R E and Andrews H L, 1972, Nuclear Radiation Physics, Second edition, New York: John Wiley and Sons.

Lovborg L, Kirkegaard P, Christiansen E M, 1976, Design of NaI(Tl) Scintillation Detectors for Use in Gamma-ray Surveys, Danish Atomic Energy Commission.

Mason B, 1966, Principles of Geochemistry, third edition, New York: John Wiley and Sons.

Mathew P J and Beretka J, 1983, Specific radioactivity of some Australian building materials, Radiation Protection in Australia, 1(2).

McSharry P J, 1973, Reducing errors in airborne gamma-ray spectrometry, Bull. Aust. Soc. Explor. Geophys., 4(1) p31.

Myers D, 1988, Lecture to Australian Society of Expl. Geophysicists, Perth.

National Radiological Protection Board, 1989, Radiation exposure of the U.K. Population- 1988 review, H.M.S.O., U.K.

Nelson D R and McCulloch M T, The ^{40}K-^{40}Ca radiogenic decay scheme- a reconnaissance study, Chemical Geology (Isotope Geoscience Section), accepted November 1987.

Parker Gay S and Lyons P B, 1978, The Benefits of Light-to-Moderate Weight Gamma-ray Spectrometer Systems in Radiometric Surveying for Uranium, American Institute of Mining Engineers meeting, Denver, Colorado (March 1978).

Pearce F, 1987, A deadly gas under the floorboards, New Scientist, 5 February 1987.

Robinson E A and Trietel S, 1980, Geophysical Signal Analysis, New Jersey: Prentice-Hall.

Salmon L, 1960, Analysis of Gamma-ray Scintillation Spectra by the Method of Least Squares, United Kingdom Atomic Energy Authority.

Saunders D F, Terry A S and Thompson C K, 1987, Test of NURE gamma-ray spectral data in petroleum reconnaissance, Geophysics 52(11) p1547.

Schlumberger, 1972, Log Interpretation and Principles, Schlumberger Limited, p57.

Schwartzer T F and Adams J A S, 1973, Rock and soil discrimination by low-altitude airborne gamma-ray spectroscopy in Payne County, Oklahoma, Econ. Geol., 68 p1297

Schwartzer T F, Cook G B and Adams J A S, 1972, Low altitude gamma-spectrometric surveys from helicopters in Puerto Rico as an example of the remote sensing of thorium, uranium and potassium in soils and rocks, Remote Sensing of Environment, 2 p83-84.

Scott J H, 1963, Computer analysis of gamma-ray logs, Geophysics, 28(3) (April 1963) p147.

Seigbahn K, 1965, Alpha-, Beta- and Gamma-ray spectroscopy, Vol 1, Amsterdam: North Holland Publ. Co.

Serra O, 1984, Fundamentals of Well-Log Interpretation, Amsterdam: Elsevier.

Smith R J, 1985, Geophysics in Australian mineral exploration, Geophysics, 50(12) (December 1985) p2637.

Spiegel M R, 1974 Theory and Problems of Fourier Analysis, New York: McGraw-Hill.

Starkey L J, 1970, Company reports, Geotechnics Pty Ltd, Perth.

The Age, 1987, 2 June-9 June weather maps, newspaper, Melbourne.

Ward D L, 1981, Surface Radiometric Surveys for Uranium using Gross and Spectral Gamma-ray Measurements, Bendix Corp., Colorado.

Weast R C, Astle M J and Beyer W H, 1984, CRC Handbook of Chemistry and Physics, 65th ed, Florida: CRC Press.

Western Mining Corporation, 1975, A General Account of the Yeelirree Uranium Deposit, quoted in Butt et al. (1977).

Wilkes P, 1976, Acquisition, Processing and Interpretation of Airborne Gamma-ray Spectrometry Data, Microform MF73, Bureau of Mineral Resources, Canberra.

Wilkes P, 1988, Computer processing of gamma ray spectrometry data, Course notes, Aust. Soc. Expl. Geoph. Conference, Melbourne, 1988.

Wormald M R and Clayton C G, 1975, Observations on the Accuracy of Gamma Spectrometry in Uranium Prospecting, United Kingdom Atomic Energy Authority, Harwell, UK.

INDEX